AN ANALYSIS OF RADAR IN TERMS OF INFORMATION THEORY AND PHYSICAL ENTROPY

by

Clifford L. Temes and Donald Schilling

Research Report No. PIBMRI-1270-65

Contract No. Nonr-839(38)

for

Office of Naval Research
Washington 25, D. C.

June 1965

POLYTECHNIC INSTITUTE OF BROOKLYN
MICROWAVE RESEARCH INSTITUTE

ELECTRICAL ENGINEERING DEPARTMENT

Research Report No. PIBMRI-1270-65

AN ANALYSIS OF RADAR IN TERMS OF INFORMATION THEORY AND PHYSICAL ENTROPY

by

Clifford L. Temes and Donald Schilling

Polytechnic Institute of Brooklyn
Microwave Research Institute
55 Johnson Street
Brooklyn 1, New York

Research Report No. PIBMRI-1270-65

Contract No. Nonr-839(38)

June 1965

Title Page
Acknowledgement
Abstract
Table of Contents
Table of Figures and Graphs
98 Pages of Text

Clifford L. Temes

Donald Schilling
Assistant Professor

Approved:

Mischa Schwartz
Head of Electrical Engineering Department

Prepared for

Office of Naval Research
Washington 25, D. C.

ACKNOWLEDGEMENT

The author would like to express his deep appreciation to Professor Donald L. Schilling for his invaluable guidance and penetrating evaluation of the work, and to Professor Mischa Schwartz and Professor Arthur E. Laemmel for enlightening discussions which solidified the central ideas.

The author is also indebted to Federal Scientific Corporation for their cooperation and support during the dissertation period.

The research described herein was supported by the Office of Naval Research, Washington, D. C. under Contract No. Nonr-839(38).

ABSTRACT

A radar is basically a measuring instrument for extracting information from a received signal voltage. The amount of information that can be extracted is ultimately limited by the noise background. The concept of measurable information has been quantitatively developed in the literature and provides a means by which substantial insight may be acquired into the generalized nature of optimum radar processing.

The presented work exhibits an interpretation of radar information consistent with intuitive views of radar processing as well as with formal definitions of information theory. The approach has led to the following specific results.

(a) A unified description of the mechanism by which both detection capability and parameter estimation are optimized simultaneously. A two-dimensional matched filter is described in which the ideal radar processing is seen to consist of a two-dimensional "involution" in which the signal's input energy area in the time-frequency plane is compressed into an interior area.

(b) The two-dimensional compression of Item (a) can be increased, in both the time and frequency domains by a factor of $\sqrt{\rho}$, where ρ is two times the signal-to-noise energy ratio, by employing an envelope detector having the characteristic of $I_o(x)$, the modified Bessel function.

(c) The definition of a "distributional" type of physical entropy that is associated with parameter information. For a given a priori surveillance window within which we search for a target, it is shown that there is a minimum threshold energy E_T required to make a meaningful measurement. Furthermore, the total amount of range and Doppler parameter information obtained is bounded such that the information is always less than the threshold entropy $E_T/\mathcal{J}$, where $\mathcal{J}$ is the equivalent noise temperature of the radar. It is also shown that the minimum signal-to-noise energy ratio required to detect the presence of a signal immersed in one noise mode (independent sample) is equal to a defined "absolute" information entropy of the noise sample, which is calculated to be unity.

(d) An equivalence between the amplitude detection threshold commonly employed in radar and the energy threshold employed in physics for setting the "reliability" of a measurement.

(e) The development of a new detection procedure based upon a defined "detection information" and the employment of the Neyman-Pearson procedure in the threshold-crossing rate domain rather than in the standard amplitude domain.

(f) A new representation of band-limited or time-limited Gaussian noise based upon the identification of independent noise "modes" in the time-frequency plane, with each mode having an energy described by the Boltzmann factor of statistical mechanics and occupying an area of one logon in the time-frequency plane.

(g) An explicit formula for parameter information in terms of a multiple-target echo ambiguity function.

(h) By defining a distributional type of information in a gas problem involving thermodynamic entropy, a formula is derived which is directly analogous to Shannon's formula for the information communicated through a noisy channel.

TABLE OF CONTENTS

Page

TABLE OF FIGURES AND GRAPHS

1. INTRODUCTION

1.1 Summary

A radar is basically a measuring instrument for extracting information from a received signal voltage. The amount of information that can be extracted about such signal parameters as range delay and Doppler frequency is ultimately limited by the noise background. Radar theory has shown that both detection capability and parameter-estimation accuracy are explicitly dependent upon the ratio of total received signal energy to noise power spectral density (for white Gaussian stationary noise). Furthermore, both detection capability and parameter estimation are optimized, within the class of linear filters, by the so-called "matched filter".

The concept of measurable information has been quantitatively developed in the literature and provides a means by which substantial insight may be acquired concerning the generalized nature of optimum radar processing. It is apparent that a radar obtains information only upon reception of a quantity of energy. Moreover, the amount of information acquired depends upon the degree of concentration (in time and frequency) of the input energy as it is introduced. The degree of concentration, in turn, is measurable in terms of the increase in physical entropy experienced by the radar instrument. We find that a greater amount of input information implies a smaller increase in entropy. In fact, a negative form of entropy (negentropy) can be defined which implies the availability of thermal work due to mixing or diffusion. This negentropy is received whenever information is obtained. If a non-dissipative process is assumed in which input energy is conserved, it is concluded that availability of thermal work is created whenever information is received. We have therefore arrived at a principle of a cybernetic nature, namely, that information (of the type considered) is interpretable as a physical entity rather than only an arbitrary "measure". (Section 3.3)*.

If the input energy is not well concentrated in time or frequency (or both) as it enters the radar, maximum information may still be extracted by using a matched filter. The role of the matched filter is interpretable as the reverse of diffusion. That is, it compresses the area occupied by the input signal energy in the time-frequency plane (with signal time-bandwidth products greater than unity). For example, suppose we are using a linear-FM (chirp) signal with a relatively wide bandwidth of B cps. The matched filter has a comparable bandwidth. At the matched filter output, the signal energy is compressed into a time interval of 1/B seconds which is also the duration of

---

* Section references in parentheses refer to sections of this dissertation where the subject is primarily developed.

an output independent noise sample. Let us assume that the input pulse has a duration of P seconds and the a priori uncertainty in our knowledge of range delay extends over a range window of T seconds. At the input to the matched filter, the received range information is measurable as $\log_2 T/P$ bits, whereas it is $\log_2 TB$ bits at the matched filter output. We now have

$$\log_2 TB > \log_2 T/P \quad , \tag{1.1}$$

since $PB > 1$ for signals with time-bandwidth products greater than unity. Therefore, the matched filter may be said to have increased the measured information (and negentropy). (Section 3.2).

Physical entropy is the ratio of an energy increment to absolute temperature and, in radar, it is shown that this is synonymous with signal-to-noise energy ratio. Thus, the analysis of optimum radar processing in terms of information theory leads to significant relations among various quantities such as information entropy, physical entropy and signal-to-noise energy ratio. Furthermore, it becomes evident that radar detection capability and (range-Doppler) parameter estimation are necessarily optimized by the same mechanism which involves a compression of the signal's energy area in the time-frequency plane. (Section 3.2).

The presented work exhibits an interpretation of radar information consistent with intuitive views of radar processing as well as with the formal definitions of information theory. Moreover, the additional insight provided by the approach has lead to the following specific results:

(a) A unified description of the mechanism by which both detection capability and parameter estimation are optimized simultaneously. A two-dimensional matched-filter concept is described in which the ideal radar processing is seen to consist of a two-dimensional "involution" in which the signal's input energy area in the time-frequency plane is compressed into an interior area. The two-dimensional matched filter is found to be a time-frequency gate which overlaps the signal's input energy area in the time-frequency plane. (Section 3.2).

(b) The two-dimensional compression of Item (a) can be increased, in both the time and frequency domains by a factor of $\sqrt{\rho}$, where

$$\rho = \frac{2E}{N_o} = \frac{2 \times \text{signal energy}}{\text{noise power spectral density}} \quad , \tag{1.2}$$

by employing an envelope detector having the characteristic of the modified Bessel function (of first kind and zero order) $I_o(x)$. (Section 3.2).

(c) The definition of a "distributional" type of physical entropy that is

associated with parameter information. For a given a priori surveillance window within which we search for a traget, it is shown that there is a minimum threshold energy E_T required to make a meaningful measurement. Furthermore, the total amount of range and Doppler parameter information obtained is bounded such that the information is always less than the threshold entropy $E_T/\mathcal{J}$, where $\mathcal{J}$ is the equivalent noise temperature of the radar. It is also shown that the minimum signal-to-noise energy ratio required to detect the presence of a signal immersed in one noise mode (independent sample) is equal to a defined "absolute" information entropy of the noise sample, which is calculated to be unity. (Sections 3.1, 3.2, 3.3).

(d) An equivalence between the amplitude detection threshold commonly employed in radar and the energy threshold employed in physics for setting the "reliability" of a measurement. (Section 3.1).

(e) The development of a new detection procedure based upon threshold-crossing rate. In this method, the amplitude threshold is set to maximize "detection information". Using this optimum amplitude threshold, a specific false-alarm threshhold-crossing rate is thereby established and accepted as normal. A data-rate threshold is then set for a selected probability of a "false-alarm type of mistake" (or Type-1 error in statistical estimation theory). If the threshold-crossing rate should exceed the established data-rate threshold, a target is judged to be present. Thus the statistical Neyman-Pearson approach is applied to the (threshold-crossing) rate variate rather than to the voltage amplitude. In one example using realistic radar parameters, it is shown that the detection-information procedure increased the detection probability from 40% (using the more conventional Neyman-Pearson procedure on amplitude) to 89% after 5 seconds of processing at a fixed overall false-alarm probability of 1% and a signal-to-noise ratio of 6 db. Furthermore, in the detection-information method, there are no "false alarms" in the usual sense which then obligate the radar to take further measures to confirm or reject the hypothesis that a target is present. That is, amplitude-threshold crossings are expected to occur on an occasional basis in the detection-information procedure. It is the increase in this threshold-crossing rate which is important. The possibility of a "false alarm type of mistake" stems from the uncertainty in determining the rate due to a finite observation time. (Sections 4.1, 4.2, 4.3 and Chapter 6).

(f) A new representation of band-limited or time-limited Gaussian noise is utilized which is analogous to a two-dimensional Karhunen-Loéve expansion. The representation is based upon the identification of independent noise "modes" in the time-frequency plane, with each mode having an energy described by the Boltzmann factor of statistical mechanics and occupying an area of one logon in the time-frequency plane. This noise representation is particularly useful in the information-analysis of

radar but should also be found helpful in other noise problems.

(g) An explicit formula for parameter information is derived in terms of a multiple-target echo ambiguity function. The formula yields results which are consistent with intuitive notions and formal definitions of information. Consideration of these results shows that contour areas may be defined similar to "ambiguity areas". An explicit interdependence coefficient between range and Doppler information is defined which is unity for linear-FM modulation and zero with no frequency modulation (pulsed-CW). The parameter-information formula may also be used for waveform evaluation. For example, the decrease in total received information may be computed for two proximate targets of various amplitudes as their spacing is decreased to zero. (Chapter 5).

(h) By defining a distributional type of information in a gas problem involving thermodynamic entropy, a formula is derived which is directly analogous to Shannon's formula for the information communicated through a noisy channel. (Section 3.3).

1.2 Historical Background

The early radars transmitted simple pulses of energy at a constant frequency. The i-f bandwidth (in cps) was empirically determined[1] to be optimum when it was chosen approximately equal to the reciprocal to the pulse width (in seconds). At that time, the expression "signal-to-noise ratio" generally referred to the ratio of rms echo signal voltage to rms noise voltage, i.e.,

$$\text{Signal-to-noise voltage ratio} = \text{SNVR} = \frac{A_{rms}}{\sigma_N} = \frac{A_{rms}}{\sqrt{N_o B}} , \qquad (1.3)$$

where

A_{rms} = rms voltage of pulsed sinusoid

σ_N = rms noise voltage

N_o = white noise power spectral density

B = i-f bandwidth.

The signal-to-noise power ratio is then

$$\text{SNPR} = \frac{A_{rms}^2}{\sigma_N^2} = \frac{A_{rms}^2}{N_o B} . \qquad (1.4)$$

If we multiply the numerator and denominator of Eq. (1.4) by the signal pulse duration P, and use the optimum i-f-bandwidth condition

$$B = \frac{1}{P} , \qquad (1.5)$$

then Eq. (1.4) becomes

$$\text{SNPR} = \frac{A_{rms}^2 P}{\sigma_N^2 P} = \frac{A_{rms}^2 P}{\sigma_N^2/B} = \frac{E}{N_o} \qquad (1.6)$$

in which

E = signal-pulse energy

N_o = noise power spectral density = $k\mathcal{T}$, where k is Boltzmann's constant and $\mathcal{T}$ is equivalent noise temperature.

Therefore, with the pulsed-CW signal, application of the optimum-bandwidth condition of Eq. (1.5) leads to the result that the SNPR is equal to a ratio of signal and noise energy quantities:

$$\text{SNER} = \frac{E}{N_o} \qquad . \qquad (1.7)$$

The SNER is a more general parameter than the SNPR or SNVR since it involves only signal and noise (energy) properties, but no explicit radar characteristics. This result is a consequence of using the optimization condition of Eq. (1.5).

The generalized importance of the SNER became more evident as the theory and practice of radar advanced beyond the use of simple sinusoidal pulses. Radar theory advanced along two distinct paths, respectively referred to as detection and parameter estimation, and the SNER attained prominence in both areas. In a paper concerned primarily with detection, North[2] showed in 1943 that, with an arbitrary signal waveshape, the linear filter which maximized the ratio of peak output signal power to mean-square output noise possessed a frequency response function which was the complex conjugate of the input signal spectrum (Fourier transform). Moreover, under these optimum-detection conditions, the ratio of output peak power to mean-square noise was found to be E/N_o for the bandpass case. Thus, for a general signal waveshape, the detection capability depended ultimately upon the SNER, whereas the SNPR and SNVR merely appeared as special cases appropriate mainly for the pulsed-CW signal. Numerous papers dealing solely with the detection problem appeared, and various approaches were developed such as the application of the Neyman-Pearson statistical estimation procedure[3-5] to output voltage amplitude, the Ideal Observer[6], the Bayes Criterion[2, 7-9], the Sequential Observer[2, 3, 7-14], Inverse Probability[15-18], zero-crossing criteria[19] and non-parametric methods[20].

In the area of parameter estimation, general waveshapes were also treated. In work by Woodward and Davies[15-17] using the approach of "inverse probability", it was shown that range delay could be measured with an ultimate accuracy of

$$\sigma_\tau = \frac{1}{\sqrt{\overline{f^2}\,\rho}} \qquad (1.8)$$

where

σ_τ = standard deviation of range-delay measurement

$\sqrt{\overline{f^2}}$ = a normalized signal bandwidth

$\rho = 2E/N_o$.

Further results[18, 21], of a more generalized nature, involving the joint estimation of range delay τ and Doppler shift ϕ, showed that the Doppler frequency could be determined to an accuracy of

$$\sigma_\phi = \frac{1}{\sqrt{\overline{t^2}\,\rho}} \quad , \qquad (1.9)$$

where,

σ_ϕ = standard deviation of Doppler frequency measurement

$\sqrt{\overline{t^2}}$ = a normalized signal duration

$\rho = 2E/N_o$.

As in the radar detection problem, the analytical results dealing with parameter estimation again revealed the preeminence of the SNER in governing the ultimate limitations of radar measurements.

A synthesis of the two areas of detection and parameter estimation tended to develop with the recognition that the same filter which optimized detection capability also implemented the required correlation operation by which the optimum parameter-estimation process was accomplished. This is the so-called North filter, or matched filter.

The concepts of information theory were originally developed in a context somewhat remote from the radar application. In 1924, Nyquist[22] considered limitations on the rate of telegraph transmission and utilized a logarithmic measure of information. This logarithmic measure was later employed by Hartley[23], and then developed into an elaborate and rigorous framework, called information theory, by Shannon[24]. The term (information) entropy was employed in connection with the concept of information evidently because of the similarity in form between the logarithmic measure of a number of alternative states to be communicated and the physical entropy of statistical mechanics which has been related to the logarithm of the number of states (or complexions) of a physical system.

Some results of information theory were related to radar applications[17], but without substantial expansion of the approach by later investigators. However, significant relations were observed by Brillouin[25] between the entropy measure used in information theory and the physical entropy of thermodynamics and physics. These were brought out by examples in various types of physical measurements.

As a result of the historical development reviewed above, the fields of radar and information theory have progressed to a point where it has become possible to take a more unified and quantitative view of generalized optimum radar processing, and to relate the amount of information received by a radar to the amount of input physical energy required to obtain it. This approach has been pursued in the present dissertation. In addition, interpretations of the role of the matched filter as a device for optimum information extraction, and various other results, have been derived as described in Section 1.1.

2. TIME-BANDWIDTH-LIMITED GAUSSIAN NOISE

2.1 Conventional Methods of Analysis

When stationary noise is treated, standard analytical techniques involve the use of an autocorrelation function[26]

$$R_x(\tau) = \lim_{T\to\infty} \frac{1}{2T} \int_{-T}^{T} x(t+\tau)x(t)\,dt \qquad (2.1)$$

where x(t) is a real noise waveform. The power spectral density is then given by the Fourier transform relation

$$S_x(f) = \int_{-\infty}^{\infty} R_x(\tau)\, e^{-j2\pi f\tau}\, d\tau \qquad (2.2)$$

by the Wiener-Khintchine theorem.[27]

If the noise is not stationary, a useful approach is that employed by Bello.[28] Letting

$$x(t) = \tilde{x}(t)\, e^{j2\pi f_o t} \qquad (2.3)$$

represent a complex narrow-band noise time function, where $\tilde{x}(t)$ is the complex modulation and f_o is the carrier frequency, then a time-varying complex autocorrelation function is defined in the time domain as

$$r(t,s) = \overline{\tilde{x}^*(t)\,\tilde{x}(s)} \qquad (2.4)$$

where t and s are two time instants, the overhead bar denotes an ensemble average, and the * represents the complex conjugate operation. If $\tilde{X}(f)$ is the Fourier transform of $\tilde{x}(t)$, then an analogous frequency-varying autocorrelation function may be defined in the frequency domain by

$$R(f,\ell) = \overline{\tilde{X}^*(f)\,\tilde{X}(\ell)} \qquad (2.5)$$

Using

$$\tilde{X}(f) = \int_{-\infty}^{\infty} \tilde{x}(t)\, e^{-j2\pi ft}\, dt \qquad (2.6)$$

in Eq. (2.5), we have

$$R(f,\ell) = \int_{-\infty}^{\infty}\int_{-\infty}^{\infty} \overline{\tilde{x}^*(t)\,\tilde{x}(s)}\; e^{-j2\pi(s\ell - ft)}\, dt\, ds$$

$$= \int_{-\infty}^{\infty}\int_{-\infty}^{\infty} r(t,s)\, e^{-j2\pi(s\ell - ft)}\, dt\, ds \qquad (2.7)$$

Eq (2.7) expresses a fundamental duality between the time and frequency domains, with the two domains being related by a double Fourier transform. It should be noted that the analysis proceeds either in the time domain or the frequency domain. However, in the following material we shall work in both domains simultaneously by dealing with areas of the time-frequency plane. This method will be found particularly useful for the information-theory approach to radar analysis.

2.2 Two-Dimensional Representation

2.2.1 Noise Occupancy in the Time-Frequency Plane

We consider first the case of white Gaussian noise which is bandpass-limited to a bandwidth of B cps. At the output of the band-limiting filter, the noise will be observed for a time duration of T seconds. By the sampling theorem for bandpass-limited noise, there are TB independent noise samples involved, with each sample having two "degrees of freedom" such as amplitude and phase (or the real and imaginary parts of the complex voltage). It is important to observe that we are not physically limiting (truncating) in both time and frequency, which cannot be rigorously defended. (That is, the Fourier transform of a truncated time function extends through an infinite range of frequencies.) We are, in fact, truncating only in frequency and then observing for a specific time. This type of noise will be described as boundary-limited in the frequency domain and window-limited in the time domain. The situation is portrayed in Fig. 2.1(a). Each rectangular sub-area represents an independent noise sample with two degrees of freedom covering an area of unity in the time-frequency plane. Such a unit of area will be called a "logon", following Gabor.[29]

The dual of the preceding case is shown in Fig. 2.1(b), where the noise has been time-gated to a duration of P seconds. The frequency axis then represents the independent noise samples as observed by a spectrum analyzer. The presence of independent noise samples in the frequency domain after time-gating may be less familiar than independent samples in the time domain after bandwidth-limiting. An experimental display of this phenomenon will be found in reference 30, Fig. 6. As in the previous dual case, each independent noise sample again occupies an area of one logon with the frequency separation between samples being 1/P cps.

2.2.2 Application of the Boltzmann Factor

The concepts of the preceding section can be conveniently formalized by an interpretation involving the Boltzmann factor of statistical mechanics. We consider a physical system at a temperature $\mathcal{T}$ which possesses n degrees of freedom, where each degree of freedom may occupy any one of M possible energy levels with equal likelihood in the absence of any other constraints. In a classical problem of physics, the question is asked, "What is the most probable energy state of the system subject

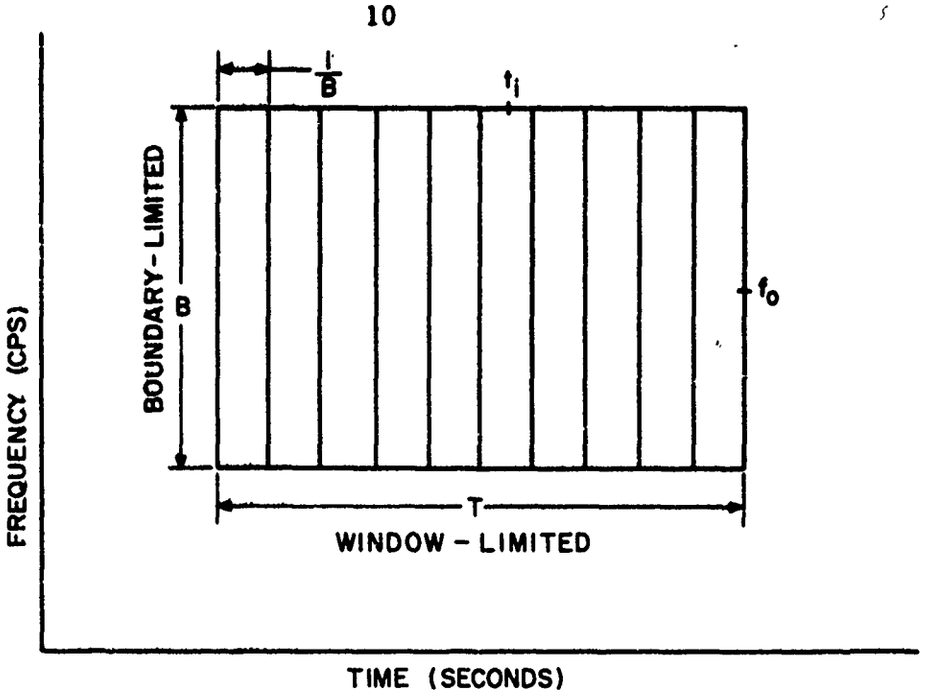

(a) Boundary-Limited in Frequency and Window-Limited In Time

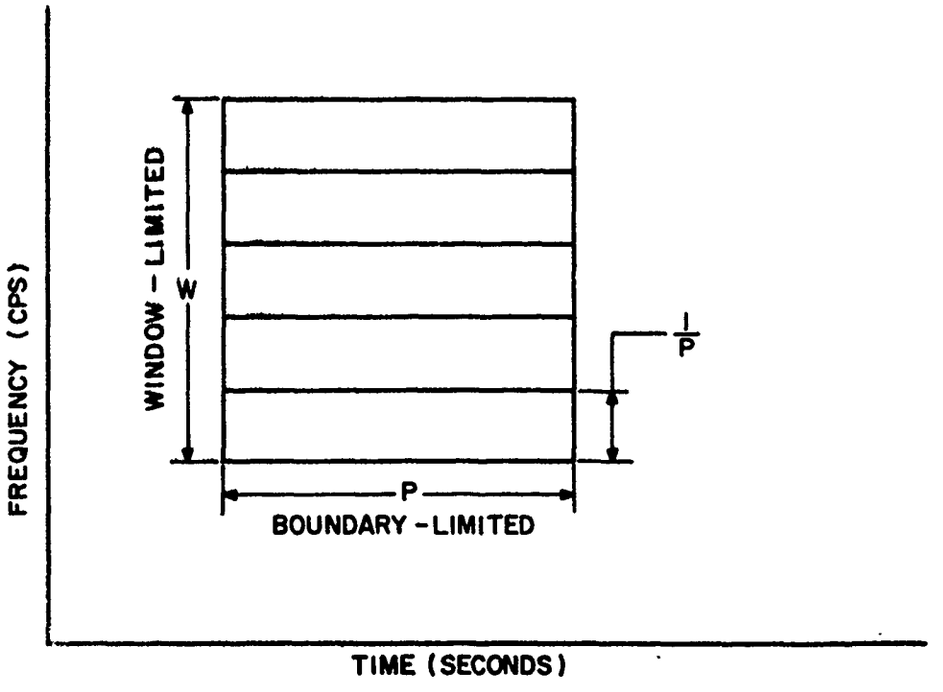

(b) Boundary-Limited in Time and Window-Limited In Frequency

Fig. 2.1 Two Types of Time-Bandwidth-Limited White Gaussian Noise

to the two constraints that: (a) the total number of degrees of freedom is a constant, and (b) the total system energy is a constant?" To solve this problem, let F_o be the overall number of ways that n degrees of freedom can occupy M energy levels. Now suppose a situation in which n_1 degrees of freedom are in level E_1, n_2 degrees of freedom are in level $E_2, \ldots,$ and n_M degrees of freedom are in level E_M. By combinatorial analysis, the number of ways in which this can occur is

$$F_1 = \frac{n!}{n_1!\, n_2! \ldots n_M!} \quad . \tag{2.8}$$

The relative frequency for this condition is

$$P = \frac{F_1}{F_o} = \frac{n!}{F_o\, n_1!\, n_2! \ldots n_M!} \quad , \tag{2.9}$$

where P may be taken as the probability of the state represented by F_1. We wish to maximize P subject to the constraints

$$n = \sum_{i=1}^{M} n_i = \text{number of degrees of freedom} = \text{a constant} \tag{2.10}$$

$$E_S = \sum_{i=1}^{M} n_i E_i = \text{total system energy} = \text{a constant} \quad . \tag{2.11}$$

Using principles of variational calculus[31, 32], it has been found that the most probable energy state of the system is such that the energy of any degree of freedom has a probability distribution

$$p(E_i) \propto e^{-\frac{E_i}{kT}} \quad , \tag{2.12}$$

where

k = Boltzmann's constant.

As the energy levels are taken closer together, the probability distribution approaches the continuous form

$$p(E) \propto e^{-\frac{E}{kT}} \tag{2.13}$$

The exponential $e^{-\frac{E}{kT}}$ is known as the Boltzmann factor.

If we assume that p(E) may be normalized directly, then

$$\int_0^\infty p(E)\, dE = \int_0^\infty \gamma\, e^{-\frac{E}{kT}}\, dE = 1 \tag{2.14}$$

where γ is the normalizing constant. Direct integration yields

$$\gamma = \frac{1}{k\mathcal{J}} \quad , \qquad (2.15)$$

and thus

$$p(E) = \frac{1}{k\mathcal{J}} e^{-\frac{E}{k\mathcal{J}}} \quad . \qquad (2.16)$$

It may be noted, however, that such an exponential probability density function is the Chi-square distribution with two degrees of freedom. This form would apply for a physical system composed of many harmonic oscillators. Each harmonic oscillator possesses two degrees of freedom and the energy variate E in Eq. (2.16) would be applicable for each harmonic oscillator as a unit. We shall call such a unit (with two degrees of freedom) a mode.

Using Eq. (2.16), it is found that the average energy of a mode is

$$\bar{E} = \int_0^\infty E\, p(E)\, dE = k\mathcal{J} \quad . \qquad (2.17)$$

The standard deviation is

$$\sigma_E = \sqrt{\int_0^\infty (E - \bar{E})^2\, p(E)\, dE} = k\mathcal{J} \quad , \qquad (2.18)$$

which is the same as the mean value.

To illustrate the applicability of these results to the noise problem, we refer back to Fig. 2.1(a). There are TB noise modes comprising the noise waveform. If the average energy of each mode is $k\mathcal{J}$, then the total average energy of the noise waveform is

$$\bar{E}_S = TB\, k\mathcal{J} \quad . \qquad (2.19)$$

Since this average energy is spread over a time T, the average power is

$$P = \frac{\bar{E}_S}{T} = k\mathcal{J}\, B \quad , \qquad (2.20)$$

which is immediately recognized as the available noise power (σ_N^2) of white noise that has been bandlimited to B. Finally, the power spectral density is given by

$$N_o = \frac{P}{B} = k\mathcal{J} \quad . \qquad (2.21)$$

Once allowing the validity of the above approach, it is seen to be a simple derivation for the power spectral density of white noise as compared, for example, with the method of reference 33. A block diagram for observing the type of random noise process being considered is shown in Fig. 2.2, which is self explanatory. The system essentially observes a manifestation of the so-called "available" noise power.

We can obtain a further result of significance by considering the voltage waveform just prior to envelope detection. This waveform is sketched in Fig. 2.3. It is possible to identify the individual modes as "packets" of energy of time duration $\Delta t \approx \frac{1}{B}$. The energy of such a mode would be given by

$$E = \frac{R^2 \Delta t}{2} = \frac{R^2}{2B} \quad , \qquad (2.22)$$

where R is the peak envelope voltage of the mode. The probability density function for R is therefore determined from the Jacobian of the transformation between E and R as

$$p(R) = p(E) \frac{dE}{dR} = \frac{R}{k \mathcal{J} B} e^{-\frac{R}{2k\mathcal{J}B}} \quad , \qquad (2.23)$$

which is the Rayleigh distribution, as would be expected. The Rayleigh distribution, of course, characterizes the amplitude of the vector sum of two orthogonal Gaussian-distributed component vectors. These component vectors represent two degrees of freedom and may be thought of as the real and imaginary parts of the complex voltage envelope, as used by Rice.[34]

2.2.3 Karhunen-Loéve Expansion in Two Dimensions

The type of noise representation developed in the preceding section involves a characterization in both the time and frequency domains simultaneously, rather that the more conventional approach of working in one domain or the other with connecting Fourier-transform transitions. The two-dimensional approach may be formalized further by using a Karhunen-Loéve type of expansion in two variables. We may, for example, define a "state function" $\psi(t, f)$ by the expansion

$$\psi(t, f) = \sum_{i=1}^{TB} a_i \psi_i (t, f) \quad , \qquad (2.24)$$

where the case in Fig. 2.1(a) is being treated. In general, the coefficients a_i may be complex. Each of the eigenfunctions $\psi_i(t, f)$ will represent a noise mode and the following orthonormality conditions will obtain

$$\int_{-\infty}^{\infty} \int_{-\infty}^{\infty} \psi_i^* (t, f) \psi_j(t, f) \, dt \, df = \delta_{ij} \quad , \qquad (2.25)$$

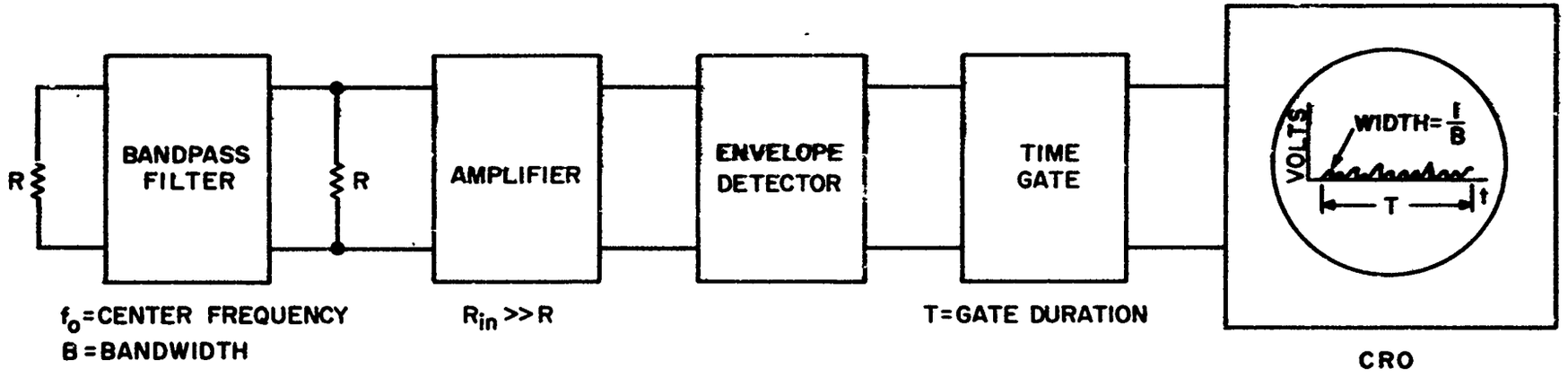

SYSTEM IS IN THERMAL EQUILIBRIUM AT ABSOLUTE TEMPERATURE $\mathcal{T}$

Fig. 2.2 Block Diagram for Observing Bandpass-Limited Noise Consisting of TB Modes

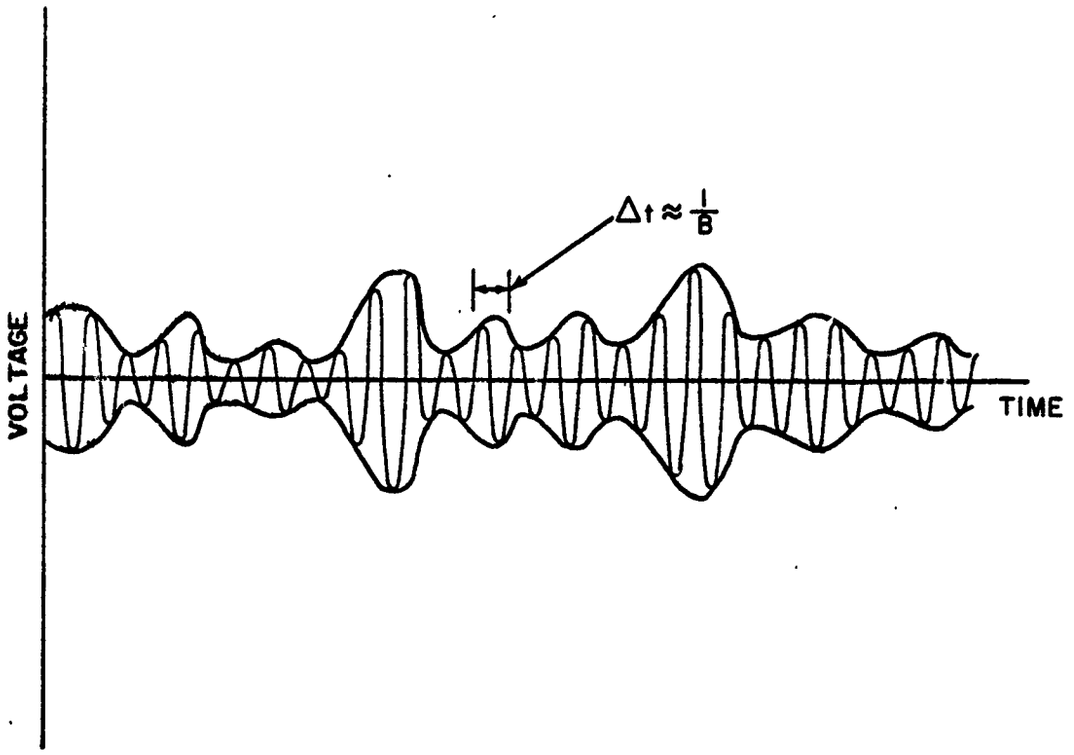

Fig. 2.3 Bandpass-Limited White Gaussian Noise Prior to Envelope Detection

where δ_{ij} is the Kronecker delta function. Since each noise mode is constrained to occupy an area of one logon in the time-frequency plane, the Heisenberg uncertainty (or indeterminacy) principle applies. There is a Fourier-transform constraint between the time and frequency axes for each mode. To illustrate this, we may consider the white noise to be composed of impulses (as is ordinarily done) as it enters the filter of bandwidth B cps. The output of the filter therefore consists of a multitude of impulse responses, many of which are too close together to be resolvable due to the finite filter bandwidth. A resolvable impulse response of the filter, however, and the filter's frequency response function (of width B in this case) are Fourier transform pairs, and together they encompass one noise mode.

Letting the center frequency of the filter be f_o and choosing equally spaced central time instants t_i for each mode, as shown in Fig. 2.1(a), with $i = 1, 2, \ldots, TB$, then the Fourier constraint may be applied as

$$\psi_i^*(t_i, f) = \int_{-\infty}^{\infty} \psi_i(t, f_o)\, e^{-j2\pi ft}\, dt \quad , \qquad (2.26a)$$

$$\psi_i(t, f_o) = \int_{-\infty}^{\infty} \psi_i^*(t_i, f)\, e^{j2\pi ft}\, df \quad , \qquad (2.26b)$$

If we consider the energy of the process to be

$$E_S = \int_{-\infty}^{\infty}\int_{-\infty}^{\infty} \psi^*(t, f)\, \psi(t, f)\, dt\, df = \sum_{i=1}^{TB} |a_i|^2 \quad , \qquad (2.27)$$

then

$$E_i = |a_i|^2 \qquad (2.28)$$

may be interpreted as the energy of the ith mode having a probability density function given by the directly-normalized Boltzmann factor and having an average value of $\bar{E}_i = k\mathcal{J}$ for all i. The absolute values $|a_i|$ are therefore Rayleigh-distributed.

We may construct an example of consistent functions satisfying the stated conditions from the situation of Fig. 2.1(a). Let

$$\psi_i(t, f) = \psi_i(t, f_o)\, \psi_i(t_i, f) \quad , \qquad (2.29)$$

which is a product of two functions. For a rectangular passband, suppose

$$\psi_i(t_i, f) = K\, \mathrm{rect}\left(\frac{f - f_o}{B}\right) e^{-j2\pi (f - f_o)\tau_i} \quad , \quad i = 1, 2, \ldots, TB \quad , \qquad (2.30)$$

where Woodward's notation[17] has been employed, namely,

$$\text{rect}(x) \triangleq 1 \quad , \quad |x| < \frac{1}{2} \quad , \qquad (2.31)$$

$$\triangleq 0 \quad , \quad |x| > \frac{1}{2} \quad ,$$

and K = a constant.

Using the constraint of Eq. (2.26b),

$$\psi_i(t, f_o) = \int_{-\infty}^{\infty} \psi_i^*(t_i, f)\ e^{j2\pi ft}\, df$$

$$= KB\ \text{sinc}\,(B(t+\tau_i))e^{j2\pi f_o t} \quad , \qquad (2.32)$$

where[17]

$$\text{sinc}(y) \triangleq \frac{\sin \pi y}{\pi y} \quad . \qquad (2.33)$$

Then Eq. (2.29) gives

$$\psi_i(t, f) = K^2 B\ \text{rect}\left(\frac{f-f_o}{B}\right)\text{sinc}\,(B(t+\tau_i))\ e^{j2\pi\left[f_o t - (f-f_o)\tau_i\right]} \quad . \qquad (2.34)$$

In order to satisfy the orthonormality conditions of Eq. (2.25), we require

$$\int_{-\infty}^{\infty}\int_{-\infty}^{\infty} \psi_i^*(t, f)\,\psi_j(t, f)\,dt\,df = \delta_{ij}$$

$$= \int_{-\infty}^{\infty}\int_{-\infty}^{\infty} K^2 B^2 \text{rect}^2\left(\frac{f-f_o}{B}\right)\text{sinc}(B(t+\tau_i))\,\text{sinc}(B(t+\tau_j))\ e^{j2\pi(f-f_o)(\tau_i-\tau_j)} \qquad (2.35)$$

$$= \int_{-\infty}^{\infty} K^4 B\,\text{rect}^2\left(\frac{f-f_o}{B}\right) e^{j2\pi(f-f_o)(\tau_i-\tau_j)}\,df \cdot \int_{-\infty}^{\infty} B\,\text{sinc}(B(t+\tau_i))\,\text{sinc}(B(t+\tau_j))\,dt.$$

This is satisfied by the conditions

$$K = \sqrt{\frac{1}{B}} \quad , \quad \tau_i = \frac{i}{B} \quad , \quad \tau_j = \frac{j}{B} \qquad (2.36)$$

since[35]

$$\int_{-\infty}^{\infty} B\ \text{sinc}\left(B\left(t+\frac{i}{B}\right)\right)\ \text{sinc}\left(B\left(t+\frac{j}{B}\right)\right)dt = \delta_{ij} \quad . \qquad (2.37)$$

Finally, the characteristic functions satisfying all specified requirements is, from Eqs. (2.34) and (2.36),

$$\psi_i(t, f) = \text{rect}\left(\frac{f-f_o}{B}\right)\text{sinc}\left(B\left(t+\frac{i}{B}\right)\right)\ e^{j2\pi\left[f_o t - \frac{(f-f_o)i}{B}\right]}; \quad i = 1, 2, \ldots, TB \quad . \qquad (2.38)$$

3. RADAR SIGNAL PROCESSING[36, 37]

3.1 Pulsed-CW Radar

3.1.1 Measurement of Range Only

In order to develop some fundamental relations involving radar information, we shall first consider a simple pulsed-CW radar for the measurement of range only. It is assumed that the target is known to be approximately stationary in space. A block diagram of such a system is shown in Fig. 3.1, where the optimum i-f bandwidth B is used. I.e.,

$$B = \frac{1}{P} \quad \text{cps} \quad , \qquad (3.1)$$

for a pulse width of P seconds.

On the CRO display, we observe noise modes having a time-width of P seconds, due to the i-f bandwidth restriction of B cps, and a signal echo response also having a width in the order of P seconds. (Ideally, for a rectangular transmitted signal envelope and a rectangular i-f filter pass band, the signal response at the output of the i-f filter is triangular with a base width of 2P seconds.) The property that the signal response has the same duration as a noise mode is characteristic of all matched-filter radars and it will be shown later that this condition is optimum in terms of the radar's efficiency in acquiring information.

Consideration of the radar output, as displayed on the CRO in Fig. 3.1, indicates the need for a threshold test to establish a measurement "reliability". Clearly we cannot accept all identifiable peaks as signal responses since most of them are due to noise. However, if a sufficiently high amplitude threshold level R_T is set, as illustrated in Fig. 3.1, then reasonable assurance can be obtained that a threshold crossing is indeed due to the presence of signal and not due to noise alone. Higher threshold settings imply greater measurement reliability but decreased sensitivity to low-level signals.

A reasonable way to evaluate the efficacy of the threshold level setting is to compute an overall false alarm probability given by

$$P_{FA} = 1 - (1 - P'_{FA})^{TB} \quad , \qquad (3.2)$$

where

TB = total number of independent opportunities for a threshold-crossing due to noise alone, within the range-delay surveillance window T

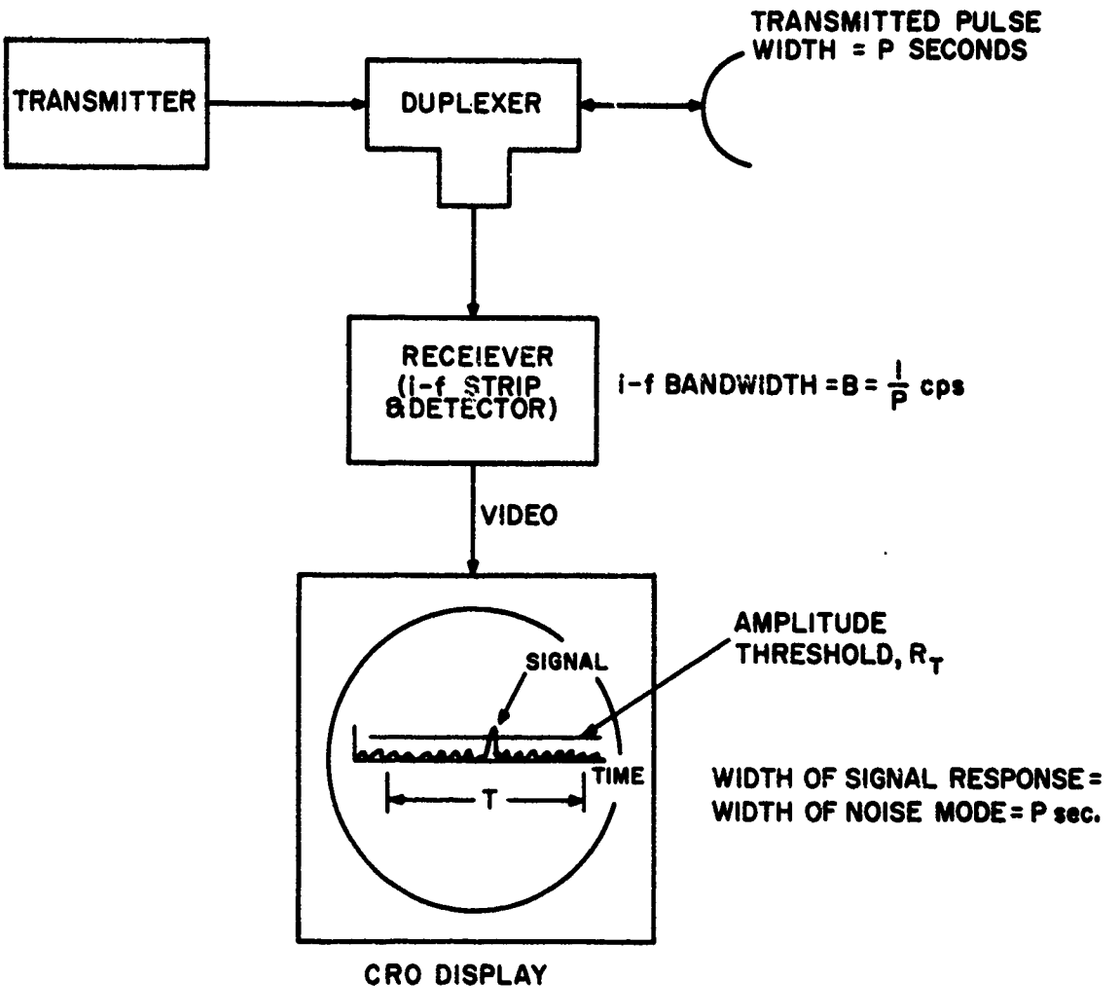

Fig. 3.1 Block Diagram of Basic Pulsed-CW Radar for the Measurement of Range Only

P'_{FA} = probability that a single noise mode will cross the amplitude threshold

P_{FA} = probability that one or more threshold crossings will occur due to noise alone.

For

$$TB\,P'_{FA} << 1 \quad , \tag{3.3}$$

as is usually the case, we have

$$P_{FA} \approx TB\,P'_{FA} \tag{3.4}$$

by use of a truncated binomial expansion. Since the measurement reliability increases with decreasing values of P_{FA}, it is reasonable to define a reliability factor[25] r, given by

$$P_{FA} = \frac{1}{r} \quad . \tag{3.5}$$

Now, from Eq. (2.16),

$$P'_{FA} = \int_{E_T}^{\infty} \frac{1}{k\mathcal{J}} e^{-\frac{E}{k\mathcal{J}}}\, dE = e^{-\frac{E_T}{k\mathcal{J}}} \quad , \tag{3.6}$$

where

E_T = modal energy threshold corresponding to amplitude threshold R_T.

Substituting Eqs. (3.5) and (3.6) into Eq. (3.4) and taking the natural logarithm of both sides of the resulting equation, it is found that

$$\frac{E_T}{k\mathcal{J}} = \ln r\,TB \quad . \tag{3.7}$$

Certainly a measurement with $r < 2$ would be sufficiently unreliable to be meaningless, since this would imply an overall false alarm probability of greater than 50%. Thus, for any meaningful physical measurement, we must have

$$\frac{E_T}{k\mathcal{J}} > \ln TB \quad . \tag{3.8}$$

Now consider the amount of information obtained by the measurement. Prior to any observation, the target range delay was presumed to be somewhere within the a priori surveillance window of T seconds. After the measurement, the signal may be localized to a range-delay interval of $1/B = P$ seconds, assuming that the threshold has been crossed. From the standard approach of information theory, the uncertainty

has been reduced by a factor of $T/P = TB$ so the acquired information is

$$I^{(2)} = \log_2 TB \quad \text{bits} \quad , \qquad (3.9)$$

where the superscript (2) indicates that a logarithmic base of 2 has been employed. The information may also be expressed in other units. For example, it may be said that the information obtained is

$$I^{(e)} = \ln TB \quad \text{natural units (called nits or nats)} \qquad (3.10)$$

or

$$I_t = k \ln TB \quad \text{thermodynamic units} \quad , \qquad (3.11)$$

where k is Boltzmann's constant. The latter form is derived by analogy with the result of statistical mechanics that thermodynamic entropy is equal to k times the natural logarithm of the number of system "complexions" in the most probable state of the system.

It is now possible to reach the conclusion that, for any meaningful measurement of range delay in the problem posed, we have

$$\frac{E_T}{k\mathcal{J}} > I^{(e)} \quad , \qquad (3.12)$$

or

$$\frac{E_T}{\mathcal{J}} > I_t \quad . \qquad (3.13)$$

That is, the signal-to-noise energy ratio $E/k\mathcal{J}$ always exceeds the information obtained, where the latter is expressed in natural units, or equivalently, the input entropy quantity $E/\mathcal{J}$ always exceeds the information expressed in thermodynamic units. In any measurement, we would like to maximize I_t as much as possible, but it can be no greater than $E_T/\mathcal{J}$. The inequalities of Eqs. (3.12) and (3.13) establish an equivalence between the SNER employed in radar terminology with the concept of physical entropy. They also specify a lower bound on the input SNER required to make a measurement which can provide a specific amount of information $I^{(e)}$. However, they do not explicitly specify what information advantage or disadvantage is incurred if a high reliability factor r is employed, or if the input SNER exceeds the threshold value by a significant amount. These questions will be more clearly formulated in the later discussions.

3.1.2 Measurement of Doppler Only

We shall here consider a pulsed-CW radar for the measurement of Doppler shift only. The basic block diagram for the system is shown in Fig. 3.2. The spectrum analyzer may be thought of as a bank of contiguous filters of bandwidth $B = 1/P$ cps, or a Coherent Memory Filter.[30,38] The surveillance window is now in the Doppler domain and is designated as W cps. The number of independent noise

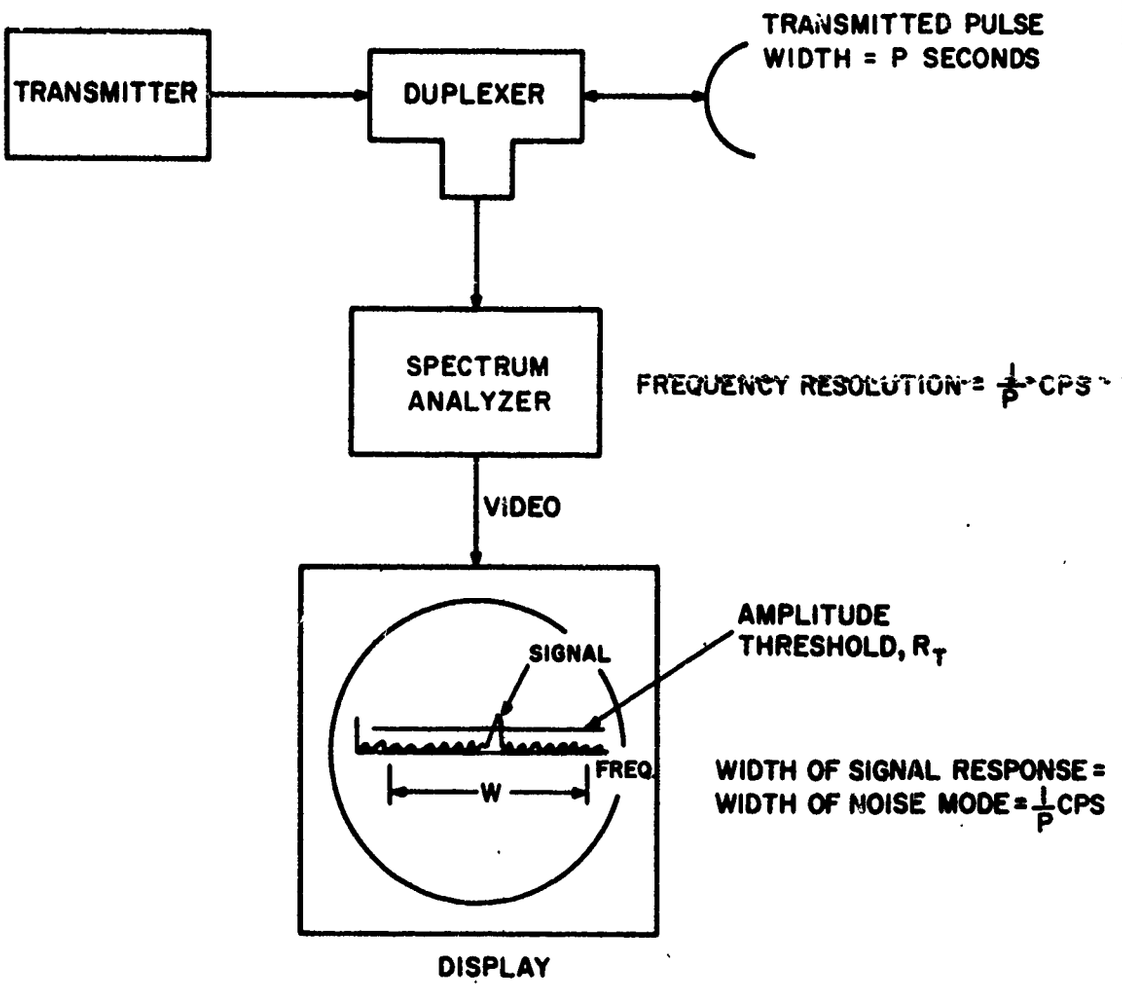

Fig. 3.2 Block Diagram of Basic Pulsed-CW Radar for the Measurement of Doppler Only

modes within the surveillance window is PW and therefore the threshold energy must be such that

$$\frac{E_T}{k\bar{J}} > \ln PW \qquad (3.14)$$

in order for the reliability factor r to be at least a value of 2. Since the information is

$$I^{(e)} = \ln PW \quad , \qquad (3.15)$$

we again have the result stated in Eq. (3.12).

3.2 Radars with General Transmitted Waveforms

3.2.1 Chirp Radars for the Measurement of Range Only[39,40]

We consider first a special waveform of major importance, namely, linear-FM modulation, as illustrated in Fig. 3.3(a) by an instantaneous frequency-vs-time plot along side of the signal spectrum. As with the pulsed-CW range-only measurement, the target is assumed stationary in this example. The matched filter has a frequency response function which is the complex conjugate of the signal spectrum shown in Fig. 3.3(a). Therefore, the output noise modes have a duration of 1/B seconds, which is the reciprocal of the matched-filter bandwidth. The signal is also compressed to a time width of 1/B seconds. The number of independent noise modes in the surveillance window is TB and therefore the threshold energy must be such that

$$\frac{E_T}{k\bar{J}} > \ln TB \quad , \qquad (3.16)$$

and Eq. (3.12) again holds. (The block diagram is shown in Fig. 3.3(b).

3.2.2. Simultaneous Measurement of Range and Doppler Shift

3.3.2.1 General Two-Dimensional Compression (Maximum-Likelihood Receiver)

3.2.2.1.1 Linear Detection

In this more general case, the theoretical radar model is as shown in Fig. 3.4. Following the method of inverse probability[17] for the joint estimation of range delay and Doppler shift (single target assumed), we wish to determine the values of τ and ϕ which maximize the a posteriori (conditional) probability $p(\tau, \phi/\zeta)$. By the Bayes equality, we have *

$$p(\tau, \phi/\zeta) = \frac{p(\tau, \phi)}{p(\zeta)} \; p(\zeta/\tau, \phi) \quad , \qquad (3.17)$$

---

* Complex signal notation is used, as reviewed in Appendix A.

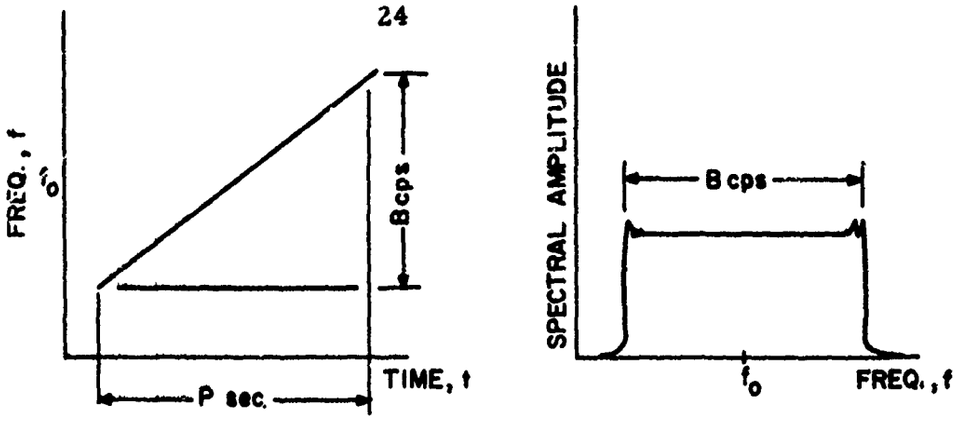

(a) Instantaneous Frequency-Vs.-Time Plot and Signal Spectrum

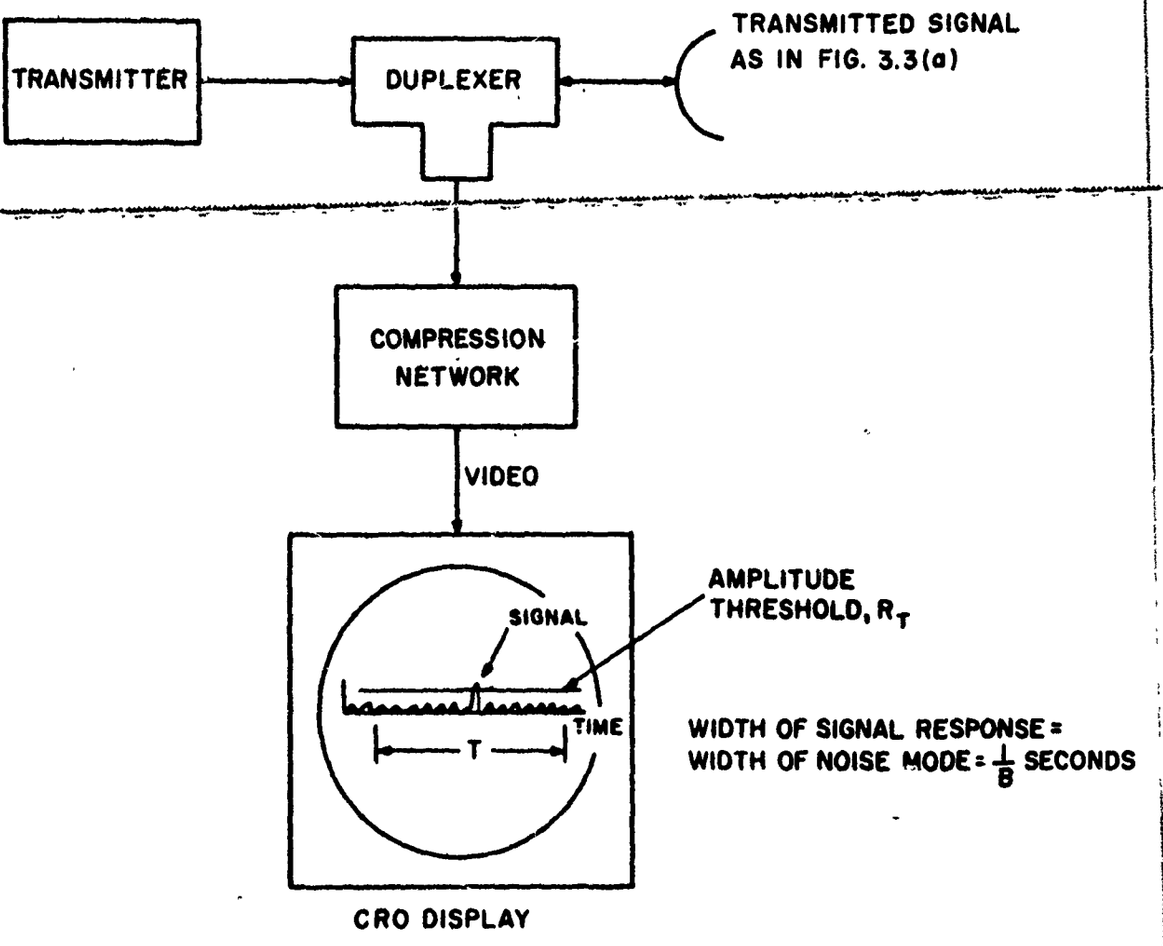

(b) Basic Block Diagram

Fig. 3.3 Chirp-Type Radar for the Measurement of Range Only

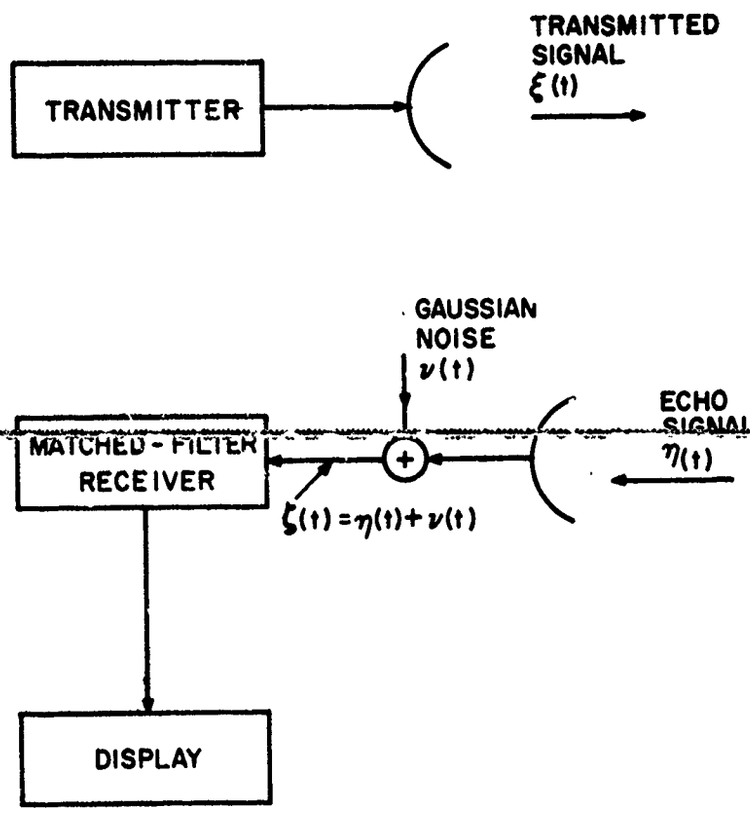

Fig. 3.4 Analytical Radar Model for the Measurement of Range and Doppler Using an Arbitrary Waveform

where

$p(\tau,\phi/\zeta)$ = conditional a posteriori density function for τ and ϕ, given the received noisy signal $\zeta(t)$ = inverse probability

$p(\tau,\phi)$ = a priori probability (before the measurement)

$p(\zeta/\tau,\phi)$ = likelihood function

$p(\zeta)$ = a normalizing function such that $\int_{-\infty}^{\infty} p(\tau,\phi)/\zeta)\, d\tau\, d\phi = 1.$

If $p(\tau,\phi)$ is uniform, it is seen that the method of inverse probability leads to a maximum likelihood estimate since maximization of $p(\tau,\phi/\zeta)$ is then equivalent to maximization of $p(\zeta/\tau,\phi)$. Following this customary assumption of a uniform a priori distribution, it follows that

$$p(\zeta/\tau,\phi) = p(\nu(t) = \zeta(t) - \eta_{\tau,\phi}(t)) \quad , \tag{3.18}$$

where

$\zeta(t)$ = a given fixed waveform observed

$\nu(t)$ = random noise process, bandlimited to some "front-end" bandwidth of W' cps

$$\eta_{\tau,\phi}(t) = A\xi(t-\tau)\, e^{j2\pi\phi t} = \text{echo signal voltage} \tag{3.19}$$

in which A is a real constant amplitude factor, and τ and ϕ are both assumed constant*.

If the receiver front-end is gated open for a time duration T', then[18]

---

* This is a powerful, though inconsistent, classical radar assumption that has led to many useful results. However, in the case of very large time-bandwidth products, the assumption is inappropriate.[41] In that case, a more exact representation is

$$\eta(t) = A\,\xi(t-\tau(t)) = A\,\tilde{\xi}(t-\tau(t))e^{j2\pi f_o(t-\tau(t))}$$

where $\tilde{\xi}(t)$ is the complex modulation and f_o is the carrier frequency. If, for example

$$\tau(t) = \tau_o + \dot{\tau}\, t,$$

then

$$\eta(t) = A\,\tilde{\xi}(t(1-\dot{\tau}) - \tau_o)\, e^{j2\pi f_o t}\, e^{-j2\pi f_o \dot{\tau} t}\, e^{-j2\pi f_o \tau_o} \quad ,$$

in which the Doppler shift may be recognized as $\dot{\phi} = -f_o\dot{\tau} = -2f_o\frac{\dot{r}}{c}$ where $\dot{r}$ is radial velocity and c is the speed of light. Also, for the very high linear velocities characteristic of space probes, satellites and astronomical bodies, relativistic effects may not be negligible.[42]

$$p(\zeta/\tau,\phi) = \frac{1}{(2\pi k\mathcal{J}W')^{T'W'}}\, e^{-\frac{1}{2k\mathcal{J}}\int_{-\infty}^{\infty}|\nu(t)|^2\,dt}$$

$$\alpha\, e^{\frac{1}{k\mathcal{J}}\,\mathrm{Re}\int_{-\infty}^{\infty}\zeta(t)\,\eta^*_{\tau,\phi}(t)\,dt} \quad , \qquad (3.20)$$

where the latter result of proportionality is derived using the identity,

$$|\nu(t)|^2 = |\zeta(t)-\eta_{\tau,\phi}(t)|^2 = |\zeta(t)|^2 - 2\,\mathrm{Re}\,\zeta(t)\eta^*_{\tau,\phi}(t) + |\eta_{\tau,\phi}(t)|^2 \quad . \qquad (3.21)$$

Defining

$$\Gamma'(\tau,\phi) = \int_{-\infty}^{\infty}\zeta(t)\eta^*_{\tau,\phi}(t)\,dt = A\int_{-\infty}^{\infty}\zeta(t)\,\xi^*(t-\tau)\,e^{-j2\pi\phi t}\,dt$$

$$= A\left[\int_{-\infty}^{\infty}\tilde{\zeta}(t)\tilde{\xi}^*(t-\tau)\,e^{-j2\pi\phi t}\,dt\right]e^{j2\pi f_o\tau} \quad , \qquad (3.22)$$

where $\tilde{\zeta}(t)$ and $\tilde{\xi}(t)$ are the complex modulations, then

$$p(\zeta/\tau,\phi)\,\alpha\, e^{\frac{1}{k\mathcal{J}}|\Gamma'(\tau,\phi)|\cos(2\pi f_o\tau + \arg\Gamma'(\tau,\phi))} \quad . \qquad (3.23)$$

The exponent reveals high-frequency fluctuations with respect to the τ variable. These are r-f phase effects which may be averaged out over one r-f cycle by defining an area-preserving smoothed version of $p(\zeta/\tau,\phi)$ given by

$$P_\zeta(\tau,\phi) = \int_{\tau-\frac{1}{2f_o}}^{\tau+\frac{1}{2f_o}} p(\zeta/\tau,\phi)\,d\tau$$

$$\alpha\int_{\tau-\frac{1}{2f_o}}^{\tau+\frac{1}{2f_o}} e^{\frac{1}{k\mathcal{J}}|\Gamma'(\tau,\phi)|\cos(2\pi f_o\tau+\arg\Gamma'(\tau,\phi))}\,d\tau$$

$$\alpha\, I_o\left(\frac{|\Gamma'(\tau,\phi)|}{k\mathcal{J}}\right) \quad , \qquad (3.24)$$

where $I_o(x)$ is the modified Bessel function of first kind and zero order.

Since the function $I_o(x)$ is a monotonic function of x, the most probable estimates of τ and ϕ may be obtained by determining those values which maximize

$$|\Gamma'(\tau,\phi)| = A\left| \int_{-\infty}^{\infty} \zeta(t)\, \xi^{*}(t-\tau)\, e^{-j2\pi\phi t}\, dt \right| \qquad (3.25a)$$

$$= A\left| \int_{-\infty}^{\infty} \hat{\zeta}(f)\hat{\xi}^{*}(f-\phi)\, e^{j2\pi\tau f}\, df \right| , \qquad (3.25b)$$

where $\hat{\zeta}(f)$ and $\hat{\xi}(f)$ are the Fourier transforms of $\zeta(t)$ and $\xi(f)$, respectively. This complex correlation process constitutes a linear operation on the received noisy echo $\zeta(t)$, followed by a linear envelope detection. The surface $|\Gamma'(\tau,\phi)|$ will be called the correlation surface and its typical appearance is as illustrated in Fig. 3.5. The maximum-likelihood estimates are $\hat{\tau}$ and $\hat{\phi}$. The range and Doppler resolutions are the widths of the correlation surface in the τ and ϕ directions, which are in the order of $1/B$ seconds and $1/P$ cps, respectively, where B cps is the signal bandwidth and P seconds is the signal duration. These resolutions are readily deduced from Eqs. (3.25a) and (3.25b). That is, Eq. (3.25a) indicates that the correlation operation on $\zeta(t)$ consists of a multiplication by a function $\xi^{*}(t-\tau)$, which is time-truncated to P seconds, followed by a Fourier transform to the ϕ domain. The surface width in the ϕ domain is therefore approximately $1/P$ cps. In the other hand, Eq. (3.25b) shows that the correlation operation can be viewed as a multiplication in the frequency domain followed by an inverse Fourier transform to the τ domain. The frequency width of $\hat{\xi}(f)$ which is also the frequency width of the matched filter) is equal to B cps, and therefore the width of the correlation surface in the τ domain is in the order of $1/B$ seconds.

The two-dimensional matched-filter process is summarized with reference to Fig. 3.6. It is assumed that the "front end" receiver characteristic passes a wide band of frequencies W' for a time duration T', the latter being taken up to a maximum of the pulse repetition period (or unambiguous range interval). The echo signal's energy arrives in the rectangle of area PB. The two-dimensional matched filter characteristic is shown to the right and it basically constitutes a time-frequency gate which overlaps the signal's energy area. The effect of the matched filter is to "involute" the signal's input energy area PB by compressing it into an essentially interior rectangle of area $1/PB$.* If $PB = 1$, there is no compression. The rectangle of area TW represents a surveillance area within which we look for targets. This surveillance area should be no larger than necessary because the number of independent noise modes

---

* In the special ambiguous case of high interdependence between τ and ϕ information, as with a linear-FM modulation, the compressed area is elongated as shown by the dotted ellipse.

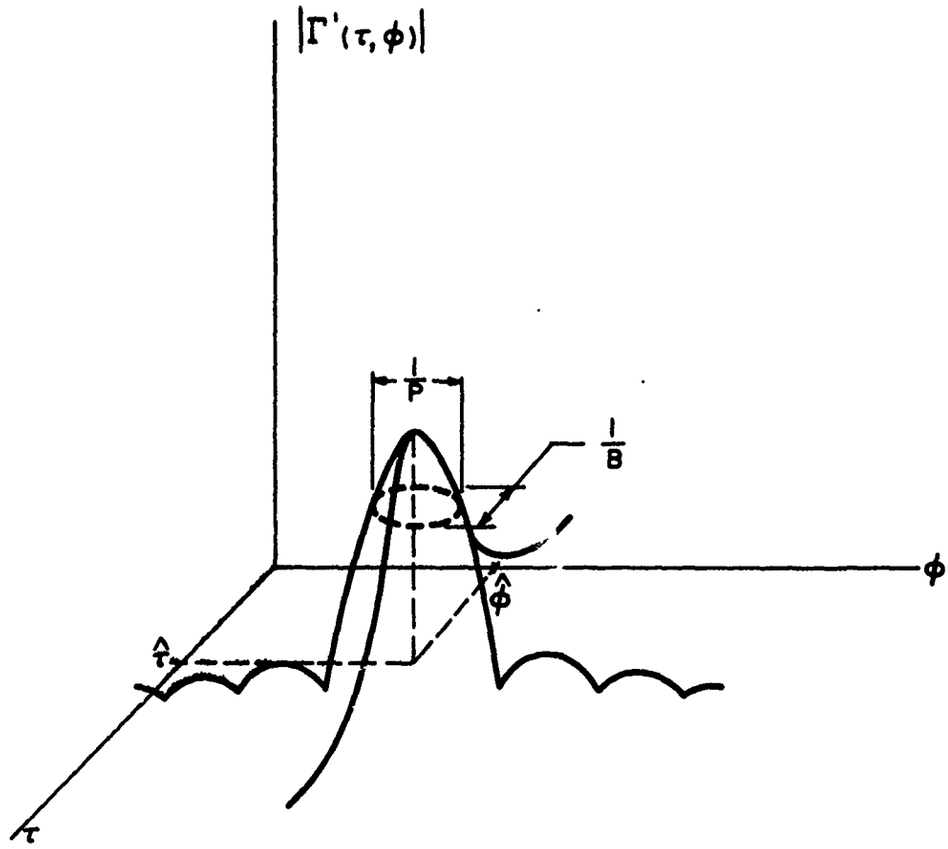

Fig. 3.5 Typical Correlation Surface

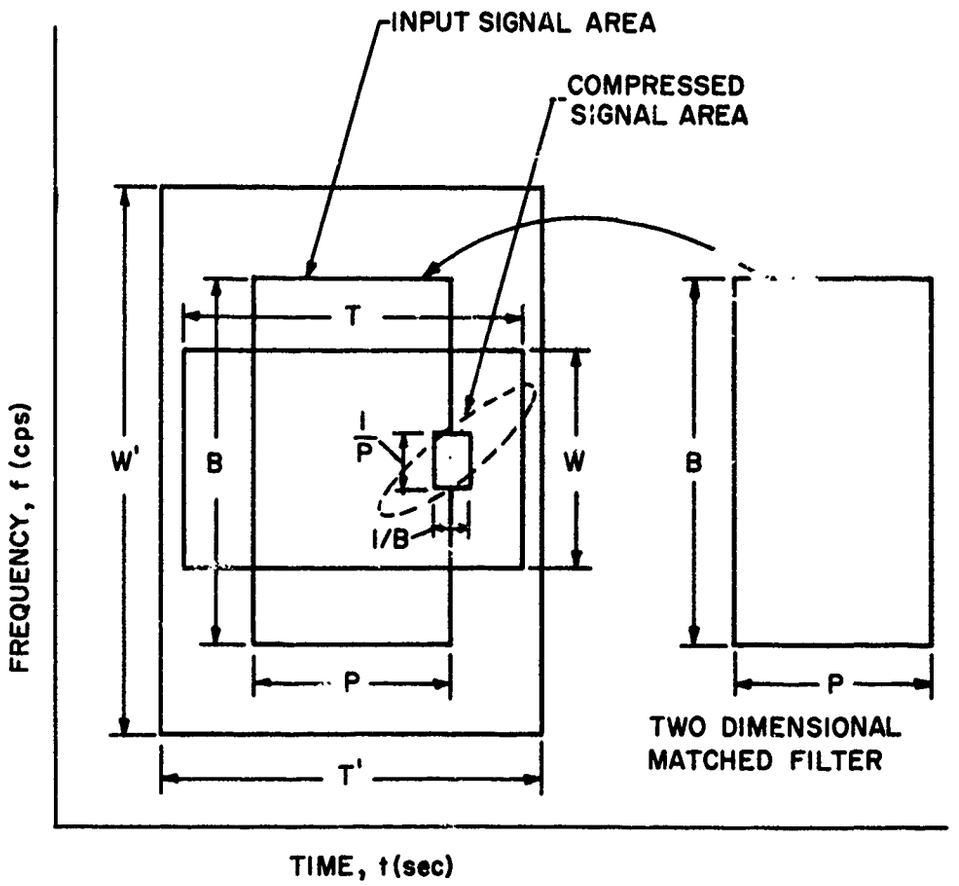

Fig. 3.6 Representation of the Two-Dimensional Matched-Filter Operation as an Involution Process

increases with the surveillance area and compels a higher amplitude-threshold setting for a given overall false-alarm probability, which implies, of course, a lower detection probability for a given signal-to-noise ratio.

3.2.2.1.2 Nonlinear Detection

The two-dimensional compression can be increased by using a nonlinear envelope detector having the characteristic of $I_o(x)$, the modified Bessel function. In particular, we generate a voltage

$$\mu(\tau,\phi) = I_o\left(\frac{|\Gamma'(\tau,\phi)}{kT}\right) , \qquad (3.26)$$

which is proportional to the exact smoothed a posteriori probability density function, as seen from Eq. (3.24). It is known that the standard deviation of the a posteriori density function is[17,18]

$$\sigma_\tau = \frac{1}{\sqrt{\overline{f^2}\,\rho}} \qquad (3.27)$$

in the τ domain and

$$\sigma_\phi = \frac{1}{\sqrt{\overline{t^2}\,\rho}} \qquad (3.28)$$

in the ϕ domain, where

$$\rho = \frac{2E}{kT} = \frac{\text{2 x received signal energy}}{\text{noise power spectral density}} \qquad (3.29)$$

$$\overline{f^2} = \frac{(2\pi)^2\int_{-\infty}^{\infty} f^2|\hat{\xi}(f)|^2\,df}{\int_{-\infty}^{\infty}|\hat{\xi}(f)|^2\,df} = \{\text{normalized signal bandwidth}\}^2 \qquad (3.30)$$

$$\overline{t^2} = \frac{(2\pi)^2\int_{-\infty}^{\infty} t^2|\hat{\xi}(t)|^2\,dt}{\int_{-\infty}^{\infty}|\hat{\xi}(t)|^2 dt} = (\text{normalized signal duration})^2 \; . \qquad (3.31)$$

The standard deviations expressed by Eqs. (3.27) and (3.28) may therefore be immediately used as an approximate measure of the resolution capabilities inherent in the Bessel-function detector of Eq. (3.26). In terms of a practical example, and a more standard resolution definition, it is observed that the 3-db width of a Gaussian distribution (from which σ_τ and σ_ϕ are derived under high SNER conditions) is about 1.6

times the standard deviation. Thus, the 3-db resolutions become

$$\Delta\tau \approx \frac{1.6}{\sqrt{f^2\rho}} \tag{3.32}$$

$$\Delta\phi \approx \frac{1.6}{\sqrt{t^2\rho}} \tag{3.33}$$

in general, for $\rho >> 1$. Furthermore, if the signal is truncated in a rectangular (chirp) characteristic, say

$$|\tilde{\xi}(t)| = \text{rect}\left(\frac{t}{P}\right) \quad \text{and} \quad |\hat{\tilde{\xi}}(f)| = \text{rect}\left(\frac{f-f_o}{B}\right), \tag{3.34}$$

then

$$\sqrt{t^2} = \frac{\pi}{\sqrt{3}}\, P = 1.81\, P \text{ and } \sqrt{f^2} = \frac{\pi}{\sqrt{3}}\, B = 1.81\, B, \tag{3.35}$$

and the resolutions are

$$\Delta\tau \approx \frac{0.9}{B\sqrt{\rho}} \tag{3.36}$$

$$\Delta\phi \approx \frac{0.9}{P\sqrt{\rho}}. \tag{3.37}$$

Eq. (3.26) may be written in a more convenient form as

$$\mu(\tau,\phi) = I_o\left(\rho\,|\Gamma(\tau,\phi)|\right) \tag{3.38}$$

where

$$|\Gamma(\tau,\phi)| = \frac{1}{2E}\,|\Gamma'(\tau,\phi)|. \tag{3.39}$$

The peak value of $|\Gamma(\tau,\phi)|$ is approximately unity under conditions of high SNER since then (neglecting noise)

$$\xi(t) = A_o\,\xi(t-\tau_o)\,e^{j2\pi\phi_o t}, \tag{3.40}$$

where

τ_o = true value of range delay

ϕ_o = true value of Doppler shift

A_o = true amplitude factor,

and therefore, from Eq. (3.25a),

$$|\Gamma'(\tau_o, \phi_o)| = |\Gamma'(\tau, \phi)|_{max} = A_o^2 \int_{-\infty}^{\infty} |\zeta(t - \tau_o)|^2 \, dt = 2E \quad . \quad (3.41)$$

Using Eq. (3.38), the Bessel function envelope detector is seen to operate as shown[43] in Fig. 3.7. The improvement in resolution resulting from such a detector characteristic is illustrated in Section 6.2.1. It may be noted that the Bessel-function detector does not alter the detection probability, although low-level response regions (such as sidelobes) are suppressed for the low-noise case. The detection and false-alarm probabilities may be established in the linear-envelope domain and these probabilities are merely transformed, along with the amplitude-detection threshold, by the nonlinear detection characteristic.

3.2.2.2 Doppler-Channel Implementation

Prior to envelope detection, it is necessary to implement the correlation surface $|\Gamma'(\tau, \phi)|$, which can be accomplished with linear systems. Two alternative approaches to this implementation are to use:[44,45] (a) Doppler channels, or (b) range channels. In this section, we shall deal with the Doppler-channel viewpoint in which ϕ in Eq. (3.25a) is quantized as ϕ_i. Now,

$$\begin{aligned} \text{Re}\, \Gamma'(\tau, \phi_i) &= A \int_{-\infty}^{\infty} \text{Re}\left[\zeta(t) \, \xi^*(t - \tau) \, e^{-j2\pi \phi_i t} \right] dt \\ &= A \int_{-\infty}^{\infty} \text{Re}\left[\zeta(t) \, e^{-j2\pi \phi_i t}\right] \text{Re}\, \xi(t - \tau) \, dt \quad . \end{aligned} \quad (3.42)$$

The latter form is readily seen to be equal to the previous form by expanding the product of the real (cosine) parts in terms of the cosine of the difference-arguments and the cosine of the sum-arguments. The integration of the term involving the cosine of the sum-arguments is zero since that term contains fluctuations at r-f frequencies.

The latter form in Eq. (3.42) can be implemented by frequency-shifting the received signal $\zeta(t)$ downward by ϕ_i cps (or passing the received signal through a filter shifted upward by ϕ_i cps from the zero-Doppler filter), and then applying the signal to a matched filter with impulse response

$$h(t) = \text{Re}\, \xi(P - t) \quad , \quad (3.43)$$

where P is the signal duration. By the convolution integral, the filter output is

$$\begin{aligned} y(t, \phi_i) &= \int_{-\infty}^{\infty} x(t') \, h(t - t') \, dt' = \int_{-\infty}^{\infty} \text{Re}\left[\zeta(t') e^{-j2\pi \phi_i t'} \right] \text{Re}\, \xi(P - t + t') \, dt' \\ &= \text{Re}\, \Gamma'(t - P, \phi_i) \quad . \end{aligned} \quad (3.44)$$

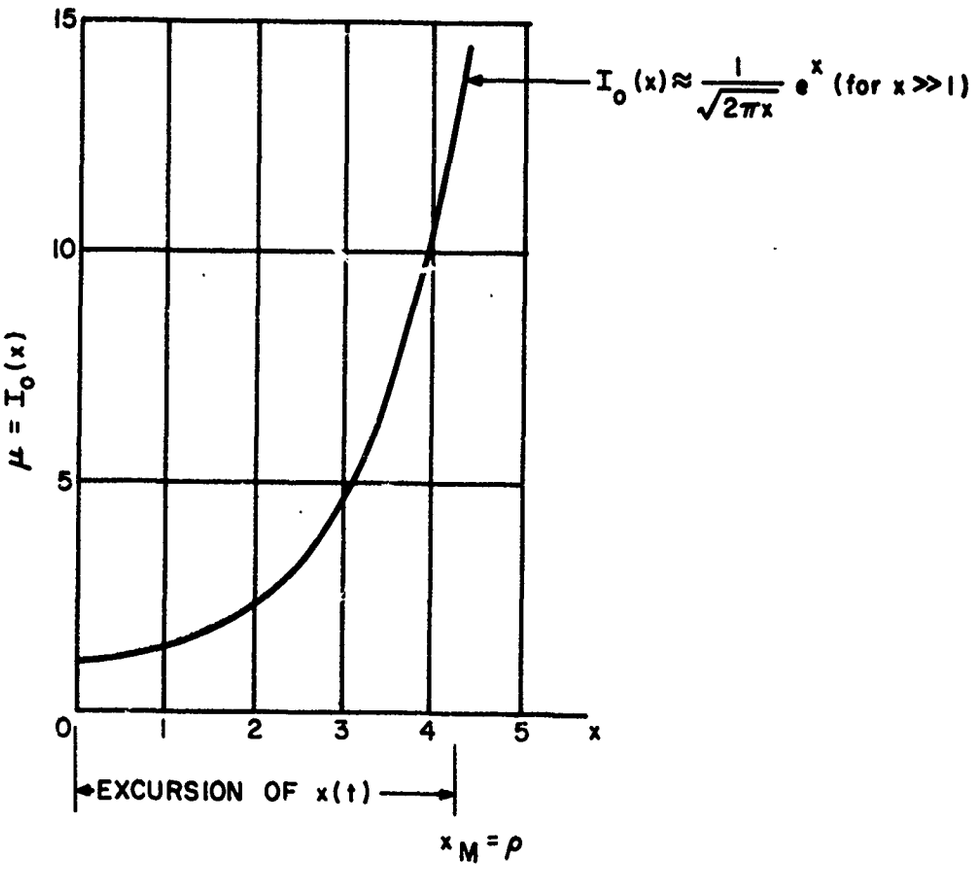

$$x = \rho \left| \Gamma(\tau, \phi) \right|$$

$0 \leq x \leq \rho$ APPROXIMATELY

Fig. 3.7 Operating Characteristic of Bessel-Function Envelope Detector

The real-time axis at the filter output is therefore the τ axis, and $|\Gamma'(\tau,\phi)|$ is the output signal envelope (see Appendix A).

Each value of ϕ_i represents a separate Doppler channel and the Doppler-channel output signal envelope traces out a cross section of the correlation surface at $\phi = \phi_i$. In order to obtain complete coverage within a surveillance window of area TW in the $\tau - \phi$ plane, a number of contiguous Doppler channels are required. They should be spaced by approximately $\Delta\phi = \frac{1}{P}$ cps, which is the linear Doppler resolution of the system. Division of the surveillance area into Doppler channels is depicted in Fig. 3.8(a).

At the output of each Doppler channel, the signal is compressed into the time-width of one noise mode, by reasoning similar to that employed in Section 3.2.1. Therefore, Eqs. (3.12) and (3.13) hold in each channel. The information in each channel is

$$I_\tau^{(e)} = \ln TB \quad , \qquad (3.45)$$

where

T = range-delay surveillance window
B = signal bandwidth,

and, in order to obtain this information, it is necessary that

$$\frac{E}{k\mathcal{T}} > I_\tau^{(e)} \quad . \qquad (3.46)$$

3.2.2.3 Range-Channel Implementation

In the range-channel viewpoint, range delay is quantized by producing the complex signal

$$\lambda(t,\tau_i) = A\,\zeta(t)\,\xi^*(t-\tau_i) \quad , \qquad (3.47)$$

the real part of which is the physical voltage. The signal $\lambda(t,\tau_i)$ can be generated by heterodyning the received signal $\zeta(t)$ by a delayed replica of the transmitted signal $\xi(t-\tau_i)$, and passing only the difference-frequency signal. Then a spectrum analysis of Re $\lambda(t,\tau_i)$ yields (see properties in Appendix A)

$$z(\tau_i,\phi) = \left|\mathcal{F}\left[\text{Re }\lambda(t,\tau_i)\right]\right| = \frac{1}{2}\left|\mathcal{F}\left[\lambda(t,\tau_i)\right]\right|$$

$$= \frac{1}{2}\left|\Gamma'(\tau_i,\phi)\right| \; ; \qquad \phi > 0 \quad , \qquad (3.48)$$

where $\mathcal{F}$ denotes the Fourier-transform operation and ϕ is the frequency argument in the transformed domain.

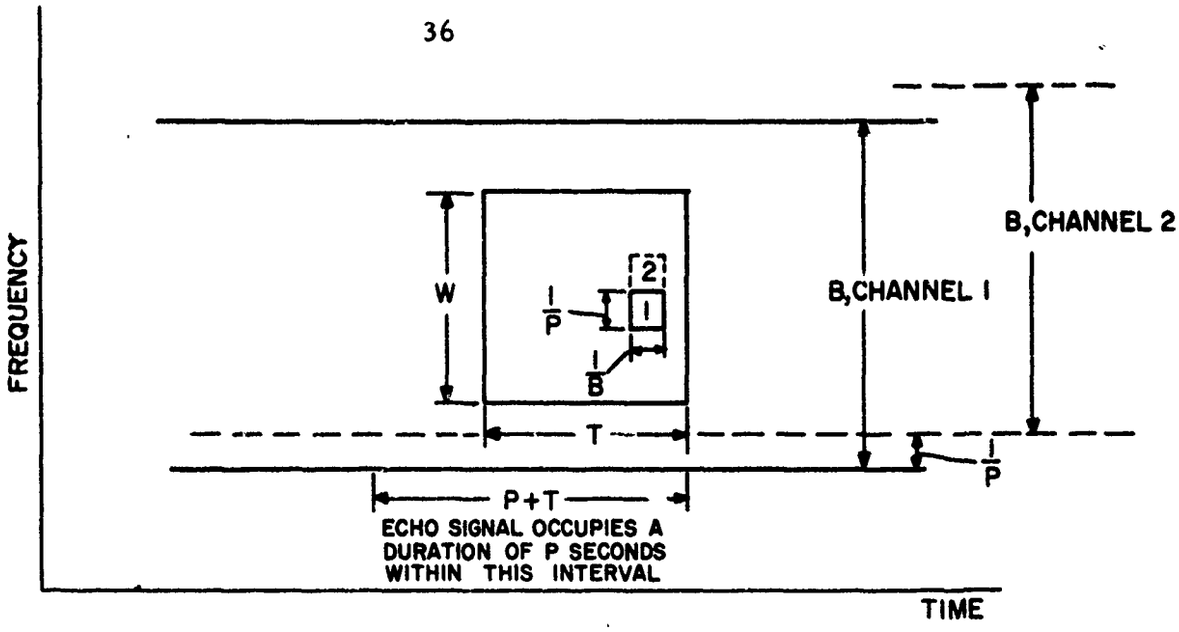

(a) Doppler-Channel Implementation

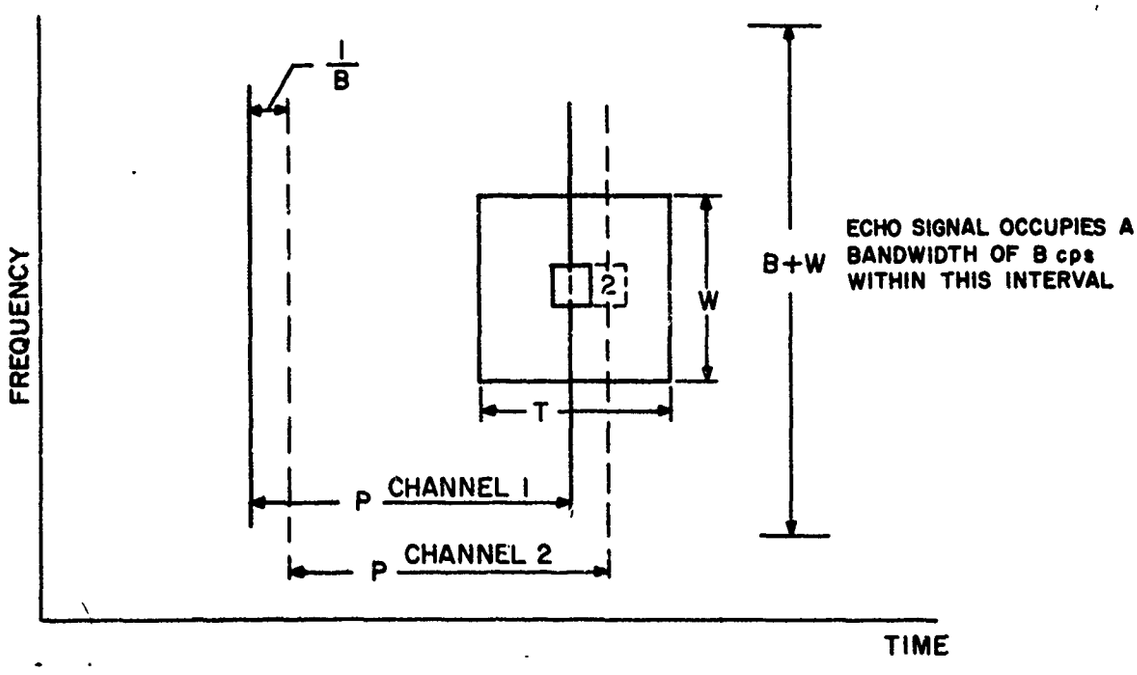

(b) Range-Channel Implementation

Fig. 3.8 Division of Surveillance Area into Doppler Channels or Range Channels

Each value of τ_i represents a separate range channel and the spectrum analysis at the range-channel output traces out a cross section of the correlation surface at $\tau = \tau_i$. In order to obtain complete coverage within a surveillance window of area TW in the $\tau - \phi$ plane, a number of contiguous range channels must be used. They should be separated by approximately $\Delta\tau = \frac{1}{B}$ seconds, which is the linear range-delay resolution of the radar. Division of the surveillance area into range channels is depicted in Fig. 3.8(a).

At the output of each range channel, the spectrum analysis has compressed the frequency width of the signal response into the width of one noise mode, by reasoning similar to that employed in Section 3.1.2. Eqs. (3.12) and (3.13) again obtain for each range channel. The information in each channel is

$$I_{\phi}^{(e)} = \ln PW \quad , \qquad (3.49)$$

where

W = Doppler surveillance window
P = signal duration,

and, in order to obtain this information, it is necessary that

$$\frac{\mathcal{E}}{k\mathcal{J}} > I_{\phi}^{(e)} \quad . \qquad (3.50)$$

3.2.2.4 Overall Two-Dimensional Information

The overall two-dimensional processing may be viewed in terms of a set of independent radar channels with the established separation between channels (linear system resolution) insuring that a signal response occurs only in a single channel. (If the signal response were to substantially spill over into other channels, which tends to occur with high $\tau - \phi$ interdependence due to elongated ambiguity areas, the channel separation should be increased.) In the linear system, the total range-Doppler information received (for a single target) is

$$I_{\tau,\phi}^{(e)} = \ln \frac{TW}{1/PB} = \ln TWPB \qquad (3.51)$$

$$= \ln TB + \ln PW = I_{\tau}^{(e)} + I_{\phi}^{(e)} \quad , \qquad (3.52)$$

regardless of whether range or Doppler channels are employed. The range and Doppler informations are therefore seen to be additive and the total information can be calculated from the (logarithm of the) ratio of the surveillance area to the compressed energy area, or simply by adding the intra-channel information to the information implied by the localization of the signal response to a particular channel. Using the

Doppler-channel implementation as an illustration, there are TB noise modes within the range-delay surveillance window of T seconds in each channel and PW Doppler channels are required to cover the Doppler surveillance window of W cps. There are therefore TBPW independent opportunities for a false alarm, so the information of Eq. (3.51) is only obtained for

$$\frac{E}{k\mathcal{J}} > \ln \text{ TBPW} \tag{3.53}$$

or

$$\frac{E}{k\mathcal{J}} > I_{\tau,\phi}^{(e)} \quad . \tag{3.54}$$

In the nonlinear system, the additional compression requires that the overall τ, ϕ information be written as

$$(N)_{I_{\tau,\phi}^{(e)}} = \ln \rho \text{ TBPW} \tag{3.55a}$$

$$= \ln \sqrt{\rho} \text{ TB} + \ln \sqrt{\rho} \text{ PW} = (N)_{I_\tau^{(e)}} + (N)_{I_\phi^{(e)}} \quad . \tag{3.55b}$$

If the reliability factor r is again introduced, the inequality in Eq. (3.53) is written as

$$\frac{E_T}{k\mathcal{J}} = \ln r \text{ TBPW} \quad , \tag{3.56}$$

in accordance with the previous development connected with Eqs. (3.7) and (3.8). We may write Eq. (3.55a) as

$$(N)_{I_{\tau,\phi}^{(e)}} = \ln \rho + \ln \text{ TBPW} \quad , \tag{3.57}$$

and Eq. (3.56) as

$$\frac{E_T}{k\mathcal{J}} = \ln r + \ln \text{ TBPW} \quad . \tag{3.58}$$

Eliminating the term ln TBPW between Eqs. (3.57) and (3.58), we have

$$\frac{E_T}{k\mathcal{J}} = (N)_{I_{\tau,\phi}^{(e)}} + \ln \frac{r}{\rho} \quad . \tag{3.59}$$

Subtracting Eq. (3.59) from the identity

$$\frac{E}{k\mathcal{J}} = \frac{E}{k\mathcal{J}} = \rho' \quad , \tag{3.60}$$

where

E = true input energy,

we obtain

$$\frac{E - E_T}{k\mathcal{J}} = \left(\frac{E}{k\mathcal{J}} - (N)_{I_{\tau,\phi}}^{(e)} \right) - \ln \frac{r}{\rho} \quad , \qquad (3.61)$$

In order to accept the presence of signal as such, we have the detection criterion

$$E - E_T > 0 \quad , \qquad (3.62)$$

and therefore, for detection,

$$\frac{E}{k\mathcal{J}} - (N)_{I_{\tau,\phi}}^{(e)} > \ln \frac{r}{\rho} \qquad (3.63)$$

or

$$\rho > r\, e^{-\left(\frac{E}{k\mathcal{J}} - (N)_{I_{\tau,\phi}}^{(e)} \right)} \quad . \qquad (3.64)$$

If we now define an information loss L by

$$L = \frac{E}{k\mathcal{J}} - (N)_{I_{\tau,\phi}}^{(e)} \quad ; \qquad (3.65)$$

where we postulate that

$$L \geq 0 \qquad (3.66)$$

by continuation of the proposition that the information does not exceed the input entropy, then

$$\rho > r\, e^{-L} \quad . \qquad (3.67)$$

For a perfectly efficient measurement we would have L = 0, which implies that

$$(N)_{I_{\tau,\phi}}^{(e)} = \frac{E}{k\mathcal{J}} \quad , \qquad (3.68)$$

and the detection criterion becomes

$$\rho > r \qquad (3.69)$$

or

$$\rho > \frac{1}{P_{FA}} \quad . \qquad (3.70)$$

The smallest that r can be for a meaningful measurement is r = 2. For this condition of minimum reliability, the detection criterion becomes

$$\frac{E}{kT} > 1 \quad . \qquad (3.71)$$

Since the single noise waveform which enters the radar is passed to all of the channels, the noise may be correlated among channels. It will now be shown that this correlation, over the τ-ϕ plane, is proportional to the ambiguity function $|\chi(\tau, \phi)|$, which in turn, is proportional to the noiseless correlation surface $|\Gamma(\tau, \phi)|$. This indicates: (1) that the two-dimensional matched filter essentially localizes the signal response into the same area shape as a noise response, even in two dimensions, and (2) that if the signal waveform design and channel spacing are such that the signal response is predominantly restricted to a single channel, then the noise between channels is largely uncorrelated. The derivation for noise correlation using the Doppler-channel model is as follows. Let $\tilde{\nu}(t)$ represent the complex envelope for a Gaussian white-noise input. (Complex signal notation will be employed and the symbol $\sim$ represents a complex modulation.) The output from one (reference) Doppler channel is

$$\tilde{\gamma}(t) = \int_{-\infty}^{\infty} \tilde{\nu}(x)\, \tilde{h}(t-x)\, dx \quad , \qquad (3.72)$$

where $\tilde{h}(t)$ is the impulse response. The output of a second Doppler channel, with impulse response $\tilde{h}'(t)$, is

$$\tilde{\gamma}'(t) = \int_{-\infty}^{\infty} \tilde{\nu}(y)\, \tilde{h}'(t-y)\, dy \quad . \qquad (3.73)$$

The cross-correlation between the two outputs is

$$\overline{\tilde{\gamma}^*(t)\ \tilde{\gamma}'(t+\tau)} = \int_{-\infty}^{\infty}\int_{-\infty}^{\infty} \overline{\tilde{\nu}^*(x)\, \tilde{\nu}(y)}\, \tilde{h}^*(t-x)\, \tilde{h}'(t+\tau-y)\, dx\, dy$$

$$= \int_{-\infty}^{\infty}\int_{-\infty}^{\infty} \overline{\tilde{\nu}^*(x)\, \tilde{\nu}(x+p)}\, \tilde{h}^*(t-x)\, \tilde{h}'(t+\tau-x-p)\, dp\, dx, \qquad (3.74)$$

where we have transformed from the variable y to p by

$$y = x + p; \quad dy = dp \quad . \qquad (3.75)$$

Now letting

$$q = t - x; \quad dq = -dx \quad , \qquad (3.76)$$

we obtain

$$R_\gamma(\tau) = \int_{-\infty}^{\infty}\int_{-\infty}^{\infty} \overline{\tilde{\nu}^*(x)\,\tilde{\nu}(x+p)}\;\tilde{h}^*(q)\,\tilde{h}'(q+\tau-p)\,dp\,dq\,. \qquad (3.77)$$

We identify the correlation functions

$$R_\nu(\tau) = \overline{\tilde{\nu}^*(t)\,\tilde{\nu}(t+\tau)} \qquad (3.78)$$

for stationary noise $\tilde{\nu}(t)$, and

$$R_{hh'}(z) = \int_{-\infty}^{\infty} \tilde{h}^*(q)\;\tilde{h}'(q+z)\,dq \qquad (3.79)$$

Then

$$R_\gamma(\tau) = \int_{-\infty}^{\infty} R_\nu(p)\,R_{hh'}(\tau-p)\,dp \qquad (3.80)$$

which is the convolution of $R_\nu(\tau)$ with $R_{hh'}(\tau)$. Now, for white noise,

$$R_\nu(\tau) = N_o\,\delta(\tau) \qquad (3.81)$$

so that

$$R_\gamma(\tau) = N_o R_{hh'}(\tau) = N_o \int_{-\infty}^{\infty} \tilde{h}^*(q)\,\tilde{h}'(q+\tau)\,dq \qquad (3.82)$$

In the Doppler-channel implementation, the only difference between the two channels is a frequency difference ϕ so that

$$\tilde{h}'(t) = \tilde{h}(t)\,e^{-j\,2\pi\,\phi\,t} \qquad (3.83)$$

Then Eq. (3.82) becomes

$$R_\gamma(\tau) = N_o R_\gamma(\tau,\phi) = N_o \int_{-\infty}^{\infty} \tilde{h}^*(q)\;\tilde{h}(q+\tau)\,e^{-j\,2\pi\,\phi\,(q+\tau)}\,dq. \qquad (3.84)$$

For a matched-filter system

$$\tilde{h}(t) = \tilde{\xi}(P-t) \qquad (3.85)$$

so

$$R_\gamma(\tau,\phi) = N_o \int_{-\infty}^{\infty} \tilde{\xi}^*(P-q)\,\tilde{\xi}(P-q-\tau)\,e^{-j2\pi\,\phi\,(q+\tau)}\,dq$$

$$= e^{-j2\pi\,\phi(\tau+P)}\,N_o \int_{-\infty}^{\infty} \tilde{\xi}^*(x)\,\tilde{\xi}(x-\tau)\,e^{j2\pi\,\phi\,x}\,dx \qquad (3.86)$$

by using

$$P - q = x \qquad (3.87)$$

and

$$dx = - dq \qquad (3.88)$$

Then

$$|R_\gamma(\tau, \phi)| = N_o \left| \int_{-\infty}^{\infty} \tilde{\xi}(x)\, \tilde{\xi}^*(x-\tau)\, e^{-j2\pi \phi x}\, dx \right| = N_o \left| \chi(\tau, \phi) \right| , \qquad (3.89)$$

which was to be shown.

In the preceding work, as well as in the former single-channel analyses, it has consistently been seen that a matched filter compresses the signal energy into the concentration occupied by a single noise mode. This property is optimum from the standpoint of information processing. For example, suppose that we consider the compressed signal area to be fixed, and postulate that more than one noise mode occurs within the signal area. (This results from a situation where the matched-filter time-frequency gate is larger than the signal's input energy area.) Then there would be more independent opportunities for a false alarm within the surveillance area. The amplitude threshold would therefore have to be raised, although the received information (which depends only upon the compressed signal area and the surveillance area) has remained constant. On the other hand, we cannot compress the signal area to less than that of a noise mode, because this would imply a matched-filter time-frequency gate which is smaller than the signal's input energy area. This situation tends to expand the compressed signal as well as the output noise modes. During such expansion, the signal tends to remain concentrated within the region of one noise mode, but information is decreasing because of the output signal expansion relative to the fixed size of the surveillance window. In summary, from the standpoint of information efficiency, the optimum filtering process is accomplished by the smallest time-frequency gate which encompasses the signal's input energy area without substantially rejecting signal energy. This is also the basic characteristic of the matched filter, which is known to be optimally suited for detection and parameter estimation.

3.3 Relation of Results to Statistical Mechanics

3.3.1 Distributional Information Defined in Terms of Physical Entropy

In the preceding sections, we dealt with various radar problems and determined equalities and inequalities between the parameter information, expressed in natural units, and the SNER required to obtain it. By a simple change of units, these relations were seen to be equivalent to relations between physical entropy and information in thermodynamic units. The associations were such as to suggest an equivalence between physical entropy and information, of the type specifically stated in Eq. (3.68). In this section, we shall be able to acquire further corroboration of such an equivalence

by starting with a thermodynamic problem and deriving similar results.

Consider a long thin thermally insulated container filled with an ideal monatomic gas, as shown in Fig. 3.9. We assume that a stationary external energy source is located somewhere along the x-axis within the region

$$0 \leq x \leq X \quad , \qquad (3.90)$$

and its location x_o is to be determined. The source injects a moderate quantity of heat energy E in such a manner that it fills a subvolume equal to 1/q times the total volume. I.e., the input energy is concentrated in an interval

$$\Delta x = \frac{X}{q} \quad , \qquad (3.91)$$

where

$$1 \leq q \leq Q \quad , \qquad (3.92)$$

with Q representing a limit on how much concentration can be physically achieved. A subvolume width Δx centered at $x = x'$ will be called subvolume (or section) $V(x')$. Intuitively, it would be said that, if $q = 1$, no information is received and if $q = Q$, the maximum information is obtained.

The introduction of a fixed amount of energy E results in an entropy increase[46,47] of

$$\Delta S' = \int_{\mathcal{T}_o}^{\mathcal{T}_o + q\Delta\mathcal{T}} \frac{dE}{\mathcal{T}} = \int_{\mathcal{T}_o}^{\mathcal{T}_o + q\Delta\mathcal{T}} \frac{C_v\,(w/q)\,d\mathcal{T}}{\mathcal{T}}$$

$$= \frac{C_v w}{q} \ln\left(1 + \frac{q\,\Delta\mathcal{T}}{\mathcal{T}_o}\right) \quad , \qquad (3.93)$$

where

$q\,\Delta\mathcal{T}$ = temperature rise in subvolume $V(x_o)$
w/q = weight of gas in subvolume $V(x_o)$
C_v = specific heat at constant volume.

If no information were obtained, then $q = 1$ and the entropy will be denoted by the unprimed value

$$\Delta S = S_p = C_v w \ln\left(1 + \frac{\Delta\mathcal{T}}{\mathcal{T}_o}\right) \qquad (3.94a)$$

$$\approx \frac{C_v w\,\Delta\mathcal{T}}{\mathcal{T}_o} = \frac{E}{\mathcal{T}_o} \quad \text{for} \quad \frac{\Delta\mathcal{T}}{\mathcal{T}_o} \ll 1 \quad , \qquad (3.94b)$$

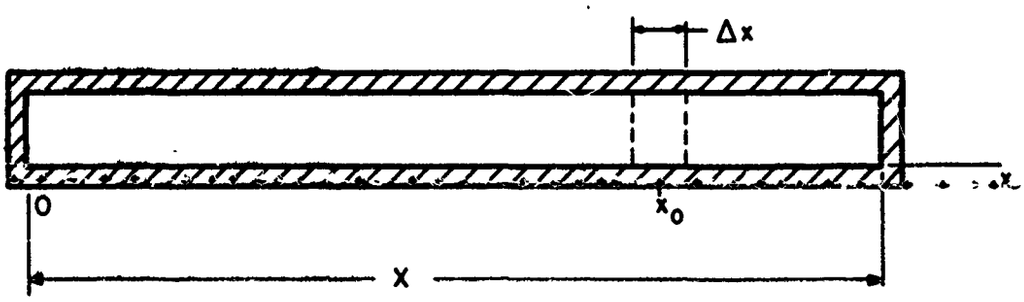

Fig. 3.9 Thermally Insulated Container Filled with Ideal Gas

and it should be observed that

$$\Delta S' \leq S_p \qquad \text{for } q \geq 1. \qquad (3.95)$$

The quantity S_p will be referred to as the entropy-equivalent of the input energy, or simply the input entropy.

We note, now, that a greater amount of received information (higher q) implies a smaller entropy rise $\Delta S'$. Since entropy represents unavailability of work, it is immediately concluded that more input information implies a greater availability of work. This result is completely compatible with the described gas model. For example, if the input energy is introduced uniformly throughout the total volume, no information is received and the thermal-equilibrium state of the system is not disturbed so that there can be no further thermal work performed due to mixing or diffusion. On the other hand, the more the fixed quantity of energy E is concentrated as it enters the container, the higher the local temperature rise in subvolume $V(x_o)$ and the more thermal work we can expect to recoup. In fact, it is proved in Appendix B that if the added heat is subsequently allowed to mix with the remainder of the volume, then the entropy increases by an amount

$$N = S_p - \Delta S' \qquad (3.96)$$

as the received information in concurrently lost. We shall associate N with information and it will be called negentropy. For a specific quantity of input energy, there then exists a principle of conservation of information and entropy such that

$$S_p = \Delta S' + N = \frac{E}{\mathcal{J}_o} \qquad (3.97)$$

To review, for a given energy E there exists an entropy-equivalent $S_p = \frac{E}{\mathcal{J}_o}$, assuming $\Delta \mathcal{J} \ll \mathcal{J}_o$. When E is introduced into subvolume $V(x_o)$, the increase in system entropy is $\Delta S'$. We also state that a further quantity N is received, which is a distributional form of entropy identified with positional information, and which is exchanged for a further increase in entropy as the added energy E diffuses throughout the volume (and information is lost). It is an interesting characteristic of this type of information that a greater input information implies a greater amount of available thermal work. In this sense, the information takes on the attribute of a physical entity rather than only an arbitrary measure, which is a fundamental conclusion of a cybernetic nature.

Although the negentropy N has thus far been associated with a measure of information, we have not yet related N to the type of information discussed in the radar application. This relation will now be clarified. From Eqs. (3.96), (3.93) and (3.94a), we have

$$N = C_v w \ln\left(1 + \frac{\Delta \mathcal{J}}{\mathcal{J}_o}\right) - \frac{C_v w}{q} \ln\left(1 + \frac{q \Delta \mathcal{J}}{\mathcal{J}_o}\right) \quad . \qquad (3.98)$$

From the theory of statistical mechanics,[48-51] it is known that

$$C_v w = \frac{kn}{2} = k m \quad , \qquad (3.99)$$

where

k = Boltzmann's constant

n = total number of degrees of freedom in overall volume

m = total number of modes, assuming two degrees of freedom per mode.

Thus,

$$N = k\left[m \ln\left(1 + \frac{\Delta \mathcal{J}}{\mathcal{J}_o}\right) - m' \ln\left(1 + \frac{q \Delta \mathcal{J}}{\mathcal{J}_o}\right)\right] \quad , \qquad (3.100)$$

where

$$m' = \frac{m}{q} = \text{number of modes in subvolume } V(x_o). \qquad (3.101)$$

But, from Eq. (3.94b) and Eq. (3.99),

$$\frac{\Delta \mathcal{J}}{\mathcal{J}_o} = \frac{E}{km\mathcal{J}_o} = \frac{SNER}{m} = \frac{\rho'}{m} \quad , \qquad (3.102)$$

where

$$SNER = \frac{E}{k\mathcal{J}_o} = \rho' \quad . \qquad (3.103)$$

Thus,

$$N = k\left[m \ln\left(1 + \frac{\rho'}{m}\right) - m' \ln\left(1 + \frac{\rho'}{m'}\right)\right] \quad . \qquad (3.104)$$

This formula for negentropy bears a remarkable similarity to Shannon's formula for the information capacity of a noisy communication channel, which will be further discussed in the subsequent section. We note here, however, that N approaches zero as ρ' approaches zero. Also, if m' is very small compared to m so that the second term is negligible (greatest received information), and if m is very large, then

$$N \approx k \rho' \quad , \qquad (3.105)$$

which shows that the greatest received information is characterized by

$$\frac{N}{k} \approx SNER \approx \frac{E}{k\mathcal{J}_o} \quad . \qquad (3.106)$$

Comparison of this result with Eq. (3.68) or Eq. (3.54) shows that we should identify N with information in thermodynamic units or N/k with information in natural units.

3.3.2 Comparison with Shannon's Formula for the Information Capacity of a Noisy Channel

From Eq. (3.104), it is seen that the distributional information $N = N^{(e)}$ (in natural units) is measured by a change in the quantity

$$N^{(e)}(m) = m \ln \left(1 + \frac{\rho'}{m}\right) , \qquad (3.107)$$

for a fixed value of ρ'. That is,

$$N^{(e)} = N^{(e)}(m) - N^{(e)}(m') . \qquad (3.108)$$

We associate $N^{(e)}(m)$ with an a priori value of information entropy, and $N^{(e)}(m')$ with an a posteriori value of information entropy, the difference being information.

For comparison, consider Shannon's formula[24, 52] for the information capacity of a noisy channel:

$$R^{(e)} = B_c \ln (1 + S/N) \quad \text{nits/sec} , \qquad (3.109)$$

where

B_c = channel bandwidth

S/N = signal-to-noise power ratio per transmitted pulse.

In a time duration T, the amount of amplitude information communicated is

$$I^{(e)} = R^{(e)} T = TB_c \ln (1 + S/N) \text{ natural units.} \qquad (3.110)$$

Now let us assume that a sequence of sinusoidal pulses, each of duration P, is being transmitted, and they are received by a matched filter having a bandwidth of $B = 1/P$, as in Eq. (1.5). Then, from Eq. (1.6),

$$S/N = SNPR = \frac{E'}{N_o} , \qquad (3.111)$$

where

E' = energy of a single pulse

$N_o = k\mathcal{T}$ = noise power spectral density.

Across the channel bandwidth B_c, we can fit a parallel group of

$$\frac{B_c}{B} = PB_c \quad \text{pulses} \qquad (3.112)$$

and, in a time T, there are T/P such pulse groups giving a total of

$$PB_c \cdot \frac{T}{P} = TB_c \quad \text{pulses} \quad . \qquad (3.113)$$

(Alternatively, we could have transmitted pulses of bandwidth B_c and would have also ended up with TB_c pulses for matched-filter reception.) Therefore, Eq. (3.111) can be written as

$$S/N = \frac{E}{TB_c\, kJ} = \frac{\rho'}{TB_c} \quad , \qquad (3.114)$$

where

E = total energy of the signal.

Finally, substitution of Eq. (3.114) into Eq. (3.110) yields,

$$I^{(e)} = m \ln \left(1 + \frac{\rho'}{m}\right) = I^{(e)}(m) \quad , \qquad (3.115)$$

where

$m = TB_c$ = number of noise modes in the time-bandwidth area occupied by the message.

For a fixed balue of ρ' (i.e., fixed total energy), the information $I^{(e)}$ is a function of on'y the number of modes m. Distributional information, as expressed by Eq. (3.108), is therefore seen to be the difference between $N^{(e)}(m)$ for the a priori surveillance region and $N^{(e)}(m')$ after reception. In a matched-filter radar, $m' = 1$ so that

$$N^{(e)} = m \ln \left(1 + \frac{\rho'}{m}\right) - \ln (1 + \rho') = H_a{}^{(e)} - H_b{}^{(e)} \quad . \qquad (3.116)$$

Thus, after the measurement, we are still left with an a posteriori uncertainity (entropy) given by

$$H_b{}^{(e)} = \ln (1 + \rho') \quad . \qquad (3.117)$$

Now, Eq. (3.115) indicates that this is the information that can still be extracted from the matched-filter output (for a signal immersed in one noise mode). In fact, this is the amplitude information about the signal. Thus $H_a{}^{(e)}$, the a priori entropy, is the sum of a distributional information term $N^{(e)}$ and an amplitude information term $H_b{}^{(e)}$.

The generality and applicability of physical-entropy and information-entropy concepts to both thermodynamic problems and electrical problems stems from the use of universal properties such as energy, temperature and degrees of freedom. In fact, the Boltzmann factor has been shown to be completely applicable to a hybrid system such as a mechanical (leaf-spring) resonator immersed in a container of gas. The spring is characterized by amplitude and phase properties[53-55] and comprises two degrees of freedom as a harmonic oscillator.

3.3.3 A Signal-Detection Criterion Relating Input Physical Entropy to "Absolute" Information Entropy of Noise Background

It is assumed, here, that the signal is immersed in one noise mode, as at the output of a matched filter. From an equation such as Eq. (3.2), we have

$$P_{FA} = 1 - (1 - P'_{FA}) = P'_{FA} \quad . \qquad (3.118)$$

Substituting Eqs. (3.5) and (3.6), it is seen that

$$\frac{E_T}{k\mathcal{J}} = \ln r \quad . \qquad (3.119)$$

The minimum useful value of r is 2 and therefore the threshold of detectability, by this criterion, is given by

$$\frac{E_T}{k\mathcal{J}} = \ln 2 = 0.74 \quad . \qquad (3.120)$$

With a slight increase in reliability to r = e, we shall (reasonably) define the detectibility by the criterion

$$\frac{E_T}{k\mathcal{J}} = \ln e = 1 \quad . \qquad (3.121)$$

Now the energy of the noise mode is characterized by the normalized Boltzmann factor of Eq. (2.16). If the energy levels were quantized to a fine interval δE, the information entropy would be approximately[52,17]

$$H_N^{(e)} = -\int_0^\infty p(E) \ln\left[p(E)\,\delta E\right] dE \qquad (3.122a)$$

$$= 1 + \ln k - \ln \delta E \quad , \qquad (3.122b)$$

by substitution of Eq. (2.16). By using the natural quantization

$$\delta E = \sigma_E = k\mathcal{J} \quad , \qquad (3.123)$$

Eq. (3.122b) reduces to

$$H_N^{(e)} = 1 \qquad \text{natural unit} \quad . \qquad (3.124)$$

Therefore, from Eqs. (3.121) and (3.124), the signal detectability threshold is given by

$$\frac{E_T}{k\mathcal{J}} = H_N^{(e)} = 1 \quad , \qquad (3.125)$$

where H_N will be referred to as the "absolute" information entropy of the noise mode.

The thermodynamic equivalent to Eq. (3.125) is

$$\frac{E_T}{\mathcal{J}} = (H_N)_t \quad , \qquad (3.126)$$

where $E_T/\mathcal{J}$ is the physical entropy increase due to signal and $(H_N)_t$ is the absolute information entropy in thermodynamic units:

$$(H_N)_t = k\, H_N^{(e)} \quad . \qquad (3.127)$$

In order to interpret the results, it should be recalled that information entropy is fundamentally defined[52] as a generalization of

$$H^{(e)} = -\ln P = \ln N \quad , \qquad (3.128)$$

where $N = 1/P$ is a number of alternative equally-likely states. Therefore $(H_N)_t$ represents the average value of the logarithm of the number of distinguishable noise amplitudes (subject to quantization $\delta E = \sigma_E$). Eq. (3.128) states that the physical entropy increase from the signal must exceed the value $(H_N)_t$ in order to be detected. This is consistent with a well known result of statistical mechanics which relates the thermodynamic entropy to the logarithm of the number of system states or "complexions". That is, assume that a system is in a condition such that n_1 degrees of freedom are in energy level E_1, n_2 degrees of freedom are in energy level $E_2, \ldots, n_M$ degrees of freedom are in energy level E_M. The number of ways in which this can occur is

$$F_1 = \frac{n!}{n_1!\, n_2! \ldots n_M!} \quad , \qquad (3.129)$$

as given by Eq. (2.8), where n is the total number of degrees of freedom. Let us add a small quantity of energy E such that one degree of freedom in level E_i jumps to a higher level E_j, with

$$E = E_j - E_i \quad . \qquad (3.130)$$

Then the number of ways that the new situation can occur is

$$F_2 = \frac{n!}{n_1! \ldots (n_i - 1)! \ldots (n_j + 1)! \ldots n_M!} \quad . \qquad (3.131)$$

Now

$$\frac{F_2}{F_1} = \frac{n_i}{n_{j+1}} \approx \frac{n_i}{n_j} \quad , \qquad \text{for } n_j \gg 1 \quad . \qquad (3.132)$$

The system is in thermal equilibrium before and after the introduction of the energy E so the Boltzmann factor of Eq. (2.12) applies. That is,

$$p(E_\ell) = \frac{n_\ell}{n} \propto e^{\frac{E_\ell}{k\mathcal{J}}} ; \quad \ell = 1, 2, \ldots, i, \ldots, j, \ldots, M \quad . \qquad (3.133)$$

Therefore Eq. (3.132) becomes

$$\frac{F_2}{F_1} = e^{\frac{E_j - E_i}{k\mathcal{J}}} = e^{\frac{E}{k\mathcal{J}}} \quad , \qquad (3.134)$$

and so

$$\frac{E}{k\mathcal{J}} = \ln \frac{F_2}{F_1} = \ln F_2 - \ln F_1 \quad . \qquad (3.135)$$

Thus, physical entropy is inherently related to the logarithm of the number of alternative states by virtue of the applicability of the exponential Boltzmann factor. The detectability criterion of Eq. (3.125) therefore is predicated upon the minimum energy that must be added to overcome the degree of randomness in the noise, as measured by the quantity $\sigma_E = k\mathcal{J}$.

4. OPTIMIZATION OF AMPLITUDE THRESHOLD LEVEL

4.1 Motivation for Amplitude-Threshold Optimization

In the previous radar discussions dealing with the nonlinear Bessel-function detector, when the input SNER was equal to the information as expressed by Eq. (3.68), the reliability factor r was equal to two times the SNER, for a barely detectible signal, as indicated in Eq. (3.69). Now, from Eqs. (3.97) and (3.116) we may write

$$\frac{E}{k\mathcal{T}_o} = N^{(e)} + \ln(1+\rho') \quad , \tag{4.1}$$

where

$N^{(e)}$ = distributional information obtained

$\Delta S' = \ln(1+\rho')$ = amplitude entropy (not yet extracted after pulse compression).

If we associate Eq. (4.1) with the radar receiver employing the linear detector, then

$$\frac{E_T}{k\mathcal{T}_o} = \ln r \; TBPW = \ln TBPW + \ln r$$

$$= I^{(e)} + \ln(1+\rho') \quad , \tag{4.2}$$

where

$$I^{(e)} = \ln TBPW = \text{distributional information of linear system} \tag{4.3a}$$

$$r = 1 + \rho' = 1 + SNER \quad . \tag{4.3b}$$

Thus, with the nonlinear detector, all of the entropy increase appears in the form of distributional information for the maximum reliability (to allow detection) of

$$r = \rho = 2\rho' \quad , \tag{4.4}$$

whereas, with the linear detector, the entropy increase may be interpreted as equivalent to the sum of distributional information plus amplitude information, with a measurement reliability of $r = 1 + \rho'$. In both cases $\rho' > 1$ implies $r > 2$, as is required for a meaningful measurement. It is intuitively consistent that no amplitude information is conveyed with the nonlinear detector because Eq. (3.38) shows that it is necessary to know ρ before we can implement the nonlinear detector and therefore no amplitude information should be expected.

With either the linear or nonlinear detector, the reliability r increases with SNER = ρ', as expressed by Eqs. (4.3b) and (4.4). This implies an increase in threshold value by virtue of Eq. (3.56), which is

$$\frac{E_T}{kT} = \ln rTBPW \quad . \qquad (4.5)$$

The conclusion that the threshold level is an increasing function of SNER, in order for the equivalence of physical entropy and information to hold, raises the question of possible optimization of the amplitude threshold for a given SNER. It is shown in this chapter that such an optimum level exists and can be usefully employed in an efficient radar detection procedure. It may also be observed, at this point, that the information lnTBPW, defined for the linear detector, does not increase with SNER. This may appear inconsistent from the viewpoint that the measurement accuracy increases with SNER as indicated by Eqs. (3.27) and (3.28), although the resolution does not. However, we are restricting our definition of positional information to a "bound" form in which a physical compression of energy is actually involved. From this standpoint, the nonlinear Bessel function detector allows the information to increase as $\ln \rho$ TBPW while the linear detector causes the information to remain constant with increasing SNER.

4.2 Detection Model

It is first assumed that the input signal-to-noise ratio is known, although a later extension of the results will show that the analysis can be employed for a given range of possible values of signal-to-noise ratio. In this procedure, we adopt the model of a binary input message x_i which has two equally likely states:

$x_o = 0$ target absent
$x_1 = 1$ target present.

At the output of a "black box", which includes a voltage-amplitude threshold test, we obtain a binary result y_j:

$y_o = 0$ target judged absent
$y_1 = 1$ target judged present.

The model is depicted in Fig. 4.1.

A detection information $I_D^{(2)}$ may be defined as

$$I_D^{(2)} = H_a^{(2)} - H_b^{(2)} \quad , \qquad (4.6)$$

where

$$H_a^{(2)} = -\sum_{i=0}^{1} p(x_i) \log_2 p(x_i) = \underline{\text{a priori}} \text{ entropy} \qquad (4.7)$$

$$H_b^{(2)} = -\sum_{i=0}^{1} \sum_{j=0}^{1} p(x_i, y_j) \log_2 p(x_i/y_j) = \underline{\text{a posteriori}} \text{ entropy.} \qquad (4.8)$$

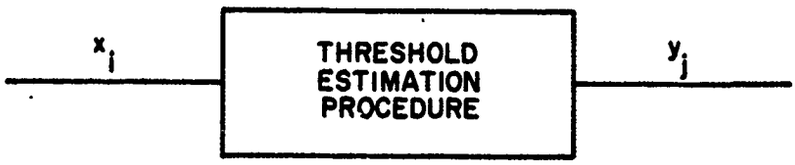

x_0 = TARGET IS NOT PRESENT

x_1 = TARGET IS PRESENT

y_0 = TARGET JUDGED NOT PRESENT

y_1 = TARGET JUDGED PRESENT

Fig. 4.1 Detection Model

The a priori entropy H_a is a constant independent of amplitude-threshold level. The maximization of information with respect to threshold level is therefore seen to be accomplished by the minimization of the a posteriori entropy, which we may write as

$$H_b^{(2)} = \sum_{j=0}^{1} p(y_j) \left[- \sum_{i=0}^{1} p(x_i(y_j) \log_2 p(x_i/y_j) \right] \quad . \tag{4.9}$$

Minimization of $H_b^{(2)}$ is equivalent to minimization of the

$$Q_j = - \sum_{j=0}^{1} p(x_i/y_j) \log_2 p(x_i/y_j) \; ; \qquad j = 0,1 \quad , \tag{4.10}$$

averaged over the $p(y_j)$. Finally, minimization of the Q_j is accomplished by producing the greatest disparity between $p(x_o/y_j)$ and $p(x_1/y_j)$, for $j = 0$ or $j = 1$ (since Q_j is itself an entropy form for two states, with maximum entropy being characterized by equal probabilities[52]). That is, given y_j, we have maximized the likelihood of distinguishing whether a target is absent (x_o) or present (x_1), where these two possibilities were equally likely before the threshold test.

H_b can be written in terms of the joint probabilities as

$$H_b^{(2)} = - \sum_{i=0}^{1} \sum_{j=0}^{1} p(x_i, y_j) \log_2 \frac{p(x_i, y_j)}{p(x_o, y_j) + p(x_1, y_j)} \quad , \tag{4.11}$$

where the joint probabilities are given by

$$p(x_i, y_j) = p(x_i)\, p(y_j/x_i) = \frac{1}{2}\, p(y_j/x_i) \quad , \tag{4.12}$$

for

$$p(x_o) = p(x_1) = \frac{1}{2} \quad . \tag{4.13}$$

The conditional probabilities $p(y_j/x_i)$ may be recognized in more familiar terms as

$$p(y_1/x_o) = P_{FA} = \text{false-alarm probability} \tag{4.14a}$$

$$p(y_1/x_1) = P_D = \text{detection probability} \tag{4.14b}$$

$$p(y_o/x_o) = P_{CD} = 1\text{-}P_{FA} = \text{correct-dismissal probability} \tag{4.14c}$$

$$p(y_o/x_1) = P_M = 1\text{-}P_D = \text{missed-signal probability} \quad . \tag{4.14d}$$

Using Eqs. (4.7), (4.11), (4.12) and (4.14), we can now write Eq. (4.6) in the form

$$I_D^{(2)} = 1 + \frac{1}{2} \left(P_D \log_2 \frac{P_D}{P_D + P_{FA}} + P_{FA} \log_2 \frac{P_{FA}}{P_D + P_{FA}} + P_M \log_2 \frac{P_M}{P_M + P_{CD}} + P_{CD} \log \frac{P_{CD}}{P_M + P_{CD}} \right) \quad , \tag{4.15}$$

which can be minimized with respect to amplitude threshold level. Typical plots of $I_D^{(2)}$ vs. threshold level are presented in Section 6.2.2, Fig. 6.5. The curves become higher and broader with increasing signal-to-noise ratio. For a given input signal-to-noise ratio, it can be seen that there is an optimum threshold level which maximizes the detection information. In the example cited in Section 6.2.2, it can be seen that the optimum ratio of threshold voltage to rms noise, $x_T = \frac{R_T}{\sigma_N}$, is not a sensitive function of signal-to-noise ratio. As a general rule, however, if we may reasonably assume, a priori, a range of possible signal-to-noise ratios, then the amplitude threshold can be set at some average value such as

$$\overline{x}_T = \frac{\int I^{(2)}_{D\,max}(S/N)\, x_T(S/N)\, d(S/N)}{\int I^{(2)}_{D\,max}(S/N)\, d(S/N)} \quad , \qquad (4.16)$$

where

$I^{(2)}_{D\,max}(S/N)$ = peak value of $I_D^{(2)}$ for a specified signal-to-noise ratio S/N ,

and the integrations are performed over the a priori expected range of S/N values. On the other hand, a radar c signer may wish to sacrifice some information at the higher S/N values and increase the information for the lower S/N values. Inspection of curves of the type illustrated in Fig. 6.5 will then allow a well-compromised selection of threshold level.

4.3 A Detection Procedure Based Upon Threshold-Crossing Rate

After one chooses the optimum amplitude threshold in accordance with the criterion described in the previous section, a specific false alarm rate is obtained which must be accepted as normal. This rate may be empirically determined as accurately as desired by observation over a long period of time while the radar is in standby operation barring, of course, variations in equivalent noise temperature due to antenna pointing angle, etc. Detection must now be based upon an increase in threshold-crossing rate resulting from the presence of signal.

A detection procedure is postulated in which an output "indicator" pulse is generated if there are one or more amplitude-threshold crossings per radar pulse. Within some observation interval $\tilde{T}$, which includes many transmitted pulses, we observe the rate at which the indicator pulses occur. If noise alone is present, the probability of exactly k indicator pulses occurring in time $\tilde{T}$ is, by the binomial distribution,

$$P(k) = \binom{\tilde{n}}{k} p_o^k \, (1 - p_o)^{\tilde{n} - k} \quad , \qquad (4.17)$$

where

p_o = P_{FA} per transmitted pulse $\approx n P'_{FA}$, where n is the number of noise modes per transmitted pulse in the surveillance region and P'_{FA} is the probability of a single noise mode crossing the threshold

$\tilde{n} = f_r \tilde{T}$ = number of transmitted pulses in time $\tilde{T}$ at a pulse repetition frequency of f_r.

Using the normal approximation that

$$P(k) \approx N(\tilde{n} p_o, \tilde{n} p_o (1 - p_o)) \qquad (4.18)$$

for[52]

$$\tilde{n} p_o (1 - p_o) \geq 3 \quad , \qquad (4.19)$$

and writing the indicator pulse rate as

$$r = \frac{k}{\tilde{T}} \quad , \qquad (4.20)$$

it is seen that the probability density function for rate with noise alone is approximately

$$P_o(r) = N\left(f_r p_o, \frac{f_r p_o (1 - p_o)}{\tilde{T}}\right) \quad . \qquad (4.21)$$

When signal is present, the indicator pulse rate increases and essentially (for $n \gg 1$) becomes equal to (a) the false alarm rate and (b) the rate with signal present but no false alarms included. This new rate has the distribution of the sum of two independent normal variables and is therefore

$$P_1(r) = N\left(f_r p_o + f_r p_1, \frac{f_r p_o (1 - p_o)}{\tilde{T}} + \frac{f_r p_1 (1 - p_1)}{\tilde{T}}\right), \qquad (4.22)$$

where

p_1 = P_D per transmitted pulse.

The two rate density functions (signal absent and signal present) are illustrated in Fig. 4.2.

A threshold rate r_T may now be set using the Neyman-Pearson procedure in the rate domain. An overall false alarm probability $\tilde{P}_{FA}$ is selected for a specified observation interval $\tilde{T}$. Since the standard deviations of the density functions $P_o(r)$ and $P_1(r)$ become narrower with increasing $\tilde{T}$, the rate threshold r_T decreases with increasing $\tilde{T}$ for a fixed overall $\tilde{P}_{FA}$. With a given signal-to-noise ratio, then, the overall detection probability $\tilde{P}_D$ will increase with $\tilde{T}$. The detection-information procedure

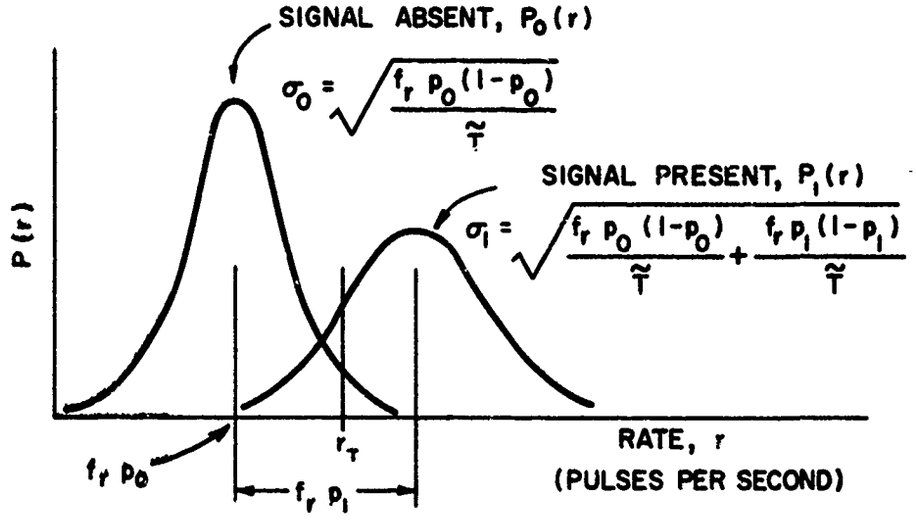

Fig. 4.2 Probability Density Functions for Indicator Pulse Rate, with Signal Absent and Signal Present

is illustrated numerically in Section 6.2.2, using the actual parameters of an advanced pulse compression radar. It was found to be substantially more efficient than the conventional approach in which the Neyman-Pearson procedure is applied in the amplitude domain. Some reflection on the nature of the difference between the two approaches will indicate how the improvement occurs. In the detection-information procedure, we have disassociated the overall false alarm and detection probabilities from the amplitude threshold setting which is optimally set by an independent criterion. It is readily seen that, under conditions of long observation time $\tilde{T}$ and low overall false alarm probability $\tilde{P}_{FA}$, the normal Neyman-Pearson procedure applied to amplitude may require amplitude thresholds which are so high as to be completely unsuited for low-level signal detection, whereas the detection-information procedure always chooses a well-compromised threshold.

5. PARAMETER INFORMATION

5.1 Basic Formula

In the previous chapters, particularly Chapter 3, the strict applicability of the concepts of information theory to radar was developed by utilizing well known results on the size of the compressed signal responses, as illustrated, for example, by Fig. 3.5 with the linear detector and Eqs. (3.32) and (3.33) for the Bessel-function detector. The basic framework developed previously can be generalized to include multiple targets with unknown echo amplitudes, range delays and Doppler shifts. The generalized results not only support the previous conclusions, but they lead to a consideration of information areas in the τ - ϕ plane as well as the definition of an interdependence coefficient between range and Doppler informations. In this section, we derive the basic formula for parameter information in a multiple-target environment. The following sections are devoted to simplifications and interpretations of the basic formula. We shall use the analytical model and complex notation employed in Fig. 3.4. Let it be assumed that there are N targets, and let

$$x = (x_1; x_2; \ldots; x_N) = (\tau_1, \phi_1, A_1; \tau_2, \phi_2, A_2; \ldots; \tau_N, \phi_N, A_N) \qquad (5.1)$$

be a vector (3N-tuple) representing the range, Doppler and amplitude parameters of the N targets. If the transmitted signal is $\xi(t)$, then the complex echo voltage is

$$\eta_{x_o}(t) = \sum_{i=1}^{N} \eta_{x_{oi}}(t) \quad , \qquad (5.2)$$

where

$$\eta_{x_{oi}}(t) = A_{oi}\, \xi(t - \tau_{oi})\, e^{j2\pi\phi_{oi}t} \quad , \qquad (5.3)$$

in which the zero subscript represents a true value.

If

$$y = \zeta(t) = \eta_{x_o}(t) + \nu(t) \quad , \qquad (5.4)$$

represents the received noisy signal, where $\nu(t)$ is noise, then, by the Bayes equality, we have

$$\frac{p(x/y)}{p(x)} = \frac{p(y/x)}{p(y)} \quad . \qquad (5.5)$$

The average parameter information is therefore

$$I_p^{(e)}(X, Y) = \int_{-\infty}^{\infty}\int_{-\infty}^{\infty} p(x, y) \ln \frac{p(x/y)}{p(x)}\, dx\, dy = \int_{-\infty}^{\infty}\int_{-\infty}^{\infty} p(x, y) \ln \frac{p(y/x)}{p(y)}\, dx\, dy \quad . \qquad (5.6)$$

Substituting,

$$p(x, y) = p(x)\, p(y/x) \tag{5.7}$$

and

$$p(y) = \int_{-\infty}^{\infty} p(x)\, p(y/x)\, dx \quad , \tag{5.8}$$

the information becomes

$$I_p^{(e)}(X, Y) = \int_{-\infty}^{\infty} p(x)\, dx \int_{-\infty}^{\infty} p(y/x) \ln \left[\frac{p(y/x)}{\int_{-\infty}^{\infty} p(x')p(y/x')dx'} \right] dy \quad , \tag{5.9}$$

which is entirely in terms of the a priori density function $p(x)$ and the likelihood function $p(y/x)$. In the analytical work dealing with information, it is most desirable to investigate the change in information as a consequence of changes in the target configuration and changes in radar waveform. In order to allow for the former consideration, the averaging with respect to $p(x)$ in Eq. (5.9) may be omitted and the formula becomes

$$I_p^{(e)}(x, Y) = \int_{-\infty}^{\infty} p(y/x) \ln \left[\frac{p(y/x)}{\int_{-\infty}^{\infty} p(x')p(y/x')\, dx'} \right] dy \quad . \tag{5.10}$$

In terms of the complex radar notation, we have

$$p(y/x) = p\,(\nu(t) = \zeta(t) - \eta_x(t)) = p\,(\nu(t) = y - \eta_x(t))$$

$$= p\,(\nu_{x,y}(t) = \zeta(t) - \eta_x(t)) \triangleq p(\nu_{x,y}) \quad , \tag{5.11}$$

where, (from Eq. (3.20)

$$p(\nu_{x,y}) = \frac{1}{(2\pi k \mathcal{T} W')^{T'W'}}\, e^{-\frac{1}{2k\mathcal{T}} \int_{-\infty}^{\infty} |\nu_{x,y}(t)|^2 dt} \quad , \tag{5.12}$$

with

$$|\nu_{x,y}(t)|^2 = |\zeta(t) - \eta_x(t)|^2 = |\zeta(t)|^2 - 2\,\mathrm{Re}\,\zeta(t)\,\eta_x^*(t) + |\eta_x(t)|^2 . \tag{5.13}$$

Thus, Eq. (5.10) becomes

$$I_p^{(e)}(x, Y) = \int_{-\infty}^{\infty} p(\nu_{x,y}) \ln \left[\frac{p(\nu_{x,y})}{\int_{-\infty}^{\infty} p(x')\, p(\nu_{x',y})dx'} \right] dy \quad . \tag{5.14}$$

For the integration

$$\int_{-\infty}^{\infty} p(x')\, p(\nu_{x',y})\, dx' \quad , \tag{5.15}$$

x' is an arbitrary variable of integration and we have

$$\nu_{x',y} = \nu_{x'y}(t) = \zeta(t) - \eta_{x'}(t)$$

$$= \nu_{x,y}(t) + \eta_x(t) - \eta_{x'}(t) \quad , \qquad (5.16)$$

where x is a given set of parameters throughout the problem and all averaging is being done over the ensemble of all possible received waveforms $y = \zeta(t)$ as determined from the multidimensional Gaussian process $\nu(t)$ added to the given $\eta_x(t)$. Substituting Eq. (5.16) into Eq. (5.14) yields

$$I_p^{(2)}(x, Y) = \int_{-\infty}^{\infty} p(\nu_{x,y}) \ln \left[\frac{p(\nu_{x,y})}{\int_{-\infty}^{\infty} p(x') p(\nu_{x,y} + \eta_x - \eta_{x'}) dx'} \right] dy \quad . \qquad (5.17)$$

First consider

$$p(\nu_{x,y} + \eta_x - \eta_{x'}) = \frac{1}{(2\pi k \mathcal{J} W')^{T'W'}} e^{-\frac{1}{2k\mathcal{J}} \int_{-\infty}^{\infty} |\nu_{x,y}(t) + \eta_x(t) - \eta_{x'}(t)|^2 dt} \quad , \qquad (5.18)$$

where

$$|\nu_{x,y}(t) + \eta_x(t) - \eta_{x'}(t)|^2 =$$

$$|\nu_{x,y}(t)|^2 + 2\,\mathrm{Re}\left[\nu^*_{x,y}(t)\,(\eta_x(t) - \eta_{x'}(t))\right] + |\eta_x(t) - \eta_{x'}(t)|^2 \quad . \qquad (5.19)$$

For wide-band signals, the center cross-correlation term involves a cosine function of a wide-band phase-modulation argument as well as a uniformly-distributed phase due to wide-band noise. After integration with respect to time, this contributes a negligible value to the total exponent in Eq. (5.18). Thus

$$p(\nu_{x,y} + \eta_x - \eta_{x'}) \approx \frac{1}{(2\pi k \mathcal{J} W')^{T'W'}} e^{-\frac{1}{2k\mathcal{J}} \int_{-\infty}^{\infty} (|\nu_{x,y}(t)|^2 + |\eta_x(t) - \eta_{x'}(t)|^2)\, dt}$$

$$\approx p(\nu_{x,y})\, e^{-\frac{1}{2k\mathcal{J}} \int_{-\infty}^{\infty} |\eta_x(t) - \eta_{x'}(t)|^2 dt} \quad , \qquad (5.20)$$

and the integration with respect to x' in Eq. (5.17) becomes

$$\int_{-\infty}^{\infty} p(x') p(\nu_{x,y} + \eta_x - \eta_{x'}) dx' = p(\nu_{x,y}) \int_{-\infty}^{\infty} p(x')\, e^{-\frac{1}{2k\mathcal{J}} \int_{-\infty}^{\infty} |\eta_x(t) - \eta_{x'}(t)|^2 dt} dx' \quad . \qquad (5.21)$$

Substituting this into Eq. (5.17) yields

$$I_p^{(e)}(x, Y) = -\int_{-\infty}^{\infty} p(\nu_{x,y}) \ln \left[\int_{-\infty}^{\infty} p(x') \, e^{-\frac{1}{2kT} \int_{-\infty}^{\infty} |\eta_x(t) - \eta_{x'}(t)|^2 \, dt} \, dx' \right] dy$$

$$= -\ln \left[\int_{-\infty}^{\infty} p(x') \, e^{-\frac{1}{2kT} \int_{-\infty}^{\infty} |\eta_x(t) - \eta_{x'}(t)|^2 dt} \, dx' \right] . \qquad (5.22)$$

Now,

$$\frac{1}{2} \int_{-\infty}^{\infty} |\eta_x(t) - \eta_{x'}(t)|^2 \, dt = \frac{1}{2} \int_{-\infty}^{\infty} (|\eta_x(t)|^2 - 2 \operatorname{Re} \eta_x^*(t) \eta_{x'}(t) + |\eta_{x'}(t)|^2) \, dt$$

$$= E + E' - \operatorname{Re} \chi_{x,x'} \qquad (5.23)$$

where

$$E = \frac{1}{2} \int_{-\infty}^{\infty} |\eta_x(t)|^2 \, dt = \text{total echo signal energy} \qquad (5.24)$$

$$E' = \frac{1}{2} \int_{-\infty}^{\infty} |\eta_{x'}(t)|^2 \, dt = \text{total echo signal energy as a function of dummy variable } x' \qquad (5.25)$$

$$\chi_{x,x'} = \int_{-\infty}^{\infty} \eta_x^*(t) \, \eta_{x'}(t) dt = \text{multiple-target echo ambiguity function} . \qquad (5.26)$$

Using the above notation, Eq. (5.22) can be expressed in the form

$$I_p^{(e)}(x, Y) = -\ln \int_{-\infty}^{\infty} e^{-\frac{E'+E}{kT}} \, e^{\frac{1}{kT} \operatorname{Re} \chi_{x,x'}} \, p(x') \, dx' , \qquad (5.27)$$

which is a general formula for parameter information that depends only upon

(1) The assumed target situation x

(2) the ratio of total echo signal energy to noise energy per mode

(3) the multiple-target echo-signal ambiguity function $\chi_{x,x'}$

(4) the a priori density function $p(x')$.

5.2 Reduced Single-Target Formula

In order to acquire further insight into Eq. (5.27) and develop it into a more useful form, the single-target problem will be considered in further detail. Thus the echo signal is of the form

$$\eta_x(t) = A \, \xi(t - \tau) \, e^{j2\pi\phi t} , \qquad (5.28)$$

where the transmitted signal is

$$\xi(t) = R(t)\, e^{j2\pi\theta(t)}\, e^{j2\pi f_o t}\, e^{j2\pi\phi t} \quad , \qquad (5.29)$$

with

R(t) = envelope modulation, having an assumed maximum value of unity

$\theta(t)$ = phase modulation

f_o = carrier frequency.

Then

$$\text{Re}\ \chi_{x,x'} = \text{Re} \int_{-\infty}^{\infty} AA'\ \xi^*(t-\tau)\, \xi(t-\tau')\, e^{j2\pi(\phi'-\phi)t}\, dt \qquad (5.30)$$

$$= \text{Re} \int_{-\infty}^{\infty} AA'\ R(t-\tau)R(t-\tau')\, e^{j2\pi[\theta(t-\tau')-\theta(t-\tau)]}\, e^{j2\pi(\phi'-\phi)t}\, e^{j2\pi f_o(\tau-\tau')}\, dt \ .$$

Letting

$$\alpha = \tau' - \tau \qquad (5.31a)$$

$$\beta = \phi' - \phi \quad , \qquad (5.31b)$$

and then

$$t - \tau = t' \ , \qquad dt = dt' \quad , \qquad (5.32)$$

it is found that

$$\text{Re}\ \chi_{x,x'} = \text{Re}\left[e^{-j2\pi(f_o\alpha-\beta\tau)} \int_{-\infty}^{\infty} AA'\ R(t')R(t'-\alpha)\, e^{j2\pi[\theta(t'-\alpha)-\theta(t')]}\, e^{j2\pi\beta t'}\, dt' \right] . \qquad (5.33)$$

We may write Eq. (5.33) as

$$\text{Re}\ \chi_{x,x'} = |\chi_{A,A'}(\alpha,\beta)| \cos\left[2\pi(f_o\alpha - \beta\tau) - \epsilon\right] \quad , \qquad (5.34)$$

where

$$\chi_{A,A'}(\alpha,\beta) = \int_{-\infty}^{\infty} AA'\ R(t')R(t'-\alpha)\, e^{j2\pi[\theta(t'-\alpha)-\theta(t')]}\, e^{j2\pi\beta t'}\, dt' \qquad (5.35)$$

and

$$\epsilon = \arg\ \chi_{A,A'}(\alpha,\beta) \quad . \qquad (5.36)$$

So Eq. (5.27) becomes

$$I_p^{(e)}(x,Y) = -\ln \int_{-\infty}^{\infty} e^{-\frac{E+E'}{kT}}\, e^{\frac{1}{kT}|\chi_{A,A'}(\alpha,\beta)|\cos[2\pi(f_o\alpha-\beta\tau)-\epsilon]}\, p(x')\, dx' \quad , \qquad (5.37)$$

where it is understood that x represents (τ, ϕ, A) and x' represents (τ', ϕ', A'). If we integrate, with respect to a, over one r-f cycle, then

$$I_p^{(e)}(x, Y) = - \ln \int_{-\infty}^{\infty} e^{-\frac{E' + E}{k\mathcal{J}}} I_o \left(\frac{|\chi_{A, A'}(\alpha, \beta)|}{k\mathcal{J}} \right) p(x') dx' \quad , \qquad (5.38)$$

where I_o is the modified Bessel function defined by

$$I_o(z) = f_o \int_{a - \frac{1}{2f_o}}^{a + \frac{1}{2f_o}} e^{z \cos(2\pi f_o a' + \gamma)} \, da' \quad . \qquad (5.39)$$

Eq. (5.38) is the desired single-target version.

5.3 Examples

5.3.1 No-Signal Case

It is assumed in this single-target example that A = E = 0, although it is not known that this is so prior to the measurement. Then Eq. (5.38) becomes

$$I_p^{(e)}(x, Y) = - \ln \int_{-\infty}^{\infty} e^{-\frac{E'}{k\mathcal{J}}} p(x') \, dx' \quad . \qquad (5.40)$$

The a priori density function p(x') is taken as the uniform distribution:

$$p(x') = \frac{1}{(\tau_B - \tau_A)(\phi_B - \phi_A)(E_B - 0)} \quad , \qquad (5.41)$$

where

$$\tau_A \leq \tau \leq \tau_B \qquad (5.42a)$$

$$\phi_A \leq \phi \leq \phi_B \qquad (5.42b)$$

$$0 \leq E \leq E_B \quad . \qquad (5.42c)$$

Then

$$I_p^{(e)}(x, Y) = - \ln \frac{1}{E_B} \int_0^{E_B} e^{-\frac{E'}{k\mathcal{J}}} \, dE'$$

$$= \ln E_B - \ln k\mathcal{J} \left(1 - e^{-\frac{E_B}{k\mathcal{J}}} \right) . \qquad (5.43)$$

Assuming that

$$E_B \gg k\mathcal{J} \quad , \qquad (5.44)$$

then

$$I_p^{(e)}(x, Y) = \ln \frac{E_B}{k\mathcal{J}} \quad . \qquad (5.45)$$

We may interpret this equation as follows. Before the measurement, the echo energy was expected to fall, with equal likelihood, between zero and the value E_B, and the range delay and Doppler shift were expected to fall uniformly in the intervals $[\tau_A, \tau_B]$ and $[\phi_A, \phi_B]$, respectively. Since, in fact, the echo energy was zero, we cannot have obtained any information about τ or ϕ. However, the energy value of zero was a possible a priori alternative within the expected energy interval. But the presence of noise prohibits us from exactly determining that the energy was truly zero. In fact, the final uncertainty in the measurement of energy is the uncertainty of the noise energy alone, which is characterized by a standard deviation of $\sigma_E = k\mathcal{J}$. Eq. (5.45) thus tells us that the measurement has permitted us to divide the a priori region of energy uncertainty $[0, E_B]$ into $N = \frac{E_B}{k\mathcal{J}}$ intervals, each of size $k\mathcal{J}$, and to declare (on the average) that the energy was in the lowest interval $E \approx 0$. The information so obtained is that given by Eq. (5.45). In this example, further support is also advanced for the choice of $\delta E = k\mathcal{J}$ as a quantization level for energy.

5.3.2 No A Priori Uncertainty

Here we assume that the true target parameters are known prior to the measurement. That is, symbolically,

$$p(x') = \delta(x' - x) \quad . \qquad (5.46)$$

Eq. (5.27) is therefore

$$I_p^{(e)}(x, Y) = -\ln \int_{-\infty}^{\infty} e^{-\frac{E' + E}{k\mathcal{J}}} e^{\frac{1}{k\mathcal{J}} \operatorname{Re} \chi_{x, x'}} \delta(x' - x)\, dx' \quad . \qquad (5.47)$$

Since, from Eq. (5.26), we have

$$\chi_{x, x} = 2E \quad , \qquad (5.48)$$

then Eq. (5.47) evaluates to

$$I_p^{(e)}(x, Y) = -\ln 1 = 0 \quad , \qquad (5.49)$$

as would be expected.

We may also consider a case regarding partial knowledge of the parameters, a priori. Suppose that, in the single-target case, we know range and Doppler but not echo energy. Then

$$p(x') = \delta(\tau' - \tau)\,\delta(\phi' - \phi)\,p(E) \tag{5.50}$$

where

$$p(E) = U(E_A, E_B) \quad . \tag{5.51}$$

Then Eq. (5.38) becomes

$$I_p^{(e)}(x, Y) = -\ln \int_{E_A}^{E_B} e^{-\frac{E' + E}{k\mathcal{J}}}\, I_o\left(\frac{|\chi_{A, A'}(0, 0)|}{k\mathcal{J}}\right) p(E')\, dE' \quad . \tag{5.52}$$

Assume, for illustration, that the signal pulse envelope (of duration P) is rectangular so that

$$E' = \frac{A'^2 P}{2} \quad . \tag{5.53}$$

Then, using

$$p(A') = p(E')\,\frac{dE'}{dA'} = \frac{A' P}{E_B - E_A} \quad , \tag{5.54}$$

Eq. (5.52) becomes

$$I_p^{(e)}(A, Y) = -\ln \int_{A_A}^{A_B} e^{-\frac{A'^2 + A^2}{2(k\mathcal{J}/P)}}\, I_o\left(\frac{AA'}{k\mathcal{J}/P}\right)\left(\frac{A' P}{E_B - E_A}\right) dA'$$

$$= -\ln\left(\frac{k\mathcal{J}}{E_B - E_A}\right) \int_{A_A}^{A_B} \frac{A'}{(k\mathcal{J}/P)}\, e^{-\frac{A'^2 + A^2}{2(k\mathcal{J}/P)}}\, I_o\left(\frac{AA'}{k\mathcal{J}/P}\right) dA' \quad . \tag{5.55}$$

The integral is now recognized as the integral of a Rice distribution and it evaluates to approximately unity if the interval $[A_A, A_B]$ includes most of the area under the density function. Thus, we have

$$I_p^{(e)}(A, Y) \approx \ln\left(\frac{E_B - E_A}{k\mathcal{J}}\right) \quad , \tag{5.56}$$

which should be compared with the simpler example leading to Eq. (5.45). It is interesting to note that

$$N = \frac{E}{k\mathcal{J}} = \frac{A^2 P}{2k\mathcal{J}} \tag{5.57}$$

quantization levels in the energy domain suggests

$$N' = \frac{\sqrt{E}}{\sqrt{k\mathcal{J}}} = \frac{A_{rms}}{\sqrt{k\mathcal{J}/P}} \tag{5.58}$$

quantization levels in the rms-amplitude domain. This implies that rms amplitude is "naturally" quantized into increments of

$$\sigma_N = \sqrt{\frac{kJ}{P}} \quad , \tag{5.59}$$

which is the rms noise at the output of a filter of bandwidth $1/P$ cps. This amount of rms noise (determined above for arbitrary phase modulation and rectangular amplitude modulation) is equal to that appearing at the output of the matched filter for a rectangular CW signal pulse.

5.3.3. The Case of High Signal-to-Noise Ratio

We shall consider the case of large values of A and A', and shall also restrict the analysis to a small neighborhood of the (τ, ϕ) point in the $\tau' - \phi'$ plane which is at the peak value of the integrand in Eq. (5.38). (This point is equivalent to the origin in the $\alpha - \beta$ plane.) We can then use the asymptotic form for the modified Bessel function, which is

$$I_o(z) \approx \frac{1}{\sqrt{2\pi z}}\, e^z \quad , \qquad z \gg 1 \quad . \tag{5.60}$$

Then Eq. (5.38) becomes

$$I_p^{(e)}(x, Y) = -\ln \int_{-\infty}^{\infty} e^{-\frac{E'+E}{kJ}} \cdot \frac{1}{\sqrt{2\pi \frac{|\chi_{A,A'}(\alpha,\beta)|}{kJ}}}\, e^{\frac{|\chi_{A,A'}(\alpha,\beta)|}{kJ}}\, p(x')dx' \quad . \tag{5.61}$$

We define

$$\chi(\alpha, \beta) = \frac{1}{AA'}\, \chi_{AA'}(\alpha, \beta) \tag{5.62a}$$

$$= \int_{-\infty}^{\infty} u(t^*)\, u(t-\alpha)\, e^{j2\pi\beta t}\, dt \quad , \tag{5.62b}$$

where

$$u(t) = R(t)e^{j2\pi\theta(t)} = \text{complex transmitted modulation} \quad . \tag{5.63}$$

Near the point $(\alpha = 0, \beta = 0)$, and for $A' \approx A$, we can represent $\chi(\alpha, \beta)$ by a truncated Maclaurin series

$$\chi(\alpha, \beta) = \chi(0, 0) + \left(\alpha \frac{\partial}{\partial\alpha} + \beta \frac{\partial}{\partial\beta}\right)\chi(0, 0) + \frac{1}{2}\left(\alpha \frac{\partial}{\partial\alpha} + \beta \frac{\partial}{\partial\beta}\right)^2 \chi(0, 0). \tag{5.64}$$

Evaluation[17, 57] of the partial derivatives and use of the spectrum

$$U(f) = \mathcal{F}\left[u(t)\right] = \int_{-\infty}^{\infty} u(t)\, e^{-j2\pi ft}\, dt \quad , \tag{5.65}$$

leads to the result:

$$\chi(\alpha,\beta) = \frac{2E}{A^2}\left(1 - \frac{1}{2}\overline{f^2}\,\alpha^2 - \frac{1}{2}\overline{t^2}\,\beta^2 + \overline{tf}\,\alpha\beta\right) , \qquad (5.66)$$

where

$$\overline{f^2} \triangleq \frac{(2\pi)^2 A^2}{2E}\int_{-\infty}^{\infty} U^*(f)\, f^2\, U(f)\, df \qquad (5.67)$$

$$\overline{t^2} \triangleq \frac{(2\pi)^2 A^2}{2E}\int_{-\infty}^{\infty} u^*(t)\, t^2\, u(t)\, dt \qquad (5.68)$$

$$\overline{tf} \triangleq \frac{(2\pi)^2 A^2}{2E}\int_{-\infty}^{\infty}\int_{-\infty}^{\infty} u^*(t)\, tf\, U(f)\, e^{\,j2\pi ft}\, df\, dt \qquad (5.69a)$$

$$= \frac{-j2\pi A^2}{2E}\int_{-\infty}^{\infty} u^*(t)\, t\, u'(t)\, dt \quad . \qquad (5.69b)$$

In a peak-power-limited radar transmitter, rectangular amplitude modulation is generally employed to obtain maximum transmitted energy. If we assume this situation, then the term $\overline{tf}$ is real-valued. We now substitute Eq. (5.66) into Eq. (5.61), while making the assumption that, for the denominator of the integrand only, we can allow the approximation

$$\chi_{A,A'}(\alpha,\beta) = AA'\ \chi(\alpha,\beta) \approx \frac{2EA'}{A} \qquad (5.70)$$

within the neighborhood of ($\alpha = 0$, $\beta = 0$) that we are considering. This is motivated by the observation that the exponential term of the integrand drops rapidly downward (as a function of α and β) during which the denominator is a slowly varying function. Thus Eq. (5.61) becomes

$$I_p^{(e)}(x,Y) \approx -\ln \int_{-\infty}^{\infty} e^{-\frac{E'+E}{kT}} \cdot \frac{1}{\sqrt{\frac{4\pi EA'}{kTA}}}\; e^{\frac{2EA'}{kTA}\left(1 - \frac{1}{2}\overline{f^2}\alpha^2 - \frac{1}{2}\overline{t^2}\beta^2 + \overline{tf}\,\alpha\beta\right)} p(x')\,dx' \quad . \qquad (5.71)$$

We shall concentrate our attention on the range and Doppler information and will, accordingly, set $A = A'$ while understanding hereafter that the integration is only over τ' and ϕ'. Eq. (5.71) then becomes

$$I_p^{(e)}(x,Y) = -\ln \int_{-\infty}^{\infty} \frac{1}{\sqrt{2\pi\rho}}\, e^{-\frac{\rho}{2}\left(\overline{f^2}\alpha^2 + \overline{t^2}\beta^2 - 2\overline{tf}\,\alpha\beta\right)} p(x')\,dx' . \qquad (5.72)$$

Letting

$$p(x') = p(\tau')p(\phi') \qquad (5.73)$$

where

$$p(\tau') = U(\tau_A, \tau_B) \quad , \qquad p(\phi') = U(\phi_A, \phi_B) \quad , \tag{5.74}$$

Eq. (5.72) may be written as

$$I_p^{(e)}(x, Y) = \ln \frac{(\tau_B - \tau_A)(\phi_B - \phi_A)}{\int \frac{1}{\sqrt{2\pi\rho}} e^{-\frac{1}{2}(\rho \overline{f^2}\, \alpha^2 + \rho \overline{t^2}\, \beta^2 - 2\rho \overline{tf}\, \alpha\beta)} \, dx'} \, . \tag{5.75}$$

The numerator is the a priori surveillance area in the τ - ϕ (or α - β) plane. For a fixed ρ, the width of the volume determined by the integration in the denominator may be measured in terms of the equation

$$\rho \overline{f^2}\, \alpha^2 - 2\rho \overline{tf}\, \alpha\beta + \rho \overline{t^2}\, \beta^2 = 1 \quad , \tag{5.76}$$

since this ellipse describes the locus of points at which the integrand is $e^{-1/2}$ times its maximum value. The area of this ellipse is[57]

$$a = \frac{\pi}{\rho \sqrt{\overline{f^2}\, \overline{t^2} - \overline{tf}^2}} \tag{5.77a}$$

$$= \frac{\pi \sigma_\tau \sigma_f}{1 - D^2} \quad , \tag{5.77b}$$

where

$$\sigma_\tau = \frac{1}{\sqrt{\rho \overline{f^2}}} \tag{5.78}$$

$$\sigma_\phi = \frac{1}{\sqrt{\rho \overline{t^2}}} \tag{5.79}$$

$$D = \frac{\overline{tf}}{\sqrt{\overline{t^2}\,\overline{f^2}}} \quad . \tag{5.80}$$

The information is therefore seen to be related to the logarithm of the ratio of the a priori surveillance area to an equivalent a posteriori area given by Eq. (5.77b). This result is comparable to an expression such as Eq. (3.51) or (3.55a), except for the additional term involving D, which we shall call the interdependence coefficient. For given values of σ_τ and σ_ϕ, maximum information is obtained when D = 0.

Since

$$\overline{tf} = \frac{-j2\pi A^2}{2E} \int_{-\infty}^{\infty} u^*(t)\, t\, u'(t)\, dt \quad , \qquad (5.81)$$

then the Schwarz inequality

$$\left| \int f^*(t)\, g(t)\, dt \right|^2 \leq \int f^*(t)\, f(t)\, dt \cdot \int g^*(t)\, g(t)\, dt \quad , \qquad (5.82)$$

with

$$f(t) = \frac{2\pi A}{\sqrt{2E}}\, u(t)\, t \qquad (5.83)$$

$$g(t) = -\frac{jA}{\sqrt{2\pi}}\, u'(t) \qquad (5.84)$$

shows that

$$|\overline{tf}| \leq \sqrt{\overline{t^2}\ \overline{f^2}} \quad . \qquad (5.85)$$

Therefore, we have

$$|D| \leq 1 \quad . \qquad (5.86)$$

In terms of D, the ellipse in Eq. (5.76) is

$$\alpha'^2 - 2D\, \alpha'\, \beta' + \beta'^2 = 1 \quad , \qquad (5.87)$$

where α' and β' are normalized variables given by

$$\alpha' = \sqrt{\rho\ \overline{f^2}}\ \alpha = \frac{\alpha}{\sigma_\tau} \qquad (5.88)$$

$$\beta' = \sqrt{\rho\ \overline{t^2}}\ \beta = \frac{\beta}{\sigma_\tau} \quad . \qquad (5.89)$$

In matrix form, the ellipse in Eq. (5.87) is

$$\begin{bmatrix} \alpha' & \beta' \end{bmatrix} \begin{bmatrix} 1 & -D \\ -D & 1 \end{bmatrix} \begin{bmatrix} \alpha' \\ \beta' \end{bmatrix} = 1 \quad . \qquad (5.90)$$

The eigenvalues of the square matrix are the roots of the characteristic equation

$$\begin{vmatrix} 1-\lambda & -D \\ -D & 1-\lambda \end{vmatrix} = 1 \quad , \qquad (5.91)$$

which are

$$\lambda_1 = 1 + D \quad , \qquad (5.92a)$$

$$\lambda_2 = 1 - D \quad . \qquad (5.92b)$$

The lengths of the semi-major and semi-minor axes are therefore

$$\frac{1}{\sqrt{\lambda_1}} \qquad \text{and} \qquad \frac{1}{\sqrt{\lambda_2}} \quad . \qquad (5.93)$$

If D = 0, then the ellipse becomes a circle and we may say that there is no interdependence between range and Doppler information. This occurs, for example, if we have rectangular amplitude modulation and no phase modulation, since then

$$\overline{tf} = \frac{j2\pi A^2}{2E} = \int_{-P/2}^{P/2} t\, R(t)\, R'(t) = 0 \quad . \qquad (5.94)$$

In another practical case, suppose that rectangular amplitude modulation is used with linear frequency modulation over a large time-bandwidth product PB. Then

$$\overline{tf} = \frac{-j2\pi}{2E} \int_{-P/2}^{P/2} A^2 e^{-j2\pi\theta(t)}\, t \left(j2\pi\, e^{j2\pi\theta(t)}\, \dot{\theta}(t)\right) dt$$

$$= \frac{(2\pi)^2}{2E} \int_{-P/2}^{P/2} A^2\, t\, \dot{\theta}(t)\, dt \quad . \qquad (5.95)$$

Letting

$$f = \dot{\theta}(t) = \frac{B}{P}\, t \,, \qquad -\frac{P}{2} \le t \le \frac{P}{2} \quad , \qquad (5.96)$$

then

$$\overline{tf} = \frac{(2\pi)^2}{2E} \int_{-P/2}^{P/2} \frac{A^2 B}{P}\, t^2\, dt = \frac{\pi^2 BP}{3} \quad . \qquad (5.97)$$

Also,

$$\overline{t^2} = \frac{(2\pi)^2}{2E} \int_{-P/2}^{P/2} A^2\, t^2\, dt = \frac{\pi^2 P^2}{3} \qquad (5.98)$$

and

$$\overline{f^2} = \frac{(2\pi)^2}{2E} \int_{-B/2}^{B/2} f^2\, df = \frac{\pi^2 B^2}{3} \quad . \qquad (5.99)$$

So

$$D = \frac{\overline{tf}}{\sqrt{\overline{t^2}\ \overline{f^2}}} = 1 \qquad (5.100)$$

The eigenvalues are therefore 0 and 2, and the ellipse has elongated to an infinite length with the interdependence coefficient reaching its maximum value. Since the semi-minor axis length is equal to $\frac{1}{\sqrt{2}}$ and the ellipse (always) intersects all four axes at ± 1, then the ellipse is readily deduced to be at an angle of 45° with respect to the coordinate $\alpha' - \beta'$ axes.

6. APPLICATION OF RESULTS

6.1 Description of an Existing Advanced FM Radar System

In this chapter, a practical radar example is considered to illustrate the application of some of the analytical results obtained previously. We shall deal with an advanced type of radar system having a high pulse-compression ratio, and demonstrate quantitatively how its performance may be improved by means of the derived concepts. Such a radar is the linear-FM (chirp-type) pulse compression system described in reference 58, which has one of the highest pulse compression ratios implemented to date in an operational radar, namely 8,000. This "range-channel" system achieves a nominal range resolution of 123 ft. and transmits sufficient energy on a single pulse to obtain a 15 db signal-to-noise ratio on a radar cross section of 0.1 m^2 at a range of approximately 1000 nautical miles. Although this radar represents an advanced state-of-the-art implementation, it will be shown that:

(a) By using the proposed nonlinear processing, the range resolution can be improved by a factor in the order of $\sqrt{\rho}$, where ρ is defined in Eq. (3.29).

(b) The detection-information criterion for setting the detection threshold leads to a procedure in which detection probability increases with time for a constant overall false-alarm probability. In a numerical example, it is shown that the new procedure is substantially more efficient than a conventional Neyman-Pearson amplitude procedure.

The radar has the following parameters:

Peak power	2.5 Mw
Pulse duration, P	2000 microseconds
Pulse repetition frequency, f_r	30 pps (period, τ_r = 33 m sec)
Beamwidth	2.2 degrees
Signal bandwidth, B	4 Mc linear frequency deviation centered at f_o = 427 Mc
Range window	16.4 nm

The system concept is readily explained from the simple block diagram in Fig. 6.1. The EXCITER generates a linear FM ramp at the radar's pulse repetition frequency. This transmitted frequency is labeled FR in Fig. 6.2. The echo pulses* E arrive at a range delay τ_o after signal transmission and, at that time, a range-tracking local-oscillator FM ramp is generated by the EXCITER, which is called the delayed

* Only one target echo ramp is shown in Fig. 6.2 for illustration but there is actually one for each target present.

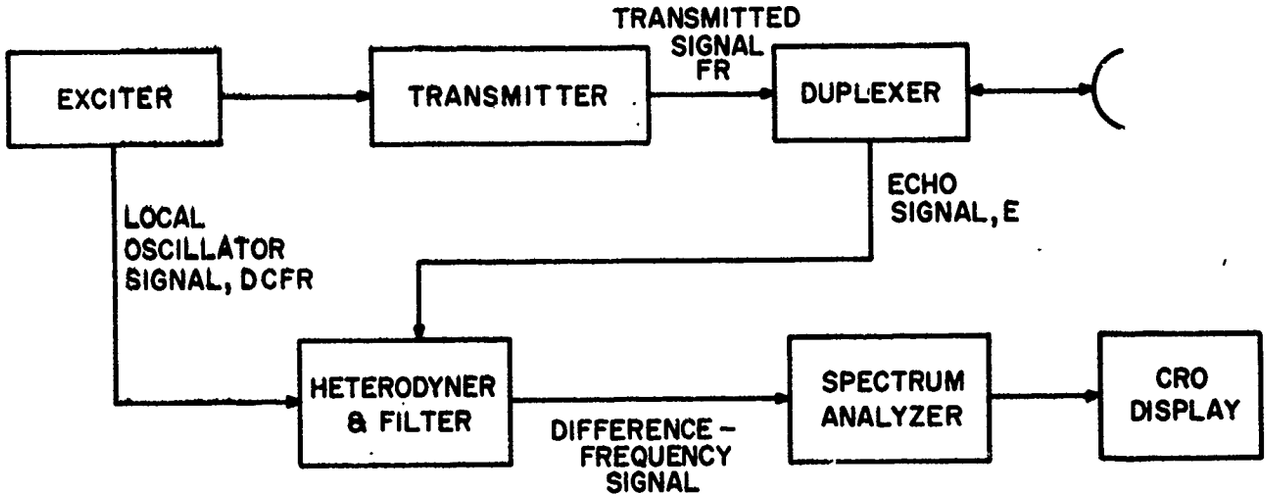

Fig. 6.1 Simplified Block Diagram of an Advanced FM Radar

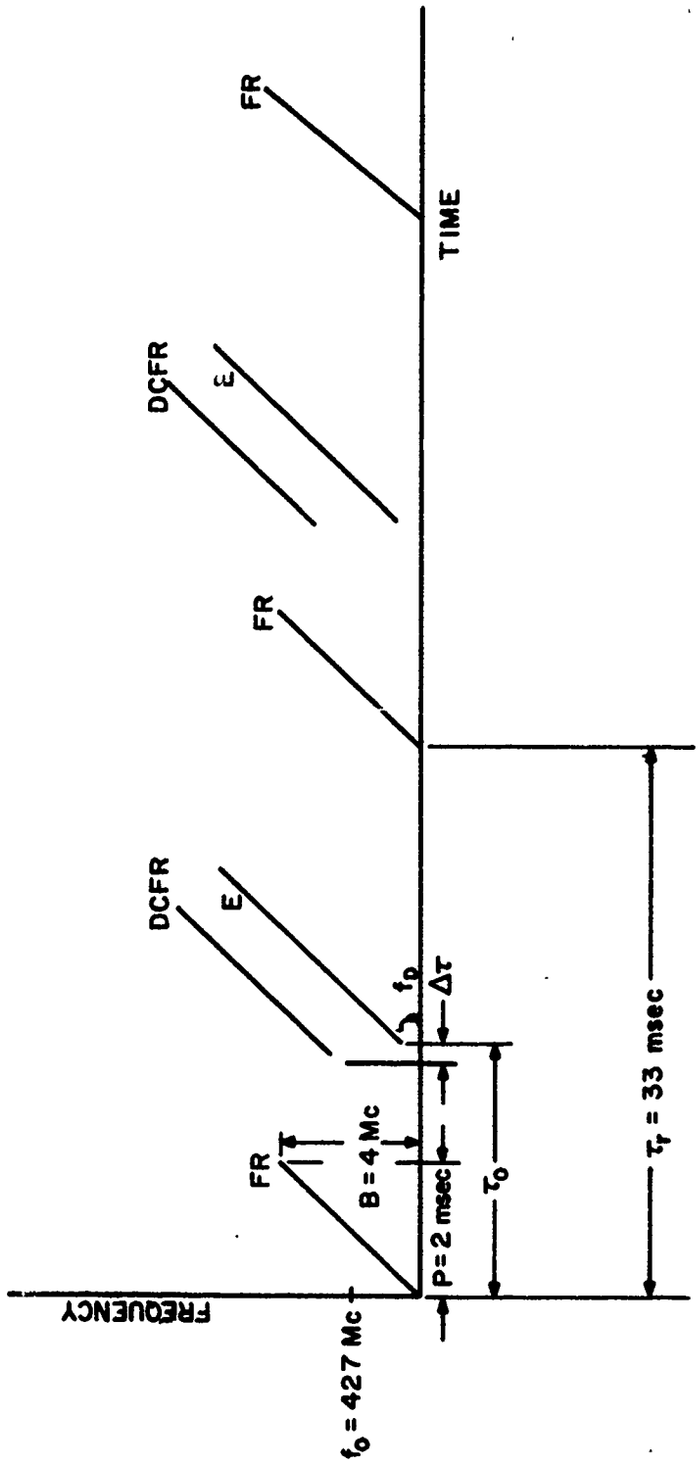

Fig. 6.2 Relative Positions of Frequency Ramps

coherent frequency ramp DCFR. The DCFR is heterodyned with the echo signal and the difference-frequency signal is passed through a real-time spectrum analyzer (Coherent Memory Filter) and displayed on an oscilloscope. If the DCFR and the echo E exactly overlap in time ($\Delta\tau = 0$), the difference-frequency signal consists of a constant-frequency pulse of duration P with a frequency of

$$f_d = f_{IF} - f_D$$

where

f_{IF} = i-f offset frequency

f_D = Doppler shift frequency.

Since the pulse width is equal to P, the spectrum analysis can determine f_D with a resolution in the order of $\frac{1}{P} = 500$ cps. In fact, we can think of the spectrum analyzer as a bank of contiguous filters, each having a bandwidth of $\frac{1}{P}$ cps which is matched to the duration of the difference-frequency pulse. The ratio of peaked mean-square signal to mean-square noise at the spectrum analyzer output is calculated from the matched-filter output ratio E/N_o, where E is input signal energy and N_o is noise power spectral density. If S_{rms} is the rms value of the difference-frequency sinusoidal pulse, then

$$\frac{E}{N_o} = \frac{S_{rms}^2 P}{N_o} = \frac{S_{rms}^2}{N_o \cdot \frac{1}{P}} \quad , \qquad (6.1)$$

which shows that the effective noise bandwidth of the radar is 1/P cps.

If the DCFR does not exactly overlap the echo E in time, then the difference frequency is

$$f_d = f_{IF} + a\,\Delta\tau - f_D \qquad (6.2)$$

where

$$a = \frac{B}{P} = \text{ramp slope} = 2000 \text{ cps/microsecond.} \qquad (6.3)$$

For

$$\Delta\tau << P \quad , \qquad (6.4)$$

the difference-frequency pulse has a duration of approximately P. So the spectrum analysis still resolves frequencies in the order of 1/P cps and therefore range-delay resolution is obtained such that

$$a\,\Delta\tau = \frac{1}{P} \quad , \qquad (6.5)$$

or

$$\Delta\tau = \frac{1}{aP} = \frac{1}{B} = 0.25 \text{ microsecond} \quad . \qquad (6.6)$$

Within the radar's range window of 16.4 nm, there are about 810 range resolution cells, which also represents the number of independent opportunities for a false alarm for each radar pulse. A characteristic property of all linear-FM systems is that there is a severe interdependence (or ambiguity) between range and Doppler information. This interdependence was demonstrated by the defined interdependence coefficient D that was shown to have the maximum value of unity for linear FM. The interdependence is clearly seen in the radar under consideration since both range and Doppler effects produce changes in the same measured variable f_d. In fact, the interdependence is so extreme that, for a number of closely-spaced targets flying at nearly the same velocities, the f_d frequency axis is used entirely as a relative range axis. (The 500 cps Doppler resolution corresponds to a coarse 578 ft/sec radial velocity resolution, while the 0.25 microsecond range resolution corresponds to a fine range resolution of 123 ft.)

6.2 Design of an Optimum Radar System

6.2.1 Resolution Improvement

A linear matched-filter radar followed by a linear envelope detector produces a voltage proportional to the correlation surface:

$$|\Gamma(\tau,\phi)| = \left| \int_{-\infty}^{\infty} \zeta(t)\, \xi^*(t-\tau)\, e^{-j2\pi\phi t} \right| dt \quad , \qquad (6.7)$$

where

$\xi(t)$ = the transmitted signal

$\zeta(t) = A_o\, \xi(t-\tau_o)\, e^{j2\pi\phi_o t} + \nu(t)$ = noisy received echo.

The width of this surface was seen to be 1/B in the τ direction and 1/P in the ϕ direction, where B and P are the signal bandwidth and duration, respectively.

Since the a posteriori probability density function $p(\tau,\phi/\zeta)$ was found to be proportional to $I_o\left(\frac{1}{k\sigma^2}\,|\Gamma(\tau,\phi)|\right)$, range and Doppler resolutions in the order of the width of $r'(\tau,\phi/\zeta)$ can be obtained by following the linear detector of the preceding linear-matched-filter implementation by a nonlinear element having the characteristic of the modified Bessel function $I_o(x)$. This would then yield resolutions of $\frac{1}{B\sqrt{\rho}}$ and $\frac{1}{P\sqrt{\rho}}$ for τ and ϕ respectively, where

$$\rho = \frac{2E}{k\mathcal{J}} = \frac{2 \text{ X echo signal energy}}{\text{noise power spectral density}} \quad . \qquad (6.8)$$

A block diagram of such a system is presented in Fig. 6.3 where a single channel is illustrated. At the output of the amplifier G, a voltage x(t) occurs having a value of $g|\Gamma(t)|$ where g is adjustable by means of the amplifier gain, G.

We wish to implement a final detected signal $S_o(t)$ that is proportional to

$$\mu(t) = I_o\left(\frac{1}{k\mathcal{J}} |\Gamma(t)|\right) \quad . \qquad (6.9)$$

From Eq. (6.7) it is seen that the maximum value of $|\Gamma(t)|$ is the matched value

$$|\Gamma(\tau_o, \phi_o)| \approx 2E \qquad (6.10)$$

where the approximation stems from the conventional neglect of the noise term $\nu(t)$, which is valid for high signal-to-noise ratios. By defining

$$\Gamma'(t) \equiv \frac{1}{2E} \Gamma(t) \quad , \qquad (6.11)$$

Eq. (6.9) can be written as

$$\mu(t) = I_o(\rho|\Gamma'(t)|) \quad , \qquad (6.12)$$

where

$$\Gamma'(t)_{max} \approx 1 \quad . \qquad (6.13)$$

The $I_o(x)$ characteristic was shown in Fig. 3.7. We may set up the system optimally for a specific signal-to-noise ratio ρ by applying such a calibration signal at the receiver input and adjusting the gain G so that the peak response corresponds to $x_M = \rho$ on the input (abscissa) axis of the implemented $I_o(x)$ characteristic. When this adjustment has been made, the noise power level is at a factor of ρ below the peak power of the signal response (or $\rho/2$ below the rms-squared value at peak response), and therefore the noise power is always concentrated below the knee of the $I_o(x)$ curve.

In the practical case, the input signal-to-noise ratio may cover a range of possible values. Now suppose that we have optimally set the gain G for a particular signal-to-noise ratio ρ_o. If a signal voltage twice as large as expected then arrives, $|\Gamma(t)|$ increases by a factor of 2, as indicated by an increase in A_o of Eq. (6.7). For the same gain G previously used, the excursion of x in Fig. 3.7 increases by a factor of 2. However, the increase in input voltage by a factor of 2 implies an increase in input ρ by a factor of 4 so that, optimally, the x-excursion should have increased by a factor of 4. Thus the system is gain-matched only for $\rho = \rho_o$. For illustration, suppose that

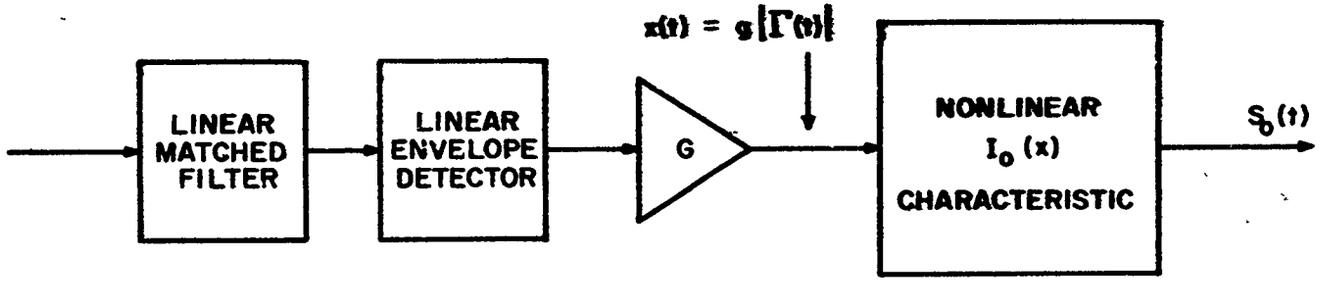

Fig. 6.3 Block Diagram of Nonlinear Receiver (Single Channel)

the input signal-to-noise ratio may vary such that

$$4 \leq \rho \leq 25 \quad (6 \text{ db to } 14 \text{ db}) \quad . \qquad (6.14)$$

As a compromise, we may set our gain G so that it is optimum for an input signal of

$$\rho_o = 10\text{db} = 10 = \frac{2E_o}{kJ} \quad . \qquad (6.15)$$

If the signal with ρ = 6db should occur, it is a factor of 4 db = 1.58 less in voltage and its peak response will only reach 10/1.58 = 6.33 on the x-axis instead of $\rho_o = 10$. On the other hand, if a signal with ρ = 14db should enter, its peak response will reach 1.58 x 10 = 15.8 on the x-axis. Fig. 6.4 shows a comparison of the normalized response $I_o(\rho|\Gamma'(t)|)/I_o(\rho)$ obtained in the above situations, where it is always assumed that the nonlinear system is set for $\rho_o = 10$; i.e., we are implementing

$$\mu(t) = I_o(\rho_o|\Gamma'(t)|) \quad , \qquad (6.16)$$

where

$$\Gamma'(t) = \frac{1}{2E_o}\Gamma(t) \quad , \qquad (6.17)$$

in which E_o is a constant while $\Gamma(t)$ changes proportionally with input voltage. Fig. 6.4(a) illustrates a typical linear response and Fig. 6.4(b) shows the gain-matched nonlinear response for $\rho = \rho_o = 10$. The significance of the improvement is best illustrated by observing that the lateral (range) jitter of the peak in Fig. 6.4(a) is characterized by a standard deviation of $1/\beta\sqrt{\rho_o}$ in range delay or $\alpha/B\sqrt{\rho_o} = 1/P\sqrt{\rho_o}$ in frequency, as indicated on the figure, where it is assumed that ρ_o is the actual input value of ρ. Thus the jitter (precision) is less than the resolution (granularity or accuracy). On the other hand, the peak width (granularity) in Fig. 6.4(b) is comparable to the lateral jitter (precision). The situation is analogous to observing an ammeter reading in which the thickness of the needle is equivalent to our resolution width. It is most desirable to have the needle width comparable to the needle jitter (as in Fig. 6.4(b)) rather than much larger (as in Fig. 6.4(a)) or much smaller. Likewise, the granularity of the scale on which we are reading should have its smallest division comparable to the jitter width (and therefore the needle width also). In Fig. 6.4(c), the response is given for an input ρ of 6 db while the receiver is set for ρ_o = 10 db. Here the noise becomes more prominant since the gain G is too high. Also, the width of the peak would be narrower than is theoretically justified so that the lateral jitter would exceed the response width. Fig. 6.4(d) shows the response for ρ = 14 db, which is higher than the set $\rho_o = 10$. Here the peak width is not as narrow as it should be and some resolution is sacrificed. In most applications, the Bessel-function detector

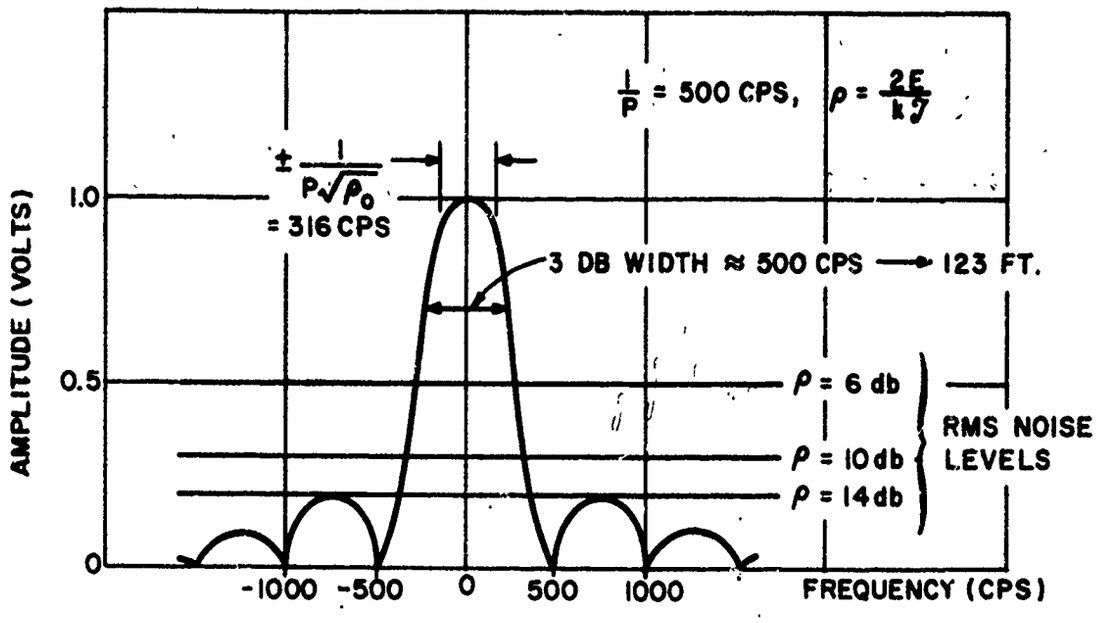

(a) Linear System

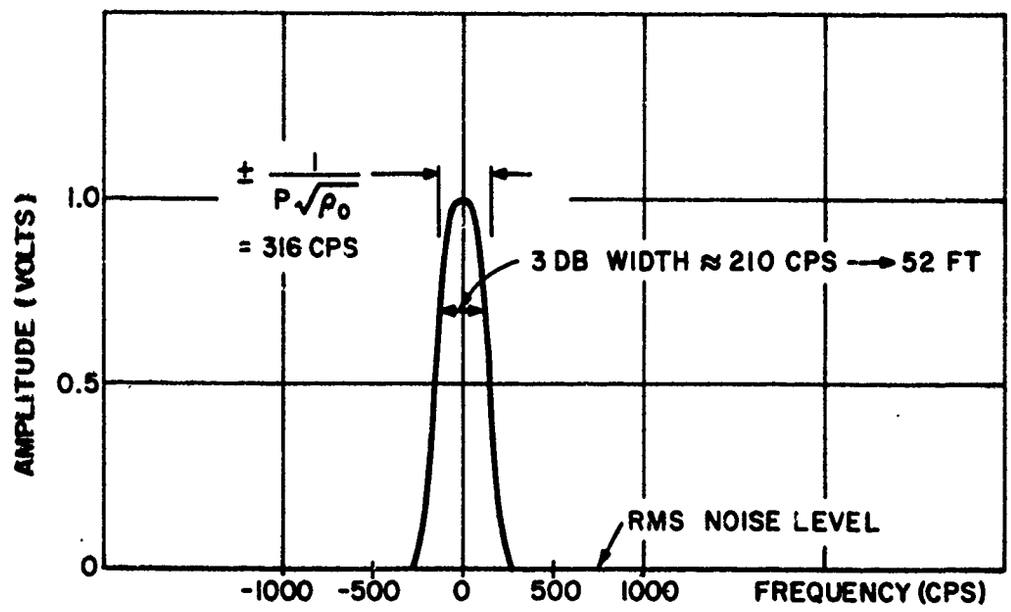

(b) Nonlinear System, $\rho = \rho_o = 10$ db

Fig. 6.4 Comparison of Linear and Nonlinear Resolutions

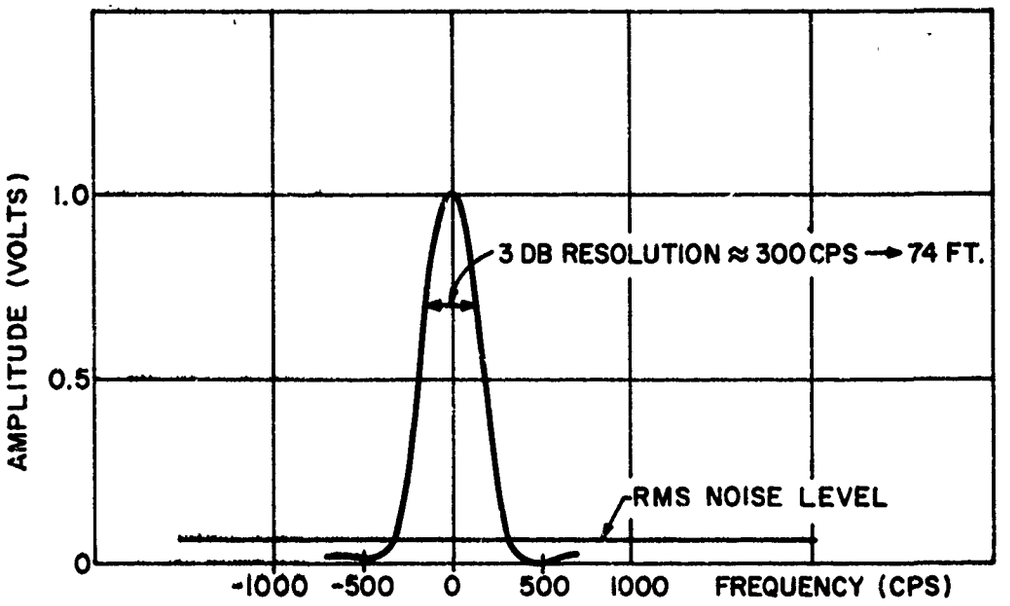

(c) Nonlinear System, ρ = 6 db , ρ_o = 10 db

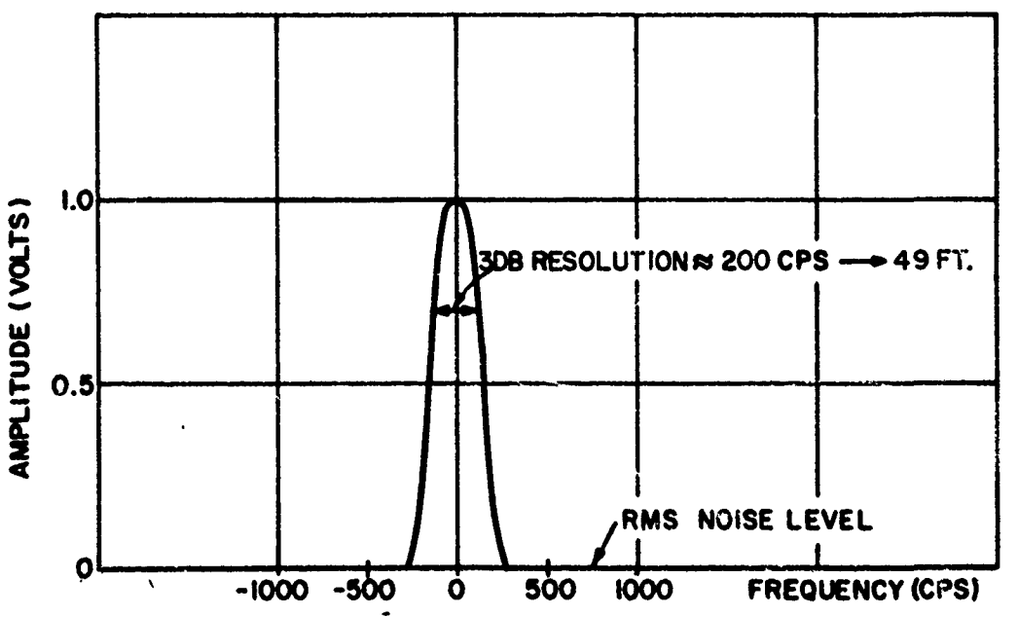

(d) Nonlinear System, ρ = 14 db, ρ_o = 10 db

Fig. 6.4 Comparison of Linear and Nonlinear Resolutions (cont' d.)

may be used in parallel with a standard linear detector and then employed for improved resolution on a target whose signal-to-noise ratio can be judged from the linear display. Thus the gain G of the nonlinear system may be properly adjusted for near-optimum performance.

An alternative to the above implementation is to replace the linear detector in Fig. 6.3 with a square-law detector. Then we are implementing an output signal $S_o(t)$ that is proportional to

$$\mu'(t) = I_o\left(\rho_o^2 \left|\Gamma'(t)\right|^2\right) \quad , \qquad (6.18)$$

where

$$\left|\Gamma'(t)\right|_{max} = 1$$

and the gain G is set so that an input calibration signal with signal-to-noise parameter ρ_o will give a maximum excursion of $x_M = \rho_o^2$. Now, however, an increase in input voltage by a factor of 2 will change the x-excursion by a factor of 4 and therefore the new maximum value x_M will be ρ^2, as it should. Therefore, this method employing a square-law detector always remains gain-matched, although we have altered the response shape because of the presence of $\left|\Gamma'(t)\right|^2$ rather than $\left|\Gamma'(t)\right|$.

6.2.2. Improvement in Detection Capability by Employment of the Detection-Information Procedure

In the radar under consideration, for each transmitted pulse there are n = 810 independent opportunities for a noise threshold crossing and one opportunity for a threshold crossing due to signal (with a single target). We shall assume that a threshold test is made for each such transmitted radar pulse. The detection probability P_D may be calculated from curves or tables of the Rice distribution for any assumed signal-to-noise ratio.[4,5,34] The false alarm probability is expressible as

$$P_{FA} = 1 - (1 - P'_{FA})^{810} \approx 810\, P'_{FA} \quad , \text{ for } \quad 810\, P'_{FA} << 1 \quad , \qquad (6.19)$$

where

P_{FA} = probability that at least one noise sample exceeds the threshold out of 810 samples, where each sample has an individual probability (Rayleigh-distributed) P'_{FA} of crossing the threshold.

We may plot I vs. threshold-to-rms noise level R_T/σ_N for various values of signal-to-noise ratio, as shown in Fig. 6.5.

As an example of the application of the above results, we shall assume that the

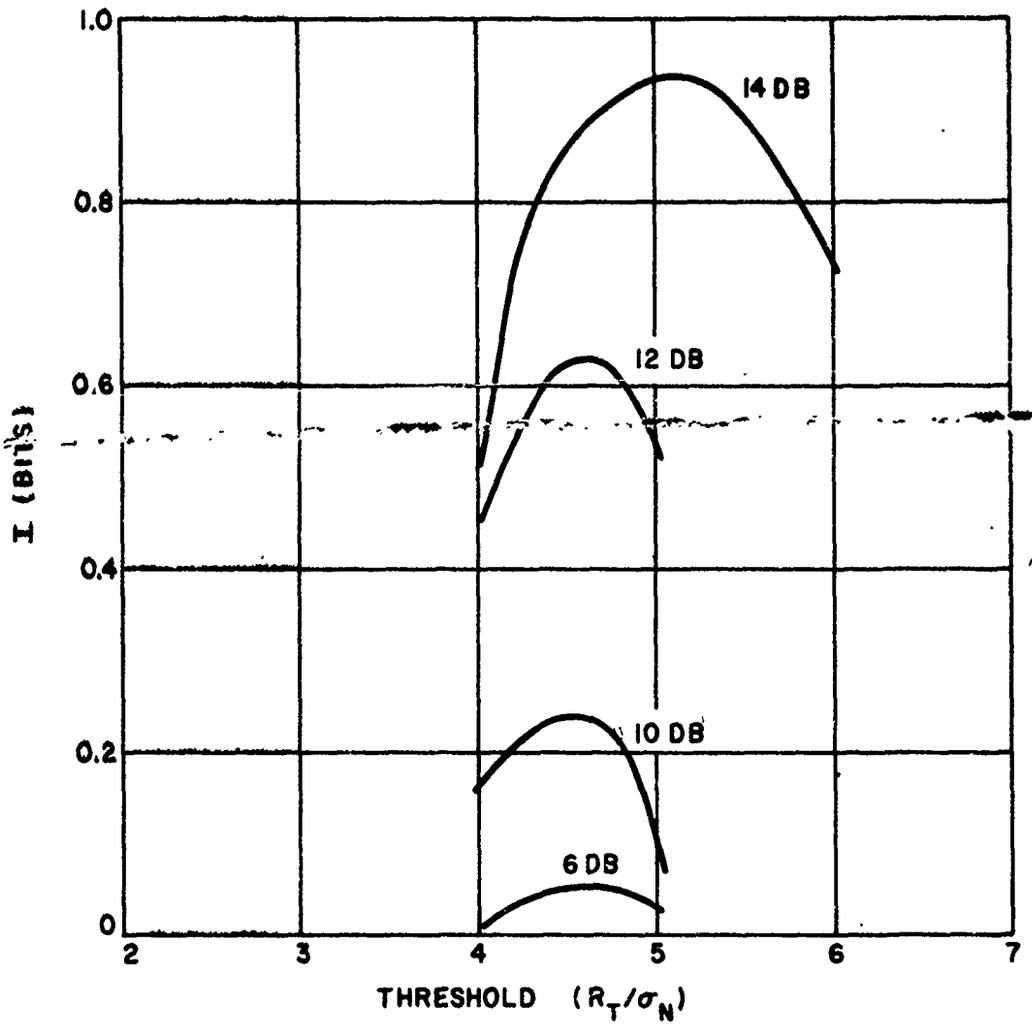

Fig. 6.5 Detection Information vs. Threshold Level For Various Values of S/N Ratio

threshold employed is 4.5. This yields maximum information for S/N ratios from at least 6 db to 12 db, although the amount of information decreases with decreasing S/N values. The false-alarm probability for a single radar pulse is then

$$P_{FA} = 810\ P'_{FA} = 0.0405 \quad , \qquad (6.20)$$

from the Rayleigh distribution. We now accept a "normal" false alarm rate based on this probability. We postulate a detection procedure in which a single output pulse is generated if there are one or more threshold crossings per radar pulse. If there is no signal present, the probability of getting such an output pulse is $P_{FA} = 0.0405$. This may be considered to be a stochastic process in which the probability of some event occurring is $p_o = 0.0405$. Then the probability of exactly k such events in $\tilde{n}$ trials is given by the binomial distribution

$$p(k) = \binom{\tilde{n}}{k} p_o^k\ (1 - p_o)^{\tilde{n}-k} \quad , \qquad (6.21)$$

which is approximately equal to the normal distribution:* $N(\tilde{n}p_o,\ \tilde{n}p_o(1 - p_o))$, for[56] $\tilde{n}p_o(1-p_o) \geq 3$. In the radar under consideration, the pulse repetition frequency is $f_r = 30$ pps so the normality approximation will hold after a time duration of about

$$\tilde{n} = \frac{3}{p_o(1-p_o)} = 77 \text{ pulses} \qquad (6.22)$$

or

$$\frac{\tilde{n}}{f_r} = \frac{77 \text{ pulses}}{30 \text{ pps}} = 2.6 \text{ seconds} \quad . \qquad (6.23)$$

The density function for output pulse rate $k/\tilde{T}$ is $N\left(\frac{\tilde{n}p_o}{\tilde{T}},\ \frac{\tilde{n}p_o(1-p_o)}{\tilde{T}^2}\right)$. The duration $\tilde{T}$ will be taken as an integral number of pulse repetition periods, so the density function may be expressed as being $N\left(f_r p_o,\ \frac{f_r p_o(1-p_o)}{\tilde{T}}\right)$. Here it is seen that the mean value of rate is constant and the variance decreases proportionally with time duration. The mean value of false-alarm rate can be determined precisely from standby observations on the radar. When a signal appears, the data rate increases and essentially becomes equal to the sum of (a) the false alarm rate and (b) the rate with signal present but no false alarms included. To a good approximation, this new rate with signal present has the distribution of the sum of two independent normal variables and is $N\left(f_r p_o + f_r p_1,\ \frac{f_r p_o(1-p_o)}{\tilde{T}} + \frac{f_r p_1(1-p_1)}{\tilde{T}}\right)$, where $p_1 = P_D$ is the probability

---

* Even when the normal approximation does not hold, however, the mean and variance are still given by np_o and $np_o(1-p_o)$, respectively.

that a signal-plus-noise sample exceeds the threshold. The two rate density functions (signal absent and signal present) were illustrated in Fig. 4.2.

We may apply the procedure by specifying some overall false-alarm probability, say $\tilde{P}_{FA} = 0.01$, after $\tilde{T}$ seconds of observation time. In the absence of signal, the density function for rate is (approximate for $\tilde{T} < 2.6$ seconds)

$$N\left(f_r p_o, \frac{f_r p_o (1-p_o)}{\tilde{T}}\right) = N\left(1.215, \frac{1.167}{\tilde{T}}\right) , \qquad (6.24)$$

where

f_r = 30 pulses per second

p_o = 0.0405 = probability of a false alarm for one radar pulse (810 noise samples).

The amplitude threshold is assumed to be set at 4.5, with respect to rms noise. For an overall false alarm probability of $\tilde{P}_{FA} = 0.01$, the data-rate threshold must be set at 2.33 standard deviations above the mean value. This data-rate threshold r_T is tabulated in Table 6.1:

TABLE 6.1 DATA-RATE THRESHOLD FOR $\tilde{P}_{FA} = 0.01$

$\tilde{T}$ (seconds)	r_T (output pulses per second)
1	3,730
2	2,880
3	2,707
4	2,474
5	2,340
6	2,264
7	2,185
8	2,122
9	2,033
10	2,012

As an example, we shall assume the sudden appearance of a signal with an rms signal-to-noise ratio of S/N = 6 db. With the chosen amplitude threshold of 4.5, the probability of a single sample of signal-plus-noise crossing the amplitude threshold is $p_1 = 0.07$. The probability density function for rate therefore changes to

$$N\left(f_r p_o + f_r p_1, \frac{f_r p_o(1-p_o)}{\tilde{T}} + \frac{f_r p_1 (1-p_1)}{\tilde{T}}\right) = N\left(3.315, \frac{3.119}{\tilde{T}}\right) \qquad (6.25)$$

Table 6.2 lists the difference between the mean value and the threshold rate r_T in standard-deviation units, and also the corresponding overall detection probability:

Table 6.2 DETECTION PROBABILITY FOR DETECTION-INFORMATION PROCEDURE, S/N = 6 db

$\tilde{T}$ (seconds)	Mean Value Minus r_T (standard deviation units)	$\tilde{P}_D$
2	0.349	0.64
3	0.592	0.72
4	0.955	0.83
5	1.235	0.89
6	1.465	0.93
7	1.695	0.96
8	1.920	0.97
9	2.190	0.99
10	2.342	0.99

For comparison, we may consider the Neyman-Pearson approach with the same radar. Again we shall assume an overall false-alarm probability of 0.01. After $\tilde{T}$ seconds, there are a total of $810 f_r \tilde{T}$ independent noise samples which can cross the amplitude threshold. The overall probability of a false alarm is

$$\tilde{P}_{FA} = 1 - (1 - P'_{FA})^{810 f_r \tilde{T}} = 24,300\, \tilde{T}\, P'_{FA} = 0.01 \quad , \qquad (6.26)$$

where

P'_{FA} = probability that a single noise sample exceeds the amplitude threshold.

The single-sample false-alarm probabilities are tabulated in Table 6.3 with the required thresholds:

Table 6.3 SINGLE-SAMPLE FALSE ALARM PROBABILITIES P'_{FA} AND THRESHOLDS FOR NEYMAN-PEARSON PROCEDURE (overall $\tilde{P}_{FA} = 0.01$)

$\tilde{T}$ (seconds)	P'_{FA}	Threshold, R_T/σ_N
2	2.06×10^{-7}	5.55
3	1.37×10^{-7}	5.63
4	1.03×10^{-7}	5.67
5	8.23×10^{-8}	5.71
6	6.86×10^{-8}	5.74
7	5.88×10^{-8}	5.76
8	5.15×10^{-8}	5.79
9	4.58×10^{-8}	5.82
10	4.12×10^{-8}	5.84

For the listed thresholds, the single-sample detection probability P'_D with S/N = 6 db ranges from 0.005 to 0.002 (using the Rice distribution)as $\tilde{T}$ varies from 2 seconds to 10 seconds. The overall probability of detection is given by

$$\tilde{P}_D = 1 - (1 - P'_D)^{f_r \tilde{T}} \qquad (6.27)$$

and is tabulated in Table 6.4:

Table 6.4 - DETECTION PROBABILITY FOR NEYMAN-PEARSON METHOD, S/N = 6 db

$\tilde{T}$ (seconds)	P'_D	$f_r \tilde{T}$	$\tilde{P}_D$
2	0.0050	60	0.26
3	0.0042	90	0.32
4	0.0038	120	0.38
5	0.0033	150	0.40
6	0.0030	180	0.44
7	0.0028	210	0.45
8	0.0025	240	0.46
9	0.0022	270	0.46
10	0.0020	300	0.46

Comparative results for the two procedures are plotted in Fig. 6.6. The higher detection efficiency of the detection-information procedure is attributed to its initial optimization of the amplitude threshold independent of the detection and false alarm probabilities. In the Neyman-Pearson amplitude approach, however, the amplitude threshold determines the false alarm probability. In the cited example, the particular overall false alarm probability that was set required an amplitude threshold that was rather high and relatively inefficient for detecting low-level signals such as the signal assumed at S/N = 6 db.

In addition to the greater efficiency of the detection-information approach, there are no "false alarms" in the sense understood in the Neyman-Pearson amplitude approach. That is, in the Neyman-Pearson amplitude method a false alarm is considered to occur whenever noise alone crosses the amplitude threshold. However, in the detection-information procedure, a certain standby threshold-crossing rate is accepted as normal. An alarm occurs only when the rate increases "significantly". Just how much of a rate increase is considered significant depends upon the confidence we wish to achieve in avoiding a "false alarm type of mistake".

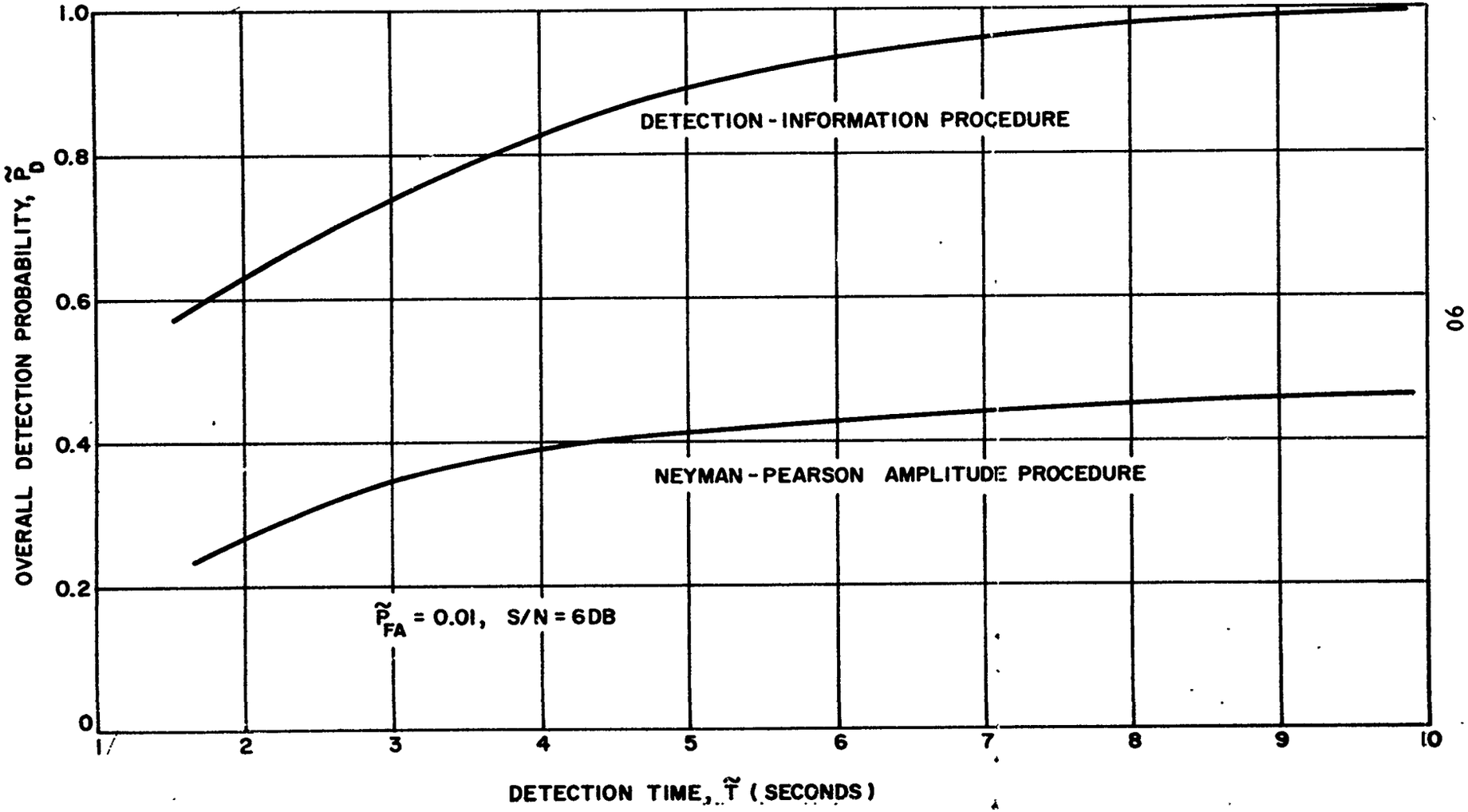

Fig. 6.6 Comparison of Detection Probabilities for Detection-Information Procedure and Neyman-Pearson Amplitude Procedure

7. CONCLUSION

7.1 General Results

By employing a strict information-theory approach to radar, it has been possible to develop a new view of radar signal processing leading to a substantial insight into "ideal" matched-filter receivers. This generalized viewpoint has yielded a number of significant results, as listed in Chapter 1, which include a method of improving radar resolution by means of a nonlinear Bessel-function envelope detector and a new radar detection philosophy based upon a defined "detection information" and a data-rate threshold. In an illustrative example dealing with an existing advanced FM radar, the new detection procedure was shown to be superior to a conventional Neyman-Pearson procedure applied to amplitude.

Of a more basic nature, theory and examples have been presented to show that the information obtained by a radar is directly related to the input physical entropy of the receiver, with this physical entropy being synonymous with signal-to-noise energy ratio (SNER). This result implies that the parameter information has the character of a physical entity rather than only an arbitrary measure. Relations were also developed which clarify the role of the SNER in improving radar detection and in improving the measurement "reliability" of the radar.

A specific formula for parameter information was also derived, in terms of a multiple-target echo ambiguity function, which may be used to evaluate the variation of the information with changes in the radar waveform or the target environment. Analysis of the formula for high signal-to-noise ratios has lead to the definition of an explicit interdependence coefficient between range and Doppler information.

A new representation and treatment of time-limited or bandwidth-limited white noise was developed which was found to be of considerable use in the information-theory approach to radar analysis. This representation in terms of modes (or degrees of freedom) should also be found useful in other noise problems.

7.2 Further Work

Considerable further work may be done along the lines pursued in this dissertation. Additional theory and examples to substantiate the physical nature of parameter information would be desirable, and possibly an experimental "transducer" to convert such information into useful work.

A major problem area in current radar design deals with waveform analysis and synthesis. It is suggested that a useful tool in such problems would be the evaluation of the expected parameter information for specific assumed target distributions.

This would appear to be a valuable adjunct to the present practice of studying the ambiguity function of the waveform. In particular, it yields a single number as a performance measure in a target situation that may be quite complex.

It was shown, for the linear receiver, that the parameter information does not exceed the input entropy. In the case of the nonlinear receiver, this condition was postulated (Eq. 3.66). A proof or demonstration of this would be desirable for the nonlinear case.

The existence of a positional type of information, and its relation to the form of Shannon's information, as in Eq. (3.116), opens the door to a more general theory of communication in which both positional and amplitude information are communicated over a channel. It would be worthwhile to explore this broader view of a communication link.

The improvement in resolution by means of a Bessel-function envelope detector, and the new radar detection procedure based upon detection information, both appear to be valuable contributions to current radar practice and should lead to effective, yet simple, means of improving radar performance. It is recommended that these techniques be implemented and their operational performance compared to that of conventional practice.

BIBLIOGRAPHY

1. L. N. Ridenour, Radar System Engineering, M. I. T. Radiation Laboratory Series, Vol. 1, McGraw-Hill Book Co., Inc., New York, N. Y., 1947, pp 33-35.

2. D. O. North, "An Analysis of the Factors Which Determine Signal/Noise Discrimination in Pulsed-Carrier Systems", RCA Tech. Rept. PTR-6C; June 25, 1943.

3A. W. W. Peterson, T. G. Birdsall, W. C. Fox, "The Theory of Signal Detectability", IRE Trans. PGIT-4; September 1954.

3B. D. Middleton, "Statistical Criteria for the Detection of Pulsed Carriers in Noise", Parts I and II, J. Appl. Phys., Vol. 24; April 1953.

4. M. Schwartz, "A Coincidence Procedure for Signal Detection", IRE Trans. PGIT-2; December 1956.

5. J. I. Marcum, "A Statistical Theory of Target Detection by Pulsed Radar", IRE Trans. PGIT-6; April 1960. Originally published as RAND Research Memo. RM-754, December 1, 1947 and RM-753, July 1, 1948.

6. J. L. Lawson, G. E. Uhlenbeck, Threshold Signals, M. I. T. Radiation Laboratory Series, Vol. 24, McGraw-Hill Book Co., Inc., New York, N. Y. 1950. Section 7.5, pp. 167-173.

7. D. Middleton, "Statistical Theory of Signal Detection", IRE Trans., PGIT-3; March 1954.

8. D. Van Meter, D. Middleton, "Modern Statistical Approaches to Reception in Communication Theory", IRE Trans. PGIT-4; September 1954.

9. D. Middleton, D. Van Meter, "Detection and Extraction of Signals in Noise from the Viewpoint of Statistical Decision Theory", J. Soc. Ind. Appl. Math., Vol. 3, December 1955 and Vol. 4, June 1956.

10. J. J. Bussgang, D. Middleton, "Optimum Sequential Detection of Signals in Noise", IRE Trans. PGIT-1, December 1955.

11. H. Blasbalg, "The Relationship of Sequential Filter Theory to Information Theory and Its Application to the Detection of Signals in Noise by Bernoulli Trials", IRE Trans. PGIT-3; June 1957.

12. H. Blasbalg, "The Sequential Detection of a Sine-Wave Carrier of Arbitrary Duty Ratio in Gaussian Noise", IRE Trans. PGIT-3; December 1957.

13. G. W. Preston, "The Search Efficiency of a Probability Ratio Sequential Search Radar", IRE Internat. Conv. Record, Vol. 8, Part 4; 1960.

14. A. Wald, Sequential Analysis, John Wiley and Sons, Inc.; New York, 1947.

15. P. M Woodward and I. L. Davies, "Information Theory and Inverse Probability in Telecommunication", Proc. I. E. E., Vol. 99, Part III; March 1952.

16. I. L. Davies, "On Determining the Presence of Signals in Noise", Proc., I. E. E., Vol. 99, Part III; March 1952.

17. P. M. Woodward, Probability and Information Theory with Applications to Radar, McGraw-Hill Book Co., Inc.; New York; 1953.

18. G. L. Turin, "A Review of Correlation, Matched-Filter, and Signal-Coding Techniques, with Emphasis on Radar Applications", Vol. 1, Tech. Memo 559, Hughes Aircraft Co., Culver City, Calif.; April 1957.

19. W. H. Huggins and D. Middleton, "A Comparison of the Phase and Amplitude Principles in Signal Detection" Proc. National Electronics Conf., Chicago, Vol. 11; 1955.

20. J. Capon, "A Nonparametric Technique for the Detection of a Constant Signal in Additive Noise", WESCON Conv. Record, Part 4; 1959.

21. R. Manasse, "Summary of Maximum Theoretical Accuracy of Radar Measurements", The Mitre Corp.; April 1960.

22. H. Nyquist, "Certain Factors Affecting Telegraph Speed", Bell System Technical Journal; April 1924.

23. R. V. L. Hartley, "Transmission of Information", Bell System Technical Journal; July 1928.

24. C. E. Shannon and W. Weaver, The Mathematic Theory of Communication, The University of Illinois Press, Urbana, Ill; 1962.

25. L. Brillouin, Science and Information Theory, Academic Press, Inc., New York; 1962.

26. W. B. Davenport, Jr. and W. L. Root, An Introduction to the Theory of Random Signals and Noise, McGraw-Hill Book Co., Inc., New York; 1958.

27. M. Schwartz, Information Transmission, Modulation, and Noise, McGraw-Hill Book Co., Inc., New York; 1959.

28. P. Bello, "Time-Frequency Duality", IEEE Trans. PGIT-10; January 1964.

29. D. Gabor, "Theory of Communication", Journ. I. E. E.; November 1946.

30. J. Capon, "On the Properties of a Time-Variable Network; The Coherent Memory Filter", Symposium on Active Networks and Feedback Systems, Polytechnic Institute of Brooklyn; April 1960.

31. D. A. Bell, Electrical Noise, D. Van Nostrand Co., Ltd., London; 1960.

32. A. van der Ziel, Noise, Prentice-Hall, Inc., Englewood Cliffs, N. J.; 1956.

33. H. Nyquist, "Thermal Agitation of Electric Charge in Conductors", Physical Review, Vol, 32; July 1928.

34. S. O. Rice, "Mathematical Analysis of Random Noise", Bell System Technical Journal; January, 1945.

35. D. Middleton, An Introduction to Statistical Communication Theory, McGraw-Hill Book Co., Inc., New York; 1960.

36. M. I. Skolnik, Introduction to Radar Systems, McGraw-Hill Book Co., Inc.; 1962.

37. A. I. Mintzer, "Advanced Radar Signal and Data Processing", Space/Aeronautics; Nov. 1962 and Jan., April, May, 1963.

38. H. Bickel, "Spectrum Analysis with Delay Line Filters", IRE WESCON Convention Record, Part 8; 1959.

39. J. R. Klauder, A. C. Price, S. Darlington, W. J. Albersheim, "The Theory and Design of Chirp Radars", Bell System Technical Journal, Vo. 39; July, 1960.

40. C. E. Cook, "Pulse Compression: Key to More Efficient Radar Transmission", Proc. IRE, Vol. 48; March 1960.

41. C. L. Temes, "An Automatic Tracking System for Coherently Processing a Wide-Band Long-Duration Pulse Sequence", Seventh Annual Radar Symposium, Un. of Michigan, Ann Arbor, Mich.; 1961.

42. C. L. Temes, "Relativistic Consideration of Doppler Shift", IRE Trans. PGANE-6; March 1959.

43. K. S. Miller, Engineering Mathematics, Rinehart and Co., Inc., New York; 1956.

44. C. L. Temes, "Implementation of the Ideal Radar Receiver Using the Coherent Memory Filter", IRE Seventh Annual East Coast Conference on Aero. and Navig. Electronics, Baltimore, Md.; 1960.

45. C. L. Temes, "Sidelobe Suppression in a Range-Channel Pulse-Compression Radar", IRE Trans. PGMIL-6, No. 2; April 1962.

46. V. M. Faires, Applied Thermodynamics, The MacMillan Co., New York, N. Y.; 1949.

47. M. W. Zemansky, Heat and Thermodynamics, McGraw-Hill Book Co., Inc., New York; 1957.

48. R. H. Fowler, Statistical Mechanics, The University Press, Cambridge, England; 1936.

49. G. Joos, Theoretical Physics, Hafner Publishing Co., New York, N. Y.; 1950.

50. H. Margenau, G. M. Murphy, The Mathematics of Physics and Chemistry, D. Van Nostrand Co., Inc., New York, N. Y.; 1956.

51. A. J. Dekker, Solid State Physics, Prentice-Hall, Inc., Englewood Cliffs, N. J.,; 1958.

52. R. M. Fano, Transmission of Information, The M. I. T. Press and John Wiley and Sons, Inc., New York, N. Y.; 1961.

53. J. P. Den Hartog, Mechanical Vibrations, McGraw-Hill Book Co., Inc., New York, N. Y., 3rd ed., 1942.

54. C. L. Temes, "An Automatic Frequency-Control System for a High-Frequency Resonant-Type Fatigue Testing Machine", Proc. of Soc. for Exper. Stress Analysis; 1956.

55. C. L. Temes, "Analysis of a Servomechanism for Fatigue-Testing Metal Blades", M. S. Thesis, Case Institute of Technology, Cleveland, Ohio; 1954.

56. E. Parzen, Modern Probability Theory and Its Applications, John Wiley and Sons, Inc., New York, N. Y.; 1960.

57. C. W. Helstrom, Statistical Theory of Signal Detection, The MacMillan Co., New York, N. Y.; 1960.

58. C. L. Temes, A. Citrin, M. A. Laviola, H. K. Boyce, J. P. Biggs, "Pulse-Compression Subsystem for a Down-Range Tracker", IEEE International Convention, Part 8, New York, N. Y.; 1963.

Appendix A. Review of Complex Notation

Assume that a general real-valued bandpass signal voltage is

$$v(t) = R(t) \cos (2\pi f_c t + 2\pi \theta(t)) \quad , \qquad \text{(A-1)}$$

where

f_c = carrier frequency

$R(t)$ = instantaneous amplitude

$2\pi\theta(t)$ = instantaneous phase.

Its complex representation is given by

$$\xi(t) = x(t)\, e^{j2\pi f_c t} = R(t)\, e^{j2\pi\theta(t)}\, e^{j2\pi f_c t} \quad , \qquad \text{(A-2)}$$

which has the properties that

(a). $x(t)$ = low-pass equivalent signal representing instantaneous amplitude and phase modulation

(b). $\mathrm{Re}\,\xi(t)$ = real physical signal

(c). $|\xi(t)| = R(t)$ = instantaneous envelope of physical signal

(d). $\hat{\xi}(f) = 2\hat{v}(f)$, for $f > 0$,
$= 0$, for $f < 0$,

where $\hat{}$ denotes the Fourier transform.

Appendix B. Entropy Increase Due to Mixing

If all of the energy E were added uniformly, the system temperature would rise from $\mathcal{T}_o$ to $\mathcal{T}_o + \Delta\mathcal{T}$. The temperature $\mathcal{T}_o + \Delta\mathcal{T}$ is also the temperature to which the system would settle after the energy E, once added to subvolume $V(x_o)$, subsequently diffused adiabatically throughout the entire volume. During such a diffusion process, the increase in system entropy is

$$\delta S = C_v w \left(1 - \frac{1}{q}\right) \int_{\mathcal{T}_o}^{\mathcal{T}_o + \Delta\mathcal{T}} \frac{d\mathcal{T}}{\mathcal{T}} + C_v \frac{w}{q} \int_{\mathcal{T}_o + q\Delta\mathcal{T}}^{\mathcal{T}_o + \Delta\mathcal{T}} \frac{d\mathcal{T}}{\mathcal{T}} \qquad \text{(B-1)}$$

$$= C_v w \ln\left(1 + \frac{\Delta\mathcal{T}}{\mathcal{T}_o}\right) - C_v \frac{w}{q} \ln\left(1 + \frac{\Delta\mathcal{T}}{\mathcal{T}_o}\right) + C_v \frac{w}{q} \ln\left(\frac{\mathcal{T}_o + \Delta\mathcal{T}}{\mathcal{T}_o + q\Delta\mathcal{T}}\right) .$$

But

$$\ln\left(\frac{\mathcal{T}_o + \Delta\mathcal{T}}{\mathcal{T}_o + q\Delta\mathcal{T}}\right) = \ln\left(1 + \frac{\Delta\mathcal{T}}{\mathcal{T}_o}\right) - \ln\left(1 + \frac{q\,\Delta\mathcal{T}}{\mathcal{T}_o}\right) , \qquad \text{(B-2)}$$

so that

$$\delta S = C_v w \ln\left(1 + \frac{\Delta\mathcal{T}}{\mathcal{T}_o}\right) - C_v \frac{w}{q} \ln\left(1 + \frac{q\Delta\mathcal{T}}{\mathcal{T}_o}\right)$$

$$= \Delta S - \Delta S' \qquad . \qquad \text{(B-3)}$$

UNCLASSIFIED BASIC DISTRIBUTION LIST

Contract No. Nonr 839(38)

Defense Documentation Center Cameron Station Building 5, 5010 Duke Street Alexandria, Virginia 22314	20 copies
Chief of Naval Research Department of the Navy Washington, D. C. 20360 Attn: Code 427	2 copies
Commanding Officer Office of Naval Research Branch Office Box 39, Navy #100 FPO New York, New York	1 copy
Commanding Officer Office of Naval Research Branch Office 207 West 24th Street New York, New York	1 copy
Director U.S. Naval Research Laboratory Washington, D. C. 20390 Attn: Technical Information Office Code 2027	6 copies

Unclassified

Security Classification

DOCUMENT CONTROL DATA - R&D

(Security classification of title, body of abstract and indexing annotation must be entered when the overall report is classified)

1. ORIGINATING ACTIVITY (Corporate author)	2a. REPORT SECURITY CLASSIFICATION
Polytechnic Institute of Brooklyn Microwave Research Institute	Unclassified
	2b. GROUP

3. REPORT TITLE

An Analysis of Radar in Terms of Information Theory and Physical Entropy

4. DESCRIPTIVE NOTES (Type of report and inclusive dates)

Research Report June 1965

5. AUTHOR(S) (Last name, first name, initial)

Temes, Clifford L., Schilling, Donald L.

6. REPORT DATE	7a. TOTAL NO. OF PAGES	7b. NO. OF REFS
June 1965	109	58

8a. CONTRACT OR GRANT NO.	9a. ORIGINATOR'S REPORT NUMBER(S)
Nonr-839(38) b. PROJECT NO.	PIBMRI-1270-65
c. d.	9b. OTHER REPORT NO(S) (Any other numbers that may be assigned this report)

10. AVAILABILITY/LIMITATION NOTICES

DDC

11. SUPPLEMENTARY NOTES	12. SPONSORING MILITARY ACTIVITY
None	Office of Naval Research Washington 25, D. C.

13. ABSTRACT

A radar is basically a measuring instrument for extracting information from a received signal voltage. Using the quantitative concepts of "measurable information", formulae are derived which relate the range and doppler information obtained by a radar to the amount of energy required to obtain it. It is shown that the received information is bounded such that it is always less than the input physical entropy $E/\mathcal{J}$, where E is the input signal energy and $\mathcal{J}$ is the equivalent noise temperature of the radar. Except for a change of units, this physical entropy is seen to be synonymous with the standard radar expression "signal-to-noise energy ratio". Improved radar resolution is obtained by means of a Bessel-function envelope detector that effectively increases the amount of range and doppler signal compression by a factor of $\frac{2E}{k\mathcal{J}}$, where k is Boltzmann's constant. A new detection procedure is developed in which an amplitude threshold is first set so as to maximize a defined "detection information". Target detection is then based upon the use of the Neyman-Pearson procedure in the threshold-crossing rate domain rather than in the conventional voltage amplitude domain.

DD FORM 1 JAN 64 1473

Unclassified

Security Classification

Unclassified
Security Classification

14 KEY WORDS	LINK A		LINK B		LINK C	
	ROLE	WT	ROLE	WT	ROLE	WT
radar, information theory, entropy, resolution, detection, matched filters, parameter estimation						

INSTRUCTIONS

1. ORIGINATING ACTIVITY: Enter the name and address of the contractor, subcontractor, grantee, Department of Defense activity or other organization *(corporate author)* issuing the report.

2a. REPORT SECURITY CLASSIFICATION: Enter the overall security classification of the report. Indicate whether "Restricted Data" is included. Marking is to be in accordance with appropriate security regulations.

2b. GROUP: Automatic downgrading is specified in DoD Directive 5200.10 and Armed Forces Industrial Manual. Enter the group number. Also, when applicable, show that optional markings have been used for Group 3 and Group 4 as authorized.

3. REPORT TITLE: Enter the complete report title in all capital letters. Titles in all cases should be unclassified. If a meaningful title cannot be selected without classification, show title classification in all capitals in parenthesis immediately following the title.

4. DESCRIPTIVE NOTES: If appropriate, enter the type of report, e.g., interim, progress, summary, annual, or final. Give the inclusive dates when a specific reporting period is covered.

5. AUTHOR(S): Enter the name(s) of author(s) as shown on or in the report. Enter last name, first name, middle initial. If military, show rank and branch of service. The name of the principal author is an absolute minimum requirement.

6. REPORT DATE: Enter the date of the report as day, month, year, or month, year. If more than one date appears on the report, use date of publication.

7a. TOTAL NUMBER OF PAGES: The total page count should follow normal pagination procedures, i.e., enter the number of pages containing information.

7b. NUMBER OF REFERENCES: Enter the total number of references cited in the report.

8a. CONTRACT OR GRANT NUMBER: If appropriate, enter the applicable number of the contract or grant under which the report was written.

8b, 8c, & 8d. PROJECT NUMBER: Enter the appropriate military department identification, such as project number, subproject number, system numbers, task number, etc.

9a. ORIGINATOR'S REPORT NUMBER(S): Enter the official report number by which the document will be identified and controlled by the originating activity. This number must be unique to this report.

9b. OTHER REPORT NUMBER(S): If the report has been assigned any other report numbers *(either by the originator or by the sponsor)*, also enter this number(s).

10. AVAILABILITY/LIMITATION NOTICES: Enter any limitations on further dissemination of the report, other than those imposed by security classification, using standard statements such as:

(1) "Qualified requesters may obtain copies of this report from DDC."

(2) "Foreign announcement and dissemination of this report by DDC is not authorized."

(3) "U. S. Government agencies may obtain copies of this report directly from DDC. Other qualified DDC users shall request through

_____."

(4) "U. S. military agencies may obtain copies of this report directly from DDC. Other qualified users shall request through

_____."

(5) "All distribution of this report is controlled. Qualified DDC users shall request through

_____."

If the report has been furnished to the Office of Technical Services, Department of Commerce, for sale to the public, indicate this fact and enter the price, if known.

11. SUPPLEMENTARY NOTES: Use for additional explanatory notes.

12. SPONSORING MILITARY ACTIVITY: Enter the name of the departmental project office or laboratory sponsoring *(paying for)* the research and development. Include address.

13. ABSTRACT: Enter an abstract giving a brief and factual summary of the document indicative of the report, even though it may also appear elsewhere in the body of the technical report. If additional space is required, a continuation sheet shall be attached.

It is highly desirable that the abstract of classified reports be unclassified. Each paragraph of the abstract shall end with an indication of the military security classification of the information in the paragraph, represented as *(TS), (S), (C), or (U)*.

There is no limitation on the length of the abstract. However, the suggested length is from 150 to 225 words.

14. KEY WORDS: Key words are technically meaningful terms or short phrases that characterize a report and may be used as index entries for cataloging the report. Key words must be selected so that no security classification is required. Identifiers, such as equipment model designation, trade name, military project code name, geographic location, may be used as key words but will be followed by an indication of technical context. The assignment of links, roles, and weights is optional.

DD FORM 1 JAN 64 1473 (BACK)

Unclassified
Security Classification